CANADIAN THESES

THÈSES CANADIENNES

NOTICE

The quality of this microfiche is heavily dependent upon the quality of the original thesis submitted for microfilming. Every effort has been made to ensure the highest quality of reproduction possible.

If pages are missing, contact the university which granted the degree.

Some pages may have indistinct print especially if the original pages were typed with a poor typewriter ribbon or if the university sent us an inferior photocopy.

Previously copyrighted materials (journal articles, published tests, etc.) are not filmed.

Reproduction in full or in part of this film is governed by the Canadian Copyright Act, R.S.C. 1970, c. C-30. Please read the authorization forms which accompany this thesis.

AVIS

La qualité de cette microfiche dépend grandement de la qualité de la thèse soumise au microfilmage. Nous avons tout fait pour assurer une qualité supérieure de reproduction.

S'il manque des pages, veuillez communiquer avec l'université qui a conféré le grade.

La qualité d'impression de certaines pages peut laisser à désirer, surtout si les pages originales ont été dactylographiées à l'aide d'un ruban usé ou si l'université nous a fait parvenir une photocopie de qualité inférieure.

Les documents qui font déjà l'objet d'un droit d'auteur (articles de revue, examens publiés, etc.) ne sont pas microfilmés.

La reproduction, même partielle, de ce microfilm est soumise à la Loi canadienne sur le droit d'auteur, SRC 1970, c. C-30. Veuillez prendre connaissance des formules d'autorisation qui accompagnent cette thèse.

THIS DISSERTATION
HAS BEEN MICROFILMED
EXACTLY AS RECEIVED

LA THÈSE A ÉTÉ
MICROFILMÉE TELLE QUE
NOUS L'AVONS REÇUE

CHAR GASIFICATION WITH CARBON DIOXIDE

by

HELEN PANOLIASKOS

A thesis submitted to the School of Graduate Studies in partial fulfilment of the requirements for the M.A.Sc. degree in Chemical Engineering

UNIVERSITY OF OTTAWA
OTTAWA, CANADA
1983

ACKNOWLEDGEMENTS

The author wishes to express her appreciation and gratitude to Dr. R.S. Mann, her research director, for his guidance and assistance during this study and his help in the preparation of this thesis.

The author also wishes to express her thanks to Dr. A. Kumar for his criticisms and suggestions; to the other graduate students for the helpful suggestions and to Mr. G. Gasperetti and his staff for the technical assistance.

ABSTRACT

The gasification of two chars, Saskatchewan lignite and Forestburg sub-bituminous, in carbon dioxide was studied by thermogravimetric analysis. The effect of variables such as carbon dioxide flow rate, char particle size, and catalysts were investigated. Experimental data were obtained in the temperature range 728-875°C and at atmospheric pressure.

A modified unreacted-core model was developed to express reaction rates of both catalyzed and uncatalyzed gasification as a function of carbon conversion.

Two catalysts, K_2CO_3 and Ni (added in the form of $Ni(NO_3)_2$) were used, K_2CO_3 was found to be more active than Ni catalyst. Catalyst effectiveness decreased with increasing concentration and gasification temperature. Gasification rates increased by as much as 6 times in the presence of catalyst.

Activation energies decreased for the lignite char doped with catalyst but not considerably, whereas for the sub-bituminous char the decrease was insignificant.

The activation energies for the lignite and sub-bituminous chars were found to be 176 and 155 kJ /mole respectively. For catalytic gasification, the activation energies were 159 kJ /mole for lignite containing 5 m % Ni, 141 kJ /mole for lignite with 10 m % K_2CO_3 and 152 kJ /mole for the sub-bituminous char with 10 m % K_2CO_3.

The results indicated that gasification of both chars was catalyzed by the impurities present in the char ash. Also lignite char was found to be more reactive than the sub-bituminous char which is in accordance with the reactivity increasing with decreasing rank of parent coal.

TABLE OF CONTENTS

LIST OF FIGURES

Page

Page

LIST OF TABLES

NOMENCLATURE

A,B	Subscripts for reactants
a	Constant
b	Molar stoichiometry of the reaction
b	Constant
C	Reactant concentration, mole l^{-1}
D	Diameter of reactor, cm
D_{AB}	Binary diffusivity of CO_2 in nitrogen, $cm^2\ s^{-1}$
De	Effective diffusivity of gaseous reactant in ash layer, $cm^2\ s^{-1}$
d	Char particle diameter, cm
E	Activation energy, kJ $mole^{-1}$
K	Equilibrium constant of C-CO_2 reaction
K_1, K_2, K_3	Kinetic parameters
k_g	Mass transfer coefficient, cm s^{-1}
k_s	Reaction rate constant, cm s^{-1}
k_1, k_2, k_3	Reaction rate constants
M	Mass rate of carbon gasification, g s^{-1}
M_c	Molecular weight of carbon
M_g	Molecular weight of CO_2
N_A	Number of moles of gaseous reactant
N_B	Number of moles of solid reactant
n	Order of reaction
nt	Number of active sites

P	Pressure, kPa
pCO	Partial pressure of CO, kPa
pCO_2	Partial pressure of CO_2, kPa
Q	Flow rate of reactant gas in reactor, cm^3
Q_A	Flux of gaseous reactant through ash layer, mole $cm^{-2}s^{-1}$
R	Gas constant, J $mole^{-1}$ K^{-1}
R_p	Radius of char particle at time, t=0, cm
r	Radius of char particle at any time, t, cm
r_c	Radius of unreacted core of char particle, cm
r_m	Experimental specific gasification rate, s^{-1}
$r_{m,D}$, $r_{m,F}$	Diffusion limited specific gasification rate, s^{-1}
S_{ex}	Surface area of char, cm^2
T	Temperature, °C or K
TGA	Thermogravimetric analysis
TGB	Thermogravimetric balance
t	Time, min
u	Velocity, $cm\ s^{-1}$
V	Volume of the char particle, cm^3
W	Weight of char, mg
α	Constant
β	Constant
Λ	Gravimetric stoichiometric coefficient
μ	Viscosity, micropoises
η_s	Effectiveness factor
ρ_B	Molar density of solid reactant, mole cm^{-3}
σ	Particle density of char, g cm^{-3}

CHAPTER 1

INTRODUCTION

In the face of the state of world reserves of primary energy sources and the steadily rising demand for energy, it has become necessary to consider alternative sources. Coal utilization has received increasing attention in the later years for the production of liquid and gaseous fuels. There are four major routes to coal utilization, pyrolysis, combustion, gasification and liquifaction.

In pyrolysis processes the volatile constituents of coal are cracked to give gaseous and liquid products, which can be separated and reacted further to provide marketable by-products. These processes represent a de-gassing of the coal, where the greater part of the feed material remains as solid char, consisting mainly of carbon and ash. The char with its high carbon content can be further utilized in gasification processes where it is used as the feed material instead of coal.

In gasification processes, char or coal can be reacted with steam (endothermic reaction) to form H_2, CO and CO_2, with hydrogen (exothermic reaction) to form CH_4, or with carbon dioxide (endothermic reaction) to form CO. The product methane is the main constituent of Synthetic Natural Gas (SNG) where mixtures of CO and H_2 gases can be used for

fuel or for feed material in the production of chemicals (Synthesis Gas). To be efficient most gasification processes are arranged so that exothermic and endothermic reactions essentially balance the opposite heat effects. Since combustion is highly exothermic, in many cases part of the char or coal is allowed to react with oxygen in order to provide the necessary heat.

Carbon dioxide is both a reactant and a product of the gasification or combustion. Thus its reaction with the carbon in coal or char plays an important role in industrial applications, and has been the subject of many investigations. It should be mentioned that research interest in the carbon-carbon dioxide reaction has also been stimulated for its role in the smelting of ores or for the lack of reaction of carbons and graphites when used as electrodes, structural carbons or moderators in atomic reactors.

Char gasification with carbon dioxide to produce carbon monoxide is a heterogeneous endothermic reaction. The gasification rates depend on the kinetics of the reaction, heat and mass transfer phenomena and flow conditions along with the intrinsic reactivity of the char.

When studying heterogeneous reactions, it is customary to obtain data which are free of heat transfer or diffusion influences in order to understand the kinetics of the reaction. The number of variables involved in these reactions is large.

Inadequate consideration of the physical and chemical characteristics of the carbon solid is often the reason for the conflicting results reported in the literature.

Many studies have been conducted on the mechanism of the carbon-carbon dioxide reaction using mostly relatively purified carbon solids and rate expressions of the Langmuir-Hinshelwood type or other have been proposed. But there is still need for further research using actual chars and in many areas.

For example each char has its own intrinsic reactivity and thus has to be studied separately. The reactivity depends on the physical and chemical characteristics of the char which in turn are determined by the origin of the parent coal and the method and conditions of char preparation. A very important factor is the change of these characteristics during reaction.

Also the rate expressions that have been proposed, except for very few cases, are for the initial reaction only. Gasification has been mostly carried out to only a few percent conversion in order to avoid burn-off complications.

Another area of great importance is catalytic gasification. Research in this area has been limited to the effectiveness of various catalysts. Information is needed on the effect of variables such as catalyst concentration, method and conditions of catalyst addition, and gasification

temperatures. Mechanistic studies are lacking and also rate expressions for catalytic gasification.

The majority of char gasification studies reported in the literature have been carried out using chars from coals of American origin. Therefore, studies are needed on char produced from Canadian coals, because of the different properties these coals have, such as mineral matter content.

In the present study, two chars, Saskatchewan lignite and Forestburg sub-bituminous, were gasified with carbon dioxide and at atmospheric pressure. The major objectives were to

i) determine the reactivities of the chars and relate them to the rank of the parent coal.

ii) investigate the effect of variables as carbon dioxide flow rate, char particle size and termperature.

iii) determine the effectiveness of two catalysts, Ni and K_2CO_3, and study the effect of catalyst concentration and temperature on gasification rates.

iv) develop a rate expression as a function of conversion for both catalyzed and uncatalyzed gasification.

v) estimate kinetic parameters from the proposed model.

The weight-loss data were obtained by thermogravimetric analysis (TGA) with all experiments carried out isothermally. A TGA balance, compared to flow reactors, can generate more experimental data in relatively shorter time, is simple to

operate and has been widely used. However there are disadvantages such as product analysis is difficult due to the small amount of product gases involved, or effects such as residence time cannot be studied. However in the char-carbon dioxide reaction, there is only one product, carbon monoxide and just weight-loss data are sufficient.

CHAPTER 2

LITERATURE SURVEY

The carbon-carbon dioxide reaction has been the subject of numerous investigations due to its importance in many industrial applications. Catalysis of the reaction has also been studied but to a lesser extent. There are several review articles on both catalyzed and non catalyzed gasification of carbon solids with carbon dioxide (1 - 8).

In this section, the kinetics of the reaction, the effect of particle size, the factors affecting the reactivities of carbon solids, the effect of catalysts and the mechanism of catalysis will be reviewed.

2.1 The Carbon-Carbon Dioxide Reaction

Carbon solids in the presence of carbon dioxide react to produce carbon monoxide. That is

$$C + CO_2 = 2\ CO \qquad (2.1)$$

The reaction is highly endothermic with an enthalpy of 147 kJ at 298 K and 101.3 kPa (3,9).

Product formation is favoured by increasing temperatures and decreasing pressures (9). Gasification temperatures are in the range of 700°C to 1400°C mainly depending on the type of carbon solid. Relatively pure solids such as graphite require higher temperatures than coal chars.

The rate of reaction of carbon with carbon dioxide depends on many factors. That is, temperature, pressure, gas composition (concentration of CO_2, CO, inert gas), pretreatment of the solid, the nature of carbon, the mineral content, the change in reactivity during reaction, the particle size if the reaction is diffusion controlled (3,10).

2.2 Heterogeneous Nature of the Reaction

The reaction of a carbon solid with carbon dioxide is heterogeneous in nature and thus can be affected by mass transport limitations. Since most carbon solids are porous, a predominant part of the reacting interface may lie within the pores of the carbon. A simplified picture of the successive steps involved in the reaction can be visualized as follows:

1. Transport of CO_2 to the exterior surface of the solid.
2. Diffusion of CO_2 into the interior of the porous solid.
3. Chemisorption of CO_2 on the pore surface and external surface.
4. Surface reaction.
5. Desorption of CO, the product of reaction.
6. Outward diffusion of CO from the interior of the solid to the external surface.
7. Transport of CO from the surface into the bulk-gas phase.

Steps 3, 4 and 5 deal with the chemical aspects of the reaction, 2 and 6 represent internal mass transport or

pore diffusion and steps 1,7 external mass transport or film diffusion.

Depending on the experimental conditions and type of carbon solid, the reaction may be controlled by any of the above steps or a combination of those. However, there is a general agreement that as temperature is increased the reaction goes through three regions.

At low temperatures the chemical aspects of the reaction predominate and the overall rate is chemically controlled. The transport processes proceed rapidly. At intermediate temperatures, the resistances offered by the transport steps 2 and 6 can no longer be considered negligible. The rates of pore diffusion are slower than those due to chemical reaction and control the overall process. At higher temperatures film diffusion becomes rate controlling.

In kinetic studies it is desired to obtain rate data which is free from mass transport limitations since only the chemical aspects need to be considered. From the results of different workers it appears that the transition from chemical reaction to pore diffusion control occurs at temperatures 900 to 1200°C (11-17).

Rao and Jalan (14) pointed out that diffusional effects increase with increasing particle size, increasing temperature and partial pressure of CO_2 in the gas phase. Turkdogan and Vinters (17) arrived at the same conclusions. They also

pointed out that one of the ground rules is to use small samples of fine particle size and relatively fast gas flow rates so that pore diffusion and film diffusion are eliminated to a large extent.

Walker and Hippo (18) stressed the importance of solid porosity and pore size distribution along with their change during reaction upon the mass transport effects.

2.3 Mechanism of the Reaction

Among the different mechanisms proposed most of the evidence (1,4,5,14,19,20) supported the view that the reaction took place in two steps. That is

$$\text{Step 1} \quad C + CO_2 \underset{k_1'}{\overset{k_1}{\rightleftharpoons}} C(O) + CO \qquad (2.2)$$

$$\text{Step 2} \quad C(O) \xrightarrow{k_2} CO + C \qquad (2.3)$$

The first step is a reversible oxygen exchange reaction during which CO_2 dissociates at an active site on the carbon surface forming a carbon-oxygen complex, and a CO molecule. Actual gasification takes place in the second step with the generation of a new active centre on the solid carbon surface. Also the well known inhibiting effect of the product carbon monoxide is through the reverse of the reaction in step 1.

Gadsby et al. (11), Blackwood and Ingeme (21), Turkdogan

and Vinters (17,22), proposed mechanisms involving chemisorption of carbon monoxide molecules on the carbon surface. These mechanisms predict that carbon monoxide retards the reaction through its chemisorption.

The two step mechanism has been substantiated from both direct (isotopic techniques) and indirect (overall rate measurements) studies.

Reif (1) ruled out mechanisms involving adsorption of CO_2 molecules on the carbon surface since this is negligible above 600°C, which is too low a temperature for gasification.

According to Ergun (19), the reverse of step 2 would result in carbon transfer from gas to solid phase. From his own and other worker's results he concluded that step 2 is not reversible.

Mentser and Ergun (4) conducted a comprehensive study of the $C-CO_2$ reaction using isotopic techniques which permit direct measurements of the kinetic constants and rates. From their results other possible reaction steps were ruled out.

Rao and Jalan (14) presented a critical evaluation of the existing theories on mechanisms and rate equations and concluded that the two step mechanism represents a substantial part of the published data.

The oxygen-exchange equilibrium constant (step 1) is given by $K = k_1/k_1'$. Johnson (5), Mentser and Ergun (4), Ergun (19), pointed out that K values should be independent of carbon

type and pressure and be function of temperature only. Therefore comparison of the experimental values of K obtained from different studies should serve as a severe test for the validity of oxygen-exchange as an essential reaction step. As shown by Johnson (5) in his recent review, K values from different studies showed a similar overall trend.

It has been supported that step 2 is the rate controlling that is the slower step. Reif (1) based on his results concluded that the oxygen-exchange reaction is faster than the gasification step. Ergun (19) pointed out that oxygen-exchange reactions occur at temperatures approximately 200°C lower than that required for gasification at comparable rates.

Experimental evidence showed that carbon monoxide strongly inhibits the reaction. From the results of Blackwood and Ingeme (21), doubling the partial pressure of CO, the reaction rate is decreased by little less than a factor of two. They also found that the inhibiting effect decreases with increasing temperatures and decreasing partial pressures of CO. Gadsby et al. (11) and other workers arrived at the same conclusions.

Mentser and Ergun (4) concluded that the retarding effect of CO is due to decrease in concentration of carbon-oxygen complexes through the reverse of step 1. The retarding effect of CO depends upon the rates of forward and reverse oxygen transfer reactions. They also pointed out that since forward activation energy is higher than the reverse, the retarding effect of CO may be predicted to decrease with increase in

temperature.

Actual gasification takes place according to step 2 with gasification rates proportional to the number of active sites available for reaction. The number of active sites would be expected to decrease with increasing solid preparation or reaction temperature for any material. For coal chars, it would also be expected to decrease with increasing coal rank (5).

2.4 Effect of Particle Size

Ergun (19) carried out experiments in a fluidized bed and at atmospheric pressure with Ceylon graphite, activated carbon and activated graphite. Particle sizes ranged from 1.8 to 0.081 mm. He found that for the porous activated carbon (700 - 1025°C) and graphite (900 - 1150°C), the reaction was independent of particle size. For the non porous Ceylon graphite (1000 - 1400°C) rate increased with decrease in size.

Ergun (20) in another study of the C-CO_2 reaction using a metallurgical coke found the reaction rate to be independent of particle size of the same range and at temperatures 900 to 1200°C.

Walker and Hippo (18) studied the effect of particle size for a lignite char and a low volatile coal char at 900°C and atmospheric pressure. A thermogravimetric balance (TGB) was used. Four particle sizes were used in the range of 0.284 to 0.044 mm. They found that the reaction rates increased with decrease in particle size indicating pore diffusion

limitations. For the lignite char reactivity increased only by a factor of 2.7 fold over the particle size range where for the other char the increase was 35 fold. The difference in the extent of pore diffusion control for each of the chars was attributed to their different internal pore structure.

Dutta et al. (15) studied the reactivities of few chars with CO_2 at 1 atm and 840 to 1100°C. Four particle sizes (0.625 to 0.147 mm) were used to see the size effect on the reactivities of the char samples at about 1000°C and was found to be negligible.

Turkdogan and Vinters (17), for electrode graphite and coconut charcoal gasification at 1 atm found that diffusion becomes controlling for particle diameter larger than 6mm and temperatures higher than 900°C. At higher pressures and the same temperature, diffusion became progressively important.

From the above it can be said that for particle diameters lower than 1mm and temperatures lower than 900°C, the particle size effect would be expected to be negligible. However it should be investigated for each type of carbon solid and at experimental conditions.

2.5 Effect of Pressure

Very few investigations have been conducted at elevated pressures. From a study at IGT (5), reaction rates were proportional to increasing pressures up to about 10 atm and then became independent of pressure. Similar results were found by Turkdogan and Vinters (17). Fuchs and Yavorsky (23) found

that the total pressure had no effect on gasification rates at pressures of 18 - 35 atm. However Blackwood and Ingeme (21) found increasing rates up to 40 atm.

Walker et al. (3) pointed out that from thermodynamic considerations, the reaction is not favoured by increasing pressures.

2.6 Factors Affecting the Reactivity of Carbon Solids

A number of workers have stressed that in order to understand the kinetics of the reaction, adequate consideration must be given to the physical structure of carbons, and the changes that occur with conversion (3,10,18,20,23,24,25). The number of carbon sites available for reaction depends on the detailed structure of the carbon and the available for reaction surface area. In addition changes of surface area during reaction may enhance or inhibit reaction rates. In this section these factors are discussed.

2.6.1 Structure of Carbon Solids

The carbon solid surface is heterogeneous itself (3). In addition to the normal sources of heterogeinity (holes and dislocations in the lattice), carbon is a multicrystalline material, which means that its surface will be composed of different crystallographic planes. The crystallites vary widely in size ranging from 10Å in some amorphous materials, up to thousands of Angstroms in natural graphite (3). The orientation of crystallites also contributes to the

heterogeinity. Structural disorders increase with decreasing coal rank, and since the number of active sites is inversely proportional to the degree of crystallographic perfection, the reactivity of chars increases with decreasing rank of parent coal (5,10,11,12,15,23).

2.6.2 Pretreatment of Carbon Solids

Johnson (5), Katta and Keairns (10) stressed the importance of solid preparation upon its reactivity with CO_2. Walker and Hippo (18) pointed out that char more or less retains the structure of the parent coal. However, if the processing temperature is high, breakage of the crosslinks between planar regions in the char results in improved alignment with loss of porosity.

Blackwood and Ingeme (21) preheated E. Marginata char in nitrogen at different temperatures from 650 to 950°C. They found that reaction rate decreased drastically with increasing temperature.

Finally, the exact structure of a char produced from a given coal can be changed by altering such variables as pretreatment temperature, coal particle size, rate of heating, time at maximum temperature, atmosphere and total pressure during heating.

2.6.3 Inherent Catalytic Effect

Mineral matter and trace elements dispersed within the carbon solid matrix can catalyze the gasification process. The possible catalytic effect of foreign matter in cokes and chars has been discussed by several investigators (3,10, 18,20,23,26).

According to Walker and Hippo (18) the catalytic activity would vary between impurities, their concentration and extent of dispersion. They studied the gasification of sixteen chars with CO_2 at 900°C and found a reasonably good linear correlation between increasing Ca and Mg content (up to 7wt% CaO, 1wt% MgO in the parent coal) and increasing reactivity. No correlations were found for Fe or Na and K. Lignites showed strong inherent catalytic effect and their demineralization resulted in decreased reactivity.

2.6.4 Porosity and Surface Area

The porosity, pore size distribution and available surface area for reaction of a carbon influences the initial reactivity of the solid. However these can change during reaction and result in a decrease or increase of the rates. In most of the kinetic studies, burn-offs were kept low (up to 10%) to avoid these complications of structural changes.

Carbons of different origin have been gasified to a certain conversion level and their structure examined (3,13, 15,18,25,27). In most cases drastic changes occurred with

the development of the internal surface area. It was supported during conversion with the consumption of carbon molecules from the solid matrix, pores enlarge, or pores previously non interconnected become available. Eventually the rate of development of new surface area will become slower than the destruction of the old one and reaction rates will decrease. More important, diffusion limitations can be understood and identified with knowledge of the structural changes during reaction.

2.7 Reaction Rate Models

Different mathematical models have been proposed for the reaction rate expression and can be divided into two groups. Those that are derived from Langmuir-Hinshelwood mechanism and power low models. A Langmuir-Hinshelwood rate expression is preferred because it reveals information about the mechanism of the reaction and can be used for extrapolation with more confidence than an empirical model. However it is subject to limitations (28) and describes only initial rates of reaction. These models will be presented here.

2.7.1 Langmuir-Hinshelwood Model

The Langmuir-Hinshelwood rate expression generally accepted to represent the $C-CO_2$ reaction is of the form

$$r = \frac{K_1 pCO_2}{1+K_2 pCO+K_3 pCO_2} \qquad (2.4)$$

where r is the specific reaction rate, K_1,K_2 and K_3 are kinetic parameters and pCO, pCO_2 are carbon monoxide and carbon dioxide partial pressures.

The kinetic parameters are related to the rate constants of the individual steps occurring during reaction. Individual rate constants and thus the kinetic parameters cannot be directly determined from reported data without knowing the concentration of active sites, nt.

The above correlation shows that the rate decreases with increasing partial pressure of carbon monoxide. Also the order of reaction varies from zero to unity depending on the conditions of pressure and temperature. At normal gasification temperatures and low CO_2 pressures the reaction will be first order.

It should also be pointed out that the Langmuir-Hinshelwood expression can be derived from different mechanisms for the C-CO_2 reaction, showing that the reaction mechanism is not uniquely defined by a specific rate equation.

The results of investigators who interpreted their data according to the above expression will be presented.

In a study conducted at the IGT (5) a bituminous coal char was gasified in CO and CO_2 mixtures, at 2-35 atm and 850 - 1000°C. The activation energies obtained for K_1,K_2, K_3 were 119 ,-26.8 , -155 kJ /mole respectively.

Gadsby et al (11) gasified coconut-shell charcoal in a

packed bed and CO_2-N_2 mixtures, at 1.3-101.3 kPa and 734 - 829°C. They found the activation energies to be 246, -188, 123 kJ /mole.

Lewis et al. (29) studied the gasification of coke and anthracite in a fluidized bed, at 1 atm and 500 - 1100°C. Feed gases were mixtures of CO_2, N_2, CO. The K_1,K_2,K_3 activation energies for coke were 199 , -62.8 , -26.4 kJ /mole and for anthracite 136 , -70.7 , -69.5 kJ /mole.

Mentser and Ergun (4) obtained activation energies of 222 , -92.1 , -20.9 kJ /mole for spheron No. 6 carbon gasification in a packed bed, with CO_2-CO mixtures at 1 atm and 750-850°C.

Katta and Keairns (10) used a simplified Langmuir-Hinshelwood expression for gasification of coke breeze and found an activation energy of 289 kJ /mole for the temperature range 920 - 1040°C and 1 atm.

Also Rao and Jalan (14) used a simplified expression and obtained an activation energy of 333 kJ /mole (1 atm, pure CO_2 feed gas, 830 - 1050°C).

In all these studies burn-offs were kept to a minimum. The results obtained could not be used over different conversion levels.

2.7.2 Power Law Models

In the power law models the reaction rate is expressed

as a function of the partial pressure of carbon dioxide raised to some power, n. The power can be zero, a fraction, unity or higher. The values of n reported in the literature vary from zero to unity.

The results of some investigators have been summarized in Table 2.1. Overall activation energies range from 180 to 289 kJ/mole for temperatures, 750 - 1300°C. In most of the studies conducted at 101.3 kPa pure carbon dioxide was the feed gas, thus it can be said that with pure CO_2 and at 101.3 kPa the order of reaction is unity (see Table 2.1).

Wen and Wu (30) and Dutta et al. (15) are of the very few ones that proposed a rate equation for up to complete conversions was proposed. Wen and Wu (30) used a volume reaction model to interpret their results. The porosity and internal surface area of the porous carbon they used remained unchanged with conversion and their model does not account for such changes. However in the work of Dutta et al. (15) the internal surface area of the chars and coals used developed drastically with conversion, affecting their reactivity. They incorporated in the rate equation a term to account for these changes.

The development of mathematical models derived to express the rates of gas-solid reactions have been discussed by a number of investigators (32 - 41).

TABLE 2.1

SUMMARY OF ACTIVATION ENERGIES

FOR THE C-CO_2 REACTION

Investigator	Sample	T, °C	P, atm	n	E, kJ/ moles
1. Turkdogen and Vinters (17)	electrode graphite	800-1300	10^{-3}-10	0.5	285
	coconut charcoal	700-1100	10^{-3}-10	0.5	285
2. Walker et al (12)	graphite	900-1200	1	1	201
		1200	1	1	109
	gas-baked carbon	900-1100	1	1	197
3. Walker and Raats (13)	graphitized carbon	970-1130	1	1	276
		1130	1	1	184
4. Wen and Wu (30)	activated charcoal	857-1092	1	1	289
5. Dutta et al (15)	hydrane char #49	859-1059	1	1	248
	synthane char	852-1078	↓	↓	↓
	IGT char No. 6	903-1050			
	Illinois coal No.6	854-1059			
	hydrane char #150	884-979			
	Pittsburg HVal coal	917-970			
6. Fuchs and Yavorsky (23)	hydrane char	750-900	18-35	0	228
	synthane char	750-900	35	0	228
7. Knight and Sergent (31)	Millnerran char	800-1038	1	-	233
	Liddel char	↓	↓	-	219
	Lithgow char			0.7	222
	Merriown char			-	227
8. Walker and Rusinko (25)	Six carbons	900-1000	1	1	180-285

2.8 Catalytic Gasification

The use of catalysts aims to enhance the reactivities of carbons and obtain higher conversions or to lower gasification temperatures. The relative effectiveness of various catalysts strongly depends on the particular experimental conditions used, the conditions and methods of catalyst addition, chemical state of catalyst, relative anounts of catalyst and carbon. Walker et al. (7) pointed out that little was known about these parameters and additional research was needed in order that the kinetics of catalytic gasification became fully understood.

Among the various catalysts investigated, alkali metal carbonates have received particular attention. Other catalysts used included alkaline earth carbonates, Iron, Nickel.

2.8.1 Type of Catalyst

Taylor and Neville (6) studied the catalytic effect of Fe_2O_3, $CaCO_3$, K_2CO_3, Na_2CO_3, NaCl and Ni (added as nitrate and reduced in H_2 at 570°C) on the C-CO_2 and C-H_2O reactions. Catalysts were added by wet impregnation to coconut-shell charcoal and gasification runs in CO_2 were carried out in a fixed bed, at 570°C and 1 atm. Ni was found to be the most effective catalyst and from the carbonates, potassium and sodium with potassium being better. While calcium carbonate and sodium chloride had little effect on the conversion Fe_2O_3 had no effect whatsoever. Except for the case of Ni, there

was a parallelism in catalyst effectiveness between the two reactions.

McKee and Chatterji (42) using one to one mixtures of alkali metal carbonates and graphite powder, carried out experiments in a TGB, 101.3 kPa and in the temperature range 25 - 1000°C. The samples were heated in CO_2 at a rate of 10°C/min and weight changes recorded. Pure graphite slowly gasified at 900°C whereas in the presence of catalyst the reaction became detectable at about 700°C. Gasification rates accelerated near the melting point of the carbonate phase. This is due to the better contact provided by the molten salt with the carbon surface. In decreasing order, the catalytic activity was $Li_2CO_3 > Cs_2CO_3 > Rb_2CO_3 > K_2CO_3 > Na_2CO_3$ which is in accordance with the increasing order of melting points of the salts except for K_2CO_3 and Na_2CO_3.

In a recent study, McKee et al. (43) used a number of coal chars doped with small amounts of alkali metal carbonates. Catalysts were added by dry mixing before or after charring of the coals at 700°C in N_2. Runs were carried out in a TGB, with low burn-offs (>10%) and at 700 to 900°C. A variation of K_2CO_3 catalytic effect (10wt% K_2CO_3) on coal char type is given in Table 2.2.

TABLE 2.2*

CATALYTIC EFFECT OF K_2CO_3

Char	Temperature (°C)	Catalyzed/non-catalyzed rate
Lignite	700	3.0
San Juan	700	12.2
Pittsburgh hvA	800	20
Illinois No. 6 hvB	700	55
Anthracite	800	110
Graphite	900	4000

* Reproduced after McKee et al. (43)

From the Table it is easily seen that the catalytic activity increased with increasing rank of parent coal. It should be noted that low rank coal chars are very reactive even without a catalyst. The investigators also compared their data as a function of metal-to-carbon ratios over an extended concentration range, and found Cs_2CO_3 to be the most active catalyst and the activity of Li_2CO_3 actually declined at high catalyst concentrations, possibly as a result of smoothering of the char surface with a film of molten Li_2CO_3 (m.p. 618°C).

The catalysts are compared on a metal-to-carbon basis, based on the results of Spiro et al. (44) for graphite. The catalytic activity of alkali carbonates is Li > Cs > K > Na and for chars Cs > K > Na > Li.

Fox and White (45) added 5wt% Na_2CO_3 to graphite and sugar char, and found the reaction rates to increase twenty-fold at 900°C and tenfold at 950°C. Jalan and Rao (46) found the reaction rates to be the same in the range 839 - 1050°C for 1.5wt% Li_2O and 3.7wt% Li_2CO_3 added by dry mixing to carbon black. It should be noted that the concentrations used correspond to the same Li content with respect to carbon.

According to Marsh and Mochida (47) the catalytic activity of potassium salts added to metallurgical coke decreased with increasing melting point (i.e. $K_2CO_3 > KCl > K_2SO_4 > K_3PO_4$) except for K_2CO_3 and KCl. Runs were carried out at 900 and 1000°C.

McKee (48) studied the effect of additions of alkaline earth carbonates on the reactivity of graphite powder in CO_2 and 1 atm. Catalysts were added by dry mixing and runs were carried out with increasing temperature at a rate of 10°C/min and isothermally in the range 700 - 1100°C. For 5 wt% content, the catalytic activity of the salts in increasing order were $MgCO_3 < CaCO_3 << SrCO_3 < BaCO_3$. The catalysts $SrCO_3$ and $BaCO_3$ increased gasification rates about three fold where as $MgCO_3$ and $CaCO_3$ increased the rate 11 and 50 times respectively at 900°C.

Walker et al. (7) added very small amounts of Fe, Ni or Co to graphite (300 ppm) by dry mixing. From their results, and

in the temperature range of 800 to 1000°C all catalysts were very active with Fe being the most. At 950°C graphite gasified at a rate of 0.0025 min^{-1}, with Ni the rate was 0.45 min^{-1}, with Co 1.0min^{-1} and Fe 1.6 min^{-1}. From burn-off vs. time isotherms it was found that the curves levelled off after some period of constant gasification rate. This was attributed to catalyst deactivation being more pronounced in the case of Fe. For burn-offs higher than 75% decreasing rates were due to destruction of surface area rather than deactivation alone.

Tashiro et al. (49) studied the catalytic effect of platinum, palladium and rhodium on the C-CO_2 reaction of active carbon at 800°C. Without catalyst the rate expressed as CO_2 conversion was about 1.5%. The catalysts (5%) increased the conversion to 32.1% (Pd), 59.8% (Pt), 70.8% (Rh).

Yamada et al. (50) added five nickel compounds to PFC char by dry mixing to a content of nickel of 0.5 atom% with respect to carbon atoms (≈2.4wt%). The nickel compounds were NiO, $Ni_3CO_3(OH)_4.4H_2O$, $Ni(NO_3)_2.6H_2O$, $NiC_2O_4.2H_2O$ and $Ni(CH_3COO)_2.4H_2O$. Samples were heated in CO_2 up to 1000°C. The catalytic activity could be correlated with the easiness of the compound to reduce to metallic nickel. It was for this reason that nickel acetate, oxalate, nitrate were good catalysts and gave conversions of 70, 50, 40 wt% respectivly up to about 900°C at which temperatures pure char was

unreactive. The other two chars were little effective.

2.8.2 Effect of Catalyst Concentration and Temperature

Very little work has been done on the effect of catalyst loading and gasification temperature. Johnson (51) pointed out that there is generally an intermediate optimum concentration beyond which either negligible or negative effects result. Also the relative catalytic effects decrease with increasing gasification temperature.

Taylor and Neville (6)used 7.5 and 20wt% Ni in coconut-shell charcoal which produced the same results indicating the optimum concentration had been reached by 7.5wt%. Also 10 and 20wt% K_2CO_3 was used. The rate increase of production of CO was 8 and 15 times respectively. This corresponded to almost a linear increase in catalyst effectiveness.

Spiro et al. (44) reported that for graphite containing alkali metal carbonates and for metal-to-carbon ratio greater than about 0.01 relatively flat loading dependence on reaction rates was observed at 900°C. For coal chars, increasing the catalyst loading ranged from accelerating (Cs_2CO_3) to inhibiting (Li_2CO_3) the rates.

Yamada et al. (50) varied the nickel loading in the PFC char. The amount of gasifiable carbon increased with the amount of nickel acetate. The conversion of PFC char below 800°C was 40,70,90 and 98wt% for nickel loading of 0.2, 0.5,

1.0 and 2 atom% (1, 2.4, 5, 10wt% respectively). However the conversion increase divided by the amount of catalyst used decreased with catalyst loading.

Fox and White (45) found that 5wt% $NaCO_3$ in graphite and sugar char increased reaction rates twentyfold at 900°C and tenfold at 950°C. Thus effectiveness of catalyst decreased with temperature. Jalan and Rao (46) arrived at similar foundings. Also they found that with 1.5wt% LiO and 3.7wt% Li_2CO_3 content in carbon black pellets, the rates increased with particle size indicating diffusion. From the isotherms and assuming a first order reaction, the rate constants for both catalysts were found with an activation energy of 93.10 $\pm$ 4.26 kJ /mole. Correcting for pore and film diffusion, the intrinsic rates constants had an activation energy of 201.1 kJ /mole. The activation energy for uncatalyzed samples was 360 kJ /mole.

McKee (48) from plots of gasification rates of graphite with 5wt% alkaline earth carbonates vs. 1/T found the activation energies to be 383 kJ /mole for pure graphite, 291 for $MgCO_3$, 253 for $CaCO_3$, 246 for $SrCO_3$ and 244 kJ /mole for $BaCO_3$. He pointed out that the apparent activation energy is not very sensitive to the catalytic species present, the main effect of the additive being to change the pre- exponential factor of the rate constant.

Walker et al. (7) studied the catalytic effect of Ni,CO and Fe, and from rate vs. 1/T graphs, the apparent activation energies were calculated to be 364 kJ /mole, 318, 218 and 159

kJ/mole for pure graphite, Ni, Co and Fe respectively. Runs for samples containing Fe were diffusion controlled.

2.9 Mechanism of Catalysis

The mechanism of catalytic gasification of carbons in CO_2 has been reviewed recently by Wen (8) and McKee (52). The surface-cleaning, oxygen-transfer, and the electron-transfer mechanism advanced in recent years. These by various investigators are discussed here.

2.9.1 Surface-Cleaning Mechanism

Taylor and Neville (6) postulated that alkali metal carbonates catalyze the C-CO_2 reaction through a surface-cleaning mechanism. Their presence accelerates the removal of surface carbon-oxygen complexes and the cleaned surface is more reactive towards carbon dioxide. They carried out adsorption experiments of carbon dioxide in the presence of carbonates to verify this mechanism. They found that the adsorption characteristics of the charcoal surface toward CO_2 increased in the presence of the catalyst. For the carbon-steam reaction, the catalytic effect of carbonates was sought to be through the catalysis of the C-CO_2 reaction based on the fact that there was a striking parallelism between the catalysts for the two reactions.

2.9.2 Oxygen-Transfer Mechanism

Fox and White (45) interpreted the catalytic effect of Na_2CO_3 on graphite and sugar char gasification with CO_2

according to the following mechanism. The carbonate reacts with carbon in the solid matrix to form vapor metal and carbon monoxide. The alkali metal vapour reacts with CO_2 to form a metal oxide and carbon monoxide. The metal oxide further reacts with CO_2 forming a metal carbonate which is drawn back to the surface and enters the reaction again. Taylor and Neville (6) rejected this oxidation-reduction cycle as the mechanism for catalysis.

McKee (48) explained the catalytic effect of alkaline earth carbonates on graphite gasification with CO_2 according to the following oxidation-reduction cycle.

$$MCO_3+C=MO+2CO \qquad (2.5)$$

$$MO+CO_2=MCO_3 \qquad (2.6)$$

where M=Mg, Ca, Sr, Ba. The termal stability of the pure salts was investigated as a function of temperature in atmospheres of flowing He and CO_2. The catalytic activity increased with increasing stability of the salts. Reaction 2.6 was verified by heating alkaline earth oxides in CO_2 at different temperatures. McKee pointed out that the uncatalyzed graphite-steam reaction is five times faster than the graphite-carbon dioxide reaction. However with the addition of 0.5wt% $BaCO_3$, both catalyzed reactions occurred at the same rate and with the same overall activation energy over the whole temperature range. Since in both reactions the first step is as given in the reaction expressed by Equation 2.5, he concluded that this

endothermic solid state reaction step is the rate determining with the second step occurring rapidly.

McKee and Chatterji (42) proposed the oxidation-reduction mechanism for the reaction catalyzed by alkali metal carbonates.

$$M_2CO_3+2C=2M+3CO \quad (2.7)$$

$$2M+CO_2=M_2O+CO \quad (2.8)$$

$$M_2O+CO_2=M_2CO_3 \quad (2.9)$$

where M=Li, Na, K, Rb. However, very recently McKee (52) and McKee et al. (43) proposed a somewhat different sequence of steps for Li_2CO_3. According to Li_2CO_3 reacts with carbon to form Li_2O which further reacts with CO_2 to form Li_2CO_3. This was based on the grounds that lithium oxide is more stable than the other alkali metal oxides and the formation of lithium metal is unlikely under gasification conditions.

McKee and Chatterji (42) also pointed out that gasification rates accelerated at temperatures near the melting points of the salts. Hot-stage observations of graphite flakes with dispersed particles of carbonates on their exposed basal planes failed to show any catalytic channeling or particle mobility at temperatures up to 1000°C. Even above the melting points of the carbonates, the droplets remained motionless on the horizontal graphite crystal surface. A gradual vaporization of the salt was observed at 1000°C, and some sublimation of the alkali metal occurred during gasification.

The observation that the rates proceed slowly below the carbonate melting point and rapidly over it is consistent with the first step of the reaction sequence being the rate determining step since the molten carbonate is in better contact with the carbon surface.

Walker et al. (7) also supported an oxidation-reduction mechanism for the catalyzed gasification of graphite containing Fe, Ni or Co.

2.9.3 Electron-Transfer Mechanism

Long and Sykes (53) explained the catalysis of carbon gasification by an electron theory. The catalyst present in the carbon matrix accepts electrons from the carbon planes. This results in delocalization of electrons in the carbon plane which in turn affects the events at an active site. The desorption of the carbon-oxygen complex is facilitated by the change of the carbon-carbon bond order from double to single while the carbon-oxygen bond of the complex changes from single to double and adsorption is also facilitated. Their theory predicts a decrease in activation energy of both adsorption and desorption steps and does not alter the mechanism of the reaction. It limits the number of active sites only to that corresponding to edge carbon atoms. They proposed this mechanism for the transition metal oxides.

Walker et al. (7) discussed some of the modifications to

this theory to account for experimental results which could not be explained otherwise.

Wen (8) showed that alkali metals can exchange electrons with a carbon layer forming intercalation structures which can react with carbon dioxide.

Kapteijn et al. (54) reported that when K_2CO_3 - activated carbon and K_2CO_3 - coal were heated in a nitrogen flow at 827°C, intercalate structures form. These were detected by X-ray analysis. These authors pointed out that in the presence of CO_2, intercalates cannot be formed.

CHAPTER 3

EXPERIMENTAL

3.1 Apparatus

The flow diagram of the experimental set up is shown in Figure 1. It consists of a reactor, a thermogravimetric balance, a furnace, a temperature programmer and an equipment for metering feed gases.

The apparatus may be divided into three sections, that is the feed section, the reactor assembly, and the control section.

3.1.1 Feed Section

Nitrogen and Carbon Dioxide, obtained from high pressure cylinders, were the feed gases. Nitrogen was used to flush the reactor, and for the heating period, until the desired temperature was reached, at which time, N_2 flow was stopped and CO_2 was introduced.

Both gas lines had a flowmeter (tube and float series 601, Matheson CO.), a pressure gauge, and a needle valve. The needle valves were used to keep the feed gases at atmospheric pressure. These stainless steel, micrometer control valves are manufactured by Nupro Company, part number SS2SG with 0.08 cm orifice. They were supplied by Ottawa Valve and Fitting Company.

SCHEMATIC DIAGRAM OF THE APPARATUS

Symbol	Item
CO_2	Carbon Dioxide Supply
F	Furnace
LTP	Linear Temperature Programmer
NV	Needle Valve
N_2	Nitrogen Supply
PI	Pressure Gauge
QR	Quartz Reactor
R	Rotameter
S	Sample Bucket
TC	Thermocouple
TGB	Thermogravimetric Balance
V	Two-way Valves for Flow Control

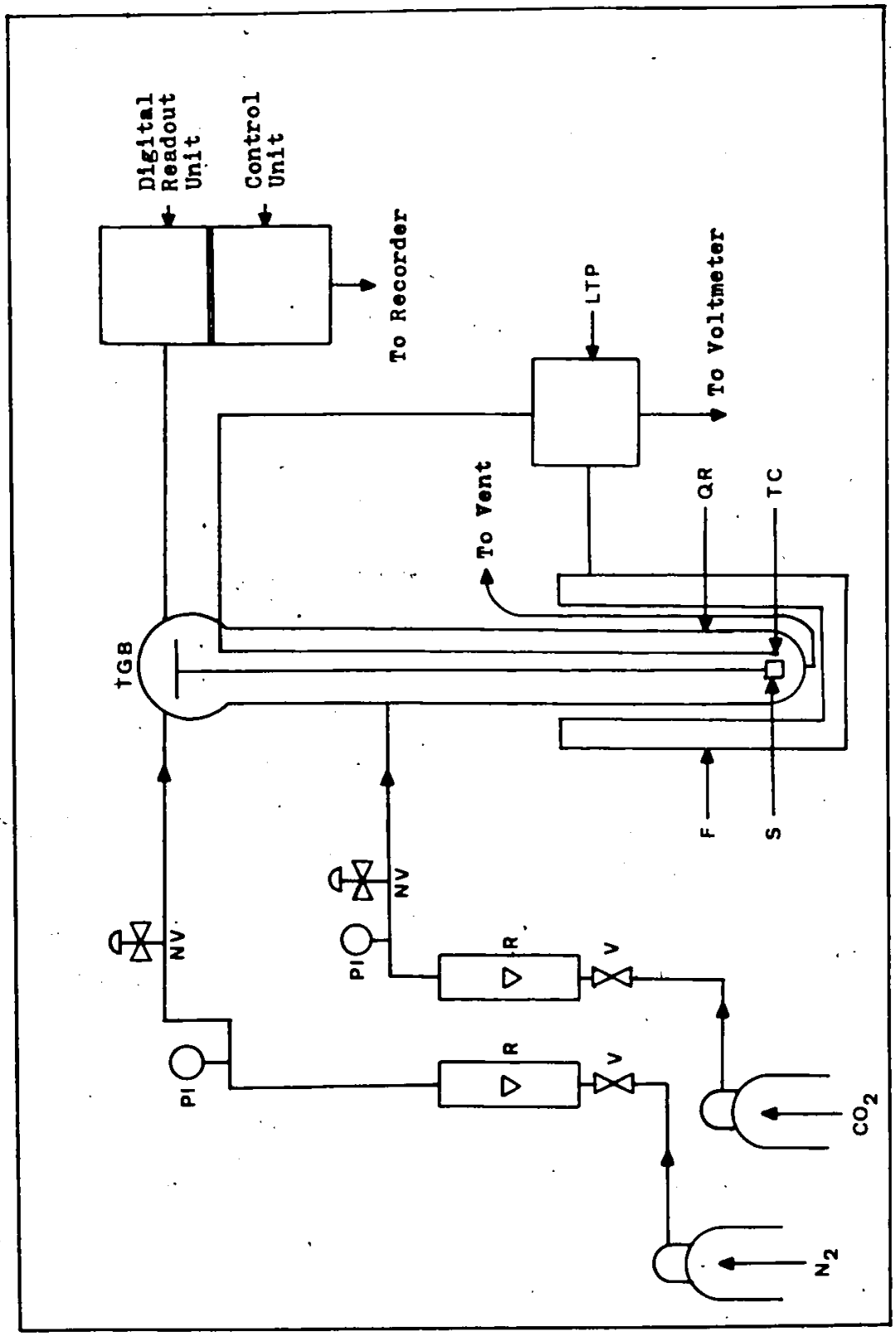

Figure 1. Schematic Diagram of the Apparatus

3.1.2 Reactor Assembly

The reactor assembly consisted of a thermogravimetric balance (TGB), hangwire and sample bucket, reactor and furnace.

The TGB (supplied by Mettler Instruments, Zurich, Switzerland) had features which provided direct weight loss data during gasification. A block diagram of the TGB is shown in Figure 2. The beam scanner (5) records the beam deflection which occurred during weighing. It controlled the control amplifier (6). The latter generated a current proportional to the weight in the moving coil of the compensation system (2) by the way of the range selector switch (7). The current generated a magnetic opposing force, which kept the beam at rest in the case of minimum deflection.

The control socket of the TGB was modified into a quartz reactor, 720 mm long 40 mm O.D. It had two side openings for the entry of N_2 and CO_2, and the exit for the product gases. The top of the reactor was clamped to the TGB.

The char sample was placed in the bucket which was made of pure platinum woven wire gauze with openings of 80 mesh (supplied by Johnson Matthay and Mallory Limited). The hangwire suspending the sample bucket was made of quartz with 600 mm length and a diameter of 0.5 mm.

A Lindberg type furnace was used to heat the reactor.

BLOCK DIAGRAM OF TGB

1	Weighing system
2	Magnetic compensation system
3	Pan brake
4	Power supply
5	Inductive beam scanning
6	Control amplifier
6a	Control for pan brake
7	Range selector
8	Measuring amplifier
9	Taxing and zero point
10	Analog output signal

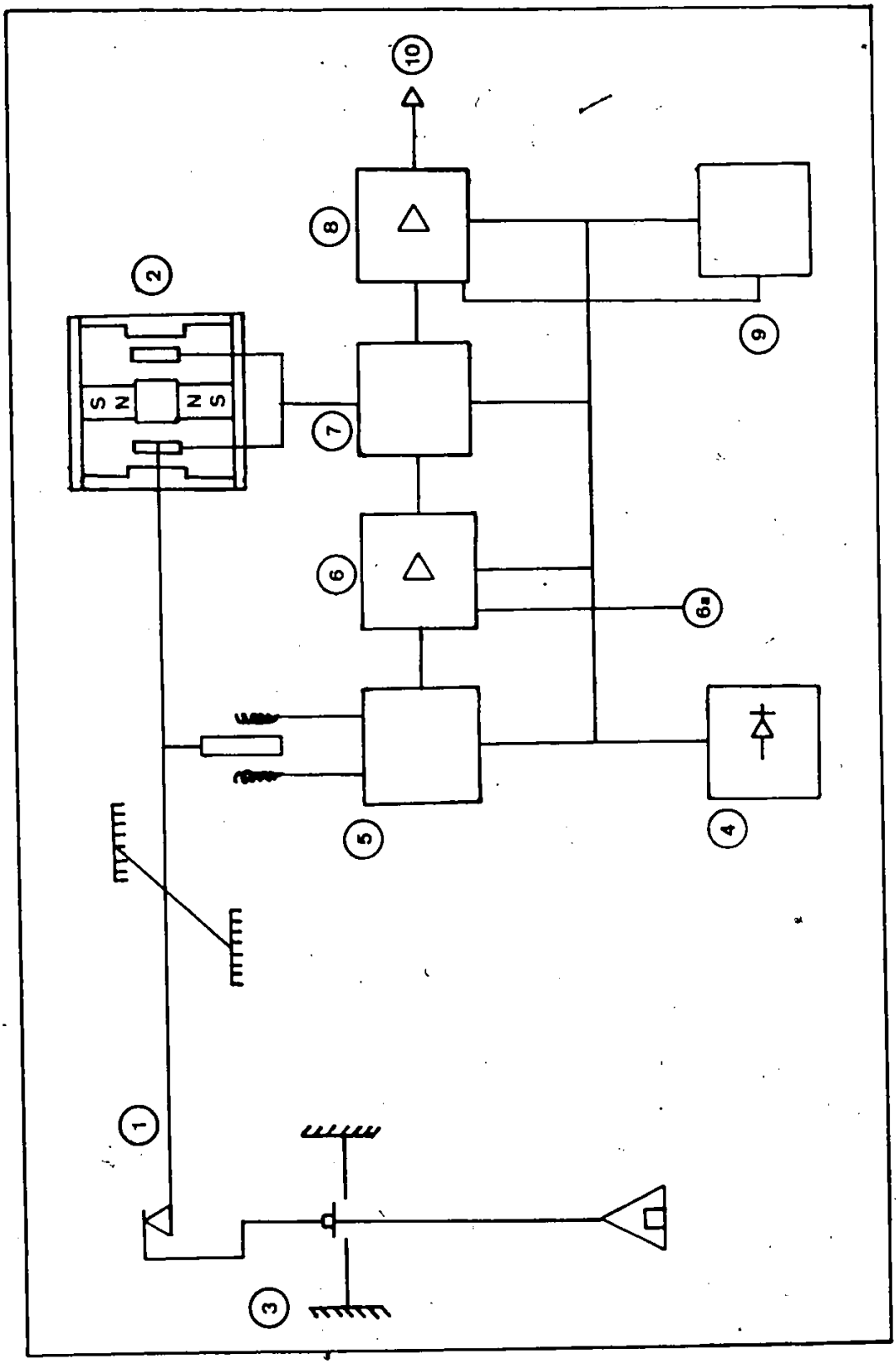

Figure 2. Block Diagram of TGB

It had two vertically split half circle heating units (2K.W.). A paste of asbestos powder mixed with water was applied to the outside of the heating elements for insulation. The asbestos was slowly dried to prevent cracking. The wires of the furnace were connected to the power and control section of the set-up.

3.1.3 Control Section

The TGB had a control unit. This was used for calibration and taring purposes. A strip chart recorder (Series B-5000, Houston Instrument, Austin, Texas) was connected to the 10 volts analog output of the control unit. The output signal in millivolts was transferred to the recorder.

A digital readout unit (Mettler ME 22) was placed on top of and connected to the control unit. The recorder and the digital readout unit gave the sample weight at any particular time.

A temperature programmer/controller (Model PC-6011, Valley Forge Instrument Company, Phoenixville, Pa.) was used. The programmer could be operated isothermally or used to maintain a change of temperature at a certain heating rate. The rate could be varied from 5-50°C/min. It had a controlled service outlet to provide power to the furnace, and required only one connection to the power line to operate the entire system. A dial indicated the temperature set point, program process,

and maximum temperature limit.

A chromel vs. alumel type K thermocouple (supplied by Thermoelectric Canada Ltd., Brampton, Ontario) was inserted into the quartz reactor, close but not touching the suspended sample bucket. The leads of the thermocouple were connected to the programmer.

A Hewlett-Packard 3435A Digital Multimeter was connected to the temperature programmer, and it gave the output signal (in millivolts) of the thermocouple at any time.

3.2 Calibration of Equipment

3.2.1 Calibration of the TGB

The thermogravimetric balance was calibrated before any experimental run. The power switch was turned on for the recorder, the control and the digital readout units of the TGB. A warming up period of about 20 minutes was allowed. With the hangwire, sample bucket and the reactor in place, a zero reading for the TGB was obtained by using the taring knob on the control unit. At the same time, the recorder was adjusted to give a zero reading. Then a 10 mg calibrating ring was hung from the TGB. The readout unit should display a 10mg reading, and the recorder 10mv. After removing the ring, zero readings should be obtained. If not the calibration steps are repeated.

3.2.2 Calibration of the Thermocouple

The thermocouple was calibrated using a mercury thermometer, and a standard chromel vs. alumel type K thermocouple attached to a temperature sensor. The sensor had a range of -60° to 2000°F (model 8520-40, Cole-Parmer Instrument Company). The two thermocouples and the thermometer were tied together with their tips joined, and were inserted into the temperature controlled furnace. The programmer was switched on, and a heating rate of 15°C/min was selected. The dial was set at 100°C and the heating started when the programmer was set at the rise to hold mode. After the temperature reached the set point, sufficient time was allowed for the temperature to stabilize. Then the voltmeter, temperature sensor, and thermometer readings were recorded. The same procedure was repeated with increasing 100°C temperature intervals, up to 900°C. Readings with the mercury thermometer were obtained only for the lower temperatures.

In Figure 3, a plot of the temperature versus the E.M.F. of the voltmeter is shown.

3.3 Experimental Procedure

Each run was carried out as follows:

With a bubble-meter connected to the outlet of the reactor, nitrogen was introduced. The flow was set at 100 ml/min, and the needle valve adjusted (if necessary) to obtain atmospheric

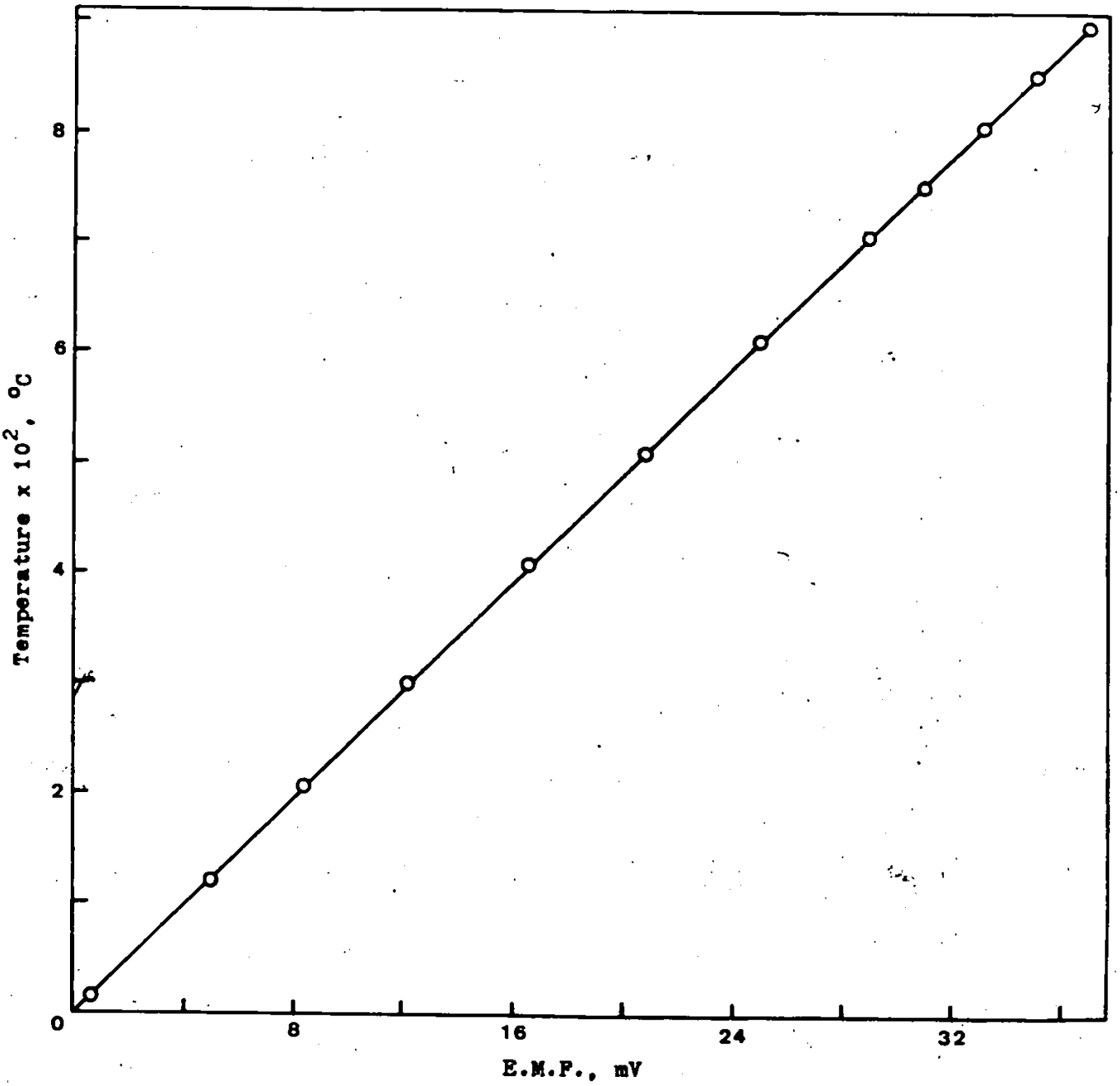

Figure 3. Calibration Curve for the Thermocouple

pressure in the system. The same procedure was repeated for carbon dioxide, but with a flow rate of 150 ml/min.

The TGB was tared and calibrated simultaneously with the analog recorder.

A char sample of 80.0±1.0mg was placed in the bucket which was then suspended by the hangwire in the reactor.

Nitrogen was allowed to flow through the reactor assembly in order to remove air. At the same time, the programmer was set at the isothermal mode at 20°C. A period of 30 minutes or more was allowed for thermal equilibrium, and purging of the assembly. The system was also checked for leaks.

With nitrogen flowing, the programmer was set at a heating rate of 15°C/min, with an upper temperature limit, and the heating started. During this period some weight loss took place due to devolatization and drying.

When the heating limit was reached, sufficient time was allowed until the temperature stabilized, and no weight loss was observed. Very quickly, the nitrogen flow was discontinued, carbon dioxide was introduced, and simultaneously the recorder's chart speed motor was turned on. The weight loss data of the sample were obtained from the strip chart of the recorder. They were periodically checked with the direct weight loss readings from the TGB. The flowmeter was also periodically checked for a constant flow rate of CO_2 The voltmeter reading (thus the temperature) was recorded.

After a certain time, or until completion of the reaction, the recorder and the programmer were turned off, the CO_2 flow was discontinued, N_2 was introduced, and the system was let to cool down.

When at room temperature, the hangwire and the bucket were removed from the reactor. The residue in the bucket was placed in a vial and stored in a desiccator for further analysis.

For some of the runs, the product gases were analyzed using a gas chromatograph (HP5750). A sampling system was connected to the exit of the reactor. Gas samples were taken on regular intervals injected into the gas chromatograph. This analysis was only qualitative.

3.4 Char Samples and Chemicals

The two chars, Saskatchewan lignite and Forestburg sub-bituminous, were obtained from Energy, Mines and Resources, Research Lab, Ottawa. The chars were produced from the respective coals by heating them in a stream of He at 927°C. The chemical composition of the chars is given in Table 3.1.

For the lignite char, the physical characteristics given in Table 3.2 and Figure 4 were provided by Micrometrics, Norcross, Ga., U.S.A.

The catalysts were supplied by the Fischer-Scientific Co., New Jersey, U.S.A.

Nitrogen and Carbon Dioxide were supplied by Liquid

TABLE 3.1

CHEMICAL ANALYSIS OF CHARS

	Lignite Char	Sub-bituminous char
Proximate Analysis, wt%		
Moisture	0.3	on dry basis
Volatile matter	0.4	9.4
Ash	17.9	11.5
Fixed carbon	77.4	79.1
Ultimate Analysis, wt%		
Ash	18.1	11.5
Carbon	78.8	81.9
Hydrogen	0.9	1.7
Sulfur	0.3	0.6
Nitrogen	0.9	1.5
Oxygen	1.0	2.8

TABLE 3.2

PHYSICAL CHARACTERISTICS OF LIGNITE CHAR

Cumulative pore volume	=	0.044 cm^3/g
Apparent density	=	1.5284 g/cm^3
Calorific value	=	11,858 BTU/lb.
B.E.T. surface area (N_2)	=	216 m^2/g

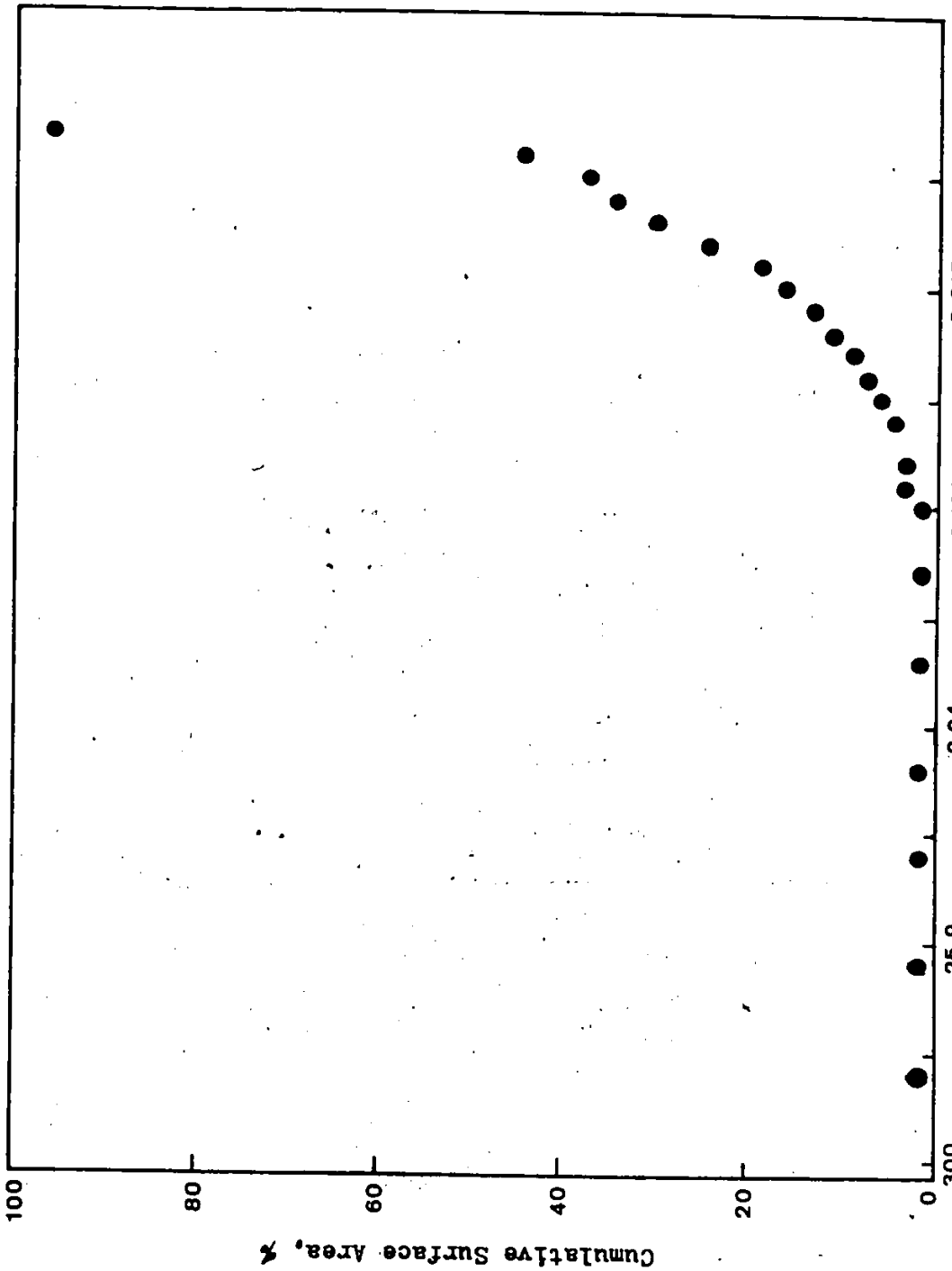

Figure 4. Surface Area Distribution Within Pores of Lignite Char

Carbonic, Ottawa, Canada.

3.5 Addition of Catalyst

Catalyzed char samples were prepared by the wet impregnation method. The chars were mixed with required amounts of solutions of $Ni(NO_3)_2$ and K_2CO_3. Then, the water was evaporated over a water bath with continuous stirring of the mixture. Finally, the mixture was oven dried at 110°C for two hours to remove the moisture. Char containing Ni was later reduced at 450°C in an atmosphere of hydrogen.

3.6 Carbon Analysis

The char residues from the reaction were analyzed for their carbon content. An Elemental Analyzer (series 99109, Perkin-Elmer, Norwalk, Connecticut, U.S.A.), a recorder (model 56, Perkin-Elmer, Waywood, Illinois, U.S.A.) and an Autobalance (series AD2Z, Perkin-Elmer, Waywood, Illinois, U.S.A.) were used.

A sample in a platinum boat was accurately weighed (1 to 3 mg) using the Autobalance. The boat was placed in the magnetically operated ladle which was inserted through the sample entrance fitting of the analyzer. The sample was pushed into the combustion chamber. The combustion products were automatically analyzed. The results were recorded in

a bar graph form on the recorder.

3.7 Pore Volume

The pore volume of the char samples was determined by carbon tetrachloride adsorption.

Char samples (1 to 2 grams) contained in small weighing bottles were first dried at 130°C for three hours. The samples were then weighed and transferred to a vacuum desiccator containing 210 cm^3 of carbon tetrachloride-cetane mixture (4.7 mole% of cetane). The desiccator, attached to a graduated cold trap, and a vacuum pump, was evacuated until about 10 cm^3 of carbon tetrachloride was vaporized and collected in the cold trap. By then all air was flushed out. The desiccator contents were then allowed to equilibrate from 10 to 20 hours at room temperature.

After the equilibration period, air was slowly admitted to the desiccator, and the cover was removed. Stoppers were put on the bottles as rapidly as possible and weighed. The pore volume was obtained from the gain in weight and the density of carbon tetrachloride.

Cetane was used to lower the vapour pressure of carbon tetrachloride to 95% of its saturation pressure.

The results are shown in Table 3.3.

TABLE 3.3

PORE VOLUME OF CHARS (cm^3/g)

Run No.	Lignite Char			Sub-bituminous char	
	None	5% Ni	10% K_2CO_3	None	10% K_2CO_3
1	0.033	0.048	0.014	0.012	0.0067
2	0.039	0.051	0.0072	0.012	0.0066
3	0.035	0.045	0.0093	0.009	0.0076
Average	0.035	0.048	0.0102	0.011	0.0070

The density of the sub-bituminous char was measured with a pycnometer. The apparent density was found to be 1.435 g/cm^3.

CHAPTER 4

KINETIC ANALYSIS

Based on many studies, the unreacted-core model is the best simple representation for the majority of gas-solid reactions. However, when the solid is very porous the reaction can be considered to take place throughout the solid, and a volume reaction model is a better representation.

The pore volumes and pore size distribution (lignite char) indicate that both chars are essentially non-porous. In that case, the char particles can be considered to be impervious to the reactant gas, and the reaction will take place at the surface of the shrinking char particles.

At first, the reaction takes place at the outside surface of the particle, but as the reaction proceeds, the surface of the reaction will move into the interior of the solid, forming an unreacted core which shrinks with time, and leaving behind inert ashes. A schematic diagram for the unreacted-core model is shown in Figure 5.

The char-carbon dioxide reaction may be represented by

$$A(\text{fluid}) + b(\text{solid}) \longrightarrow \text{fluid and solid products}$$

where b is the stoichiometric coefficient and it is equal to 1. In the unreacted-core model, it can be visualized that five steps occur in succession during reaction.

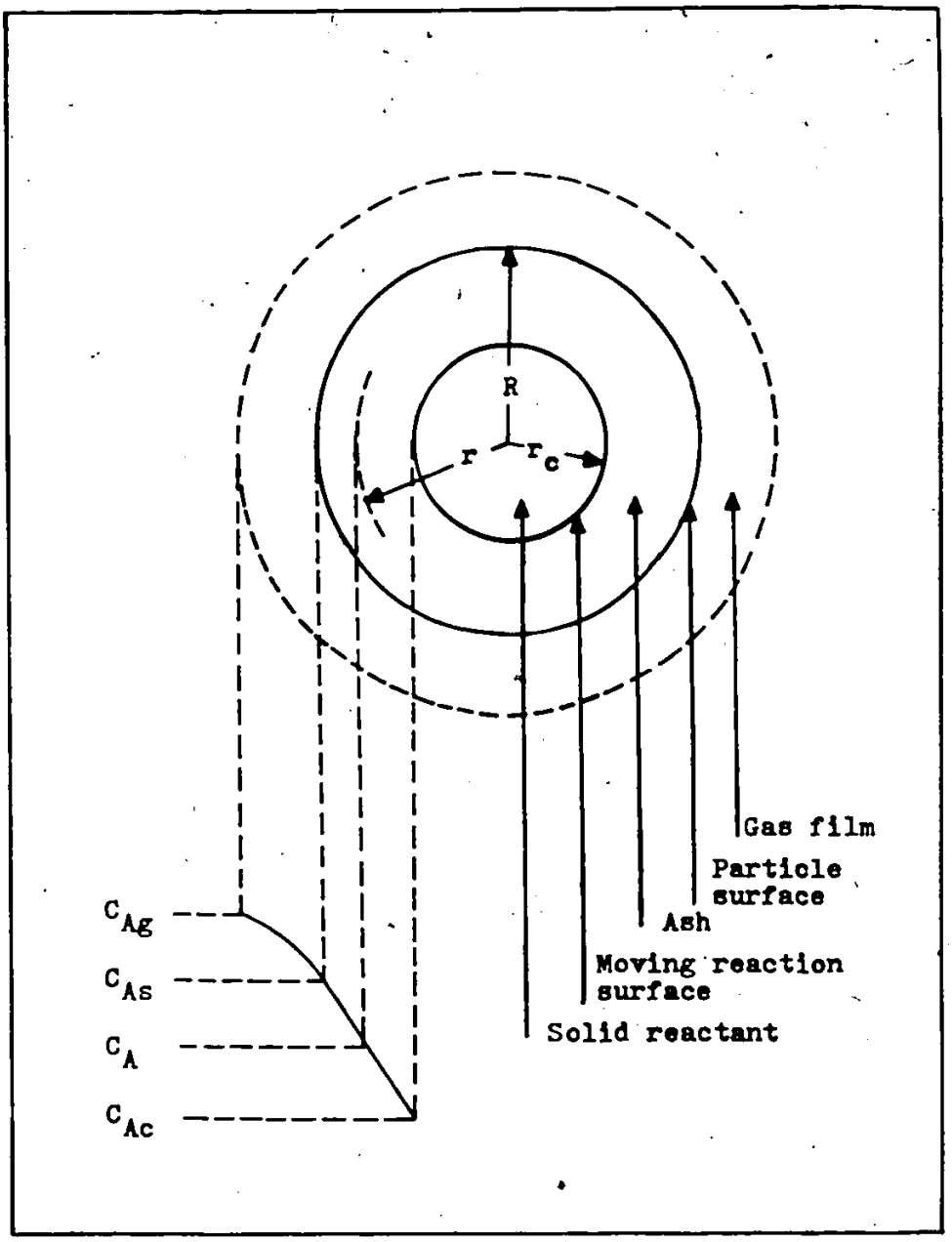

Figure 5. Schematic Diagram of Concentracion Profile for the Unreacted-Core Model

Step 1. Diffusion of gaseous reactant A through the film surrounding the particle to the surface of the solid.

Step 2. Penetration and diffusion of A through the blanket of ash to the surface of the unreacted core.

Step 3. Reaction of gaseous A with solid at this reaction surface.

Step 4. Diffusion of gaseous products through the ash back to the exterior surface of the solid.

Step 5. Diffusion of gaseous products through the gas film back into the main body of fluid.

The reaction is assumed to be irreversible, that is steps 4 and 5 do not contribute to the resistance to reaction. The mathematical analysis of the unreacted-core model as described by Levenspiel (55) and Wen (32), is reproduced here.

The following assumptions are made

1. The particles are spherical
2. The external radius of the particles remains the same, that is the ash layer is non-deformable.
3. The overall reaction is first order.
4. Each particle reacts independently without being affected by neighbouring particles, that is conversion is the same for all particles at all times.

b) Diffusion Through Gas Film Controls

From Figure 5 we see that whenever the resistance of the gas film controls, C_{As} is equal to C_{Ac} and the concentration

force is given by $(C_{Ag}-C_{As})$. Based on the external surface area of the particle, the rate expression is given by

$$-\frac{1}{S_{ex}}\frac{dN_B}{dt} = -\frac{1}{4\pi R_p^2}\frac{dN_B}{dt} = -\frac{1}{4\pi R_p^2}\frac{dN_A}{dt} = k_g(C_{Ag}-C_{AS})$$

$$= k_g C_{Ag} = \text{constant} \qquad (4.1)$$

The decrease in volume or radius of unreacted core accompanying the disappearance of dN_B moles of solid reactant or bdN_A moles of fluid reactant is given by

$$-dN_B = -\rho_B dV = -dN_A = -\rho_B d(\tfrac{4}{3} r_c^3) = -4\pi\rho_B r_c^2 dr_c \qquad (4.2)$$

where ρ_B is the molar density of B in the solid, and V is the volume of the particle. Combining the above equations, the rate of reaction in terms of the shrinking radius of unreacted core is obtained as

$$-\frac{1}{S_{ex}}\frac{dN_B}{dt} = \frac{\rho_B r_c^2}{R_p^2}\frac{dr_c}{dt} = k_g C_{Ag} \qquad (4.3)$$

Rearranging and integrating Equation 4.3

$$t = \frac{\rho_B R_p}{3k_g C_{Ag}}\left[1-\left(\frac{r_c}{R_p}\right)^3\right] \qquad (4.4)$$

where k_g is the mass transfer coefficient between fluid and particle. The radius of unreacted core can be written in terms of fractional conversion of B

$$1-X = \frac{\text{volume of unreacted core}}{\text{total volume of particle}} = \left(\frac{r_c}{R_p}\right)^3 \qquad (4.5)$$

Combining Equations 4.4 and 4.5

$$t = \frac{\rho_B R_p X}{3 k_g C_{Ag}} \qquad (4.6)$$

Thus a relationship between time, radius of particle and conversion B in solid is obtained.

ii) Diffusion through Ash Layer Controls

For a partially reacted particle, both reactant A and the boundary of the unreacted core move inward toward the centre of the particle. But the shrinkage of the unreacted core is slower than the flow rate of A towards the unreacted core by a factor of about 1000, which is roughly the ratio of densities of solid to gas. Therefore, it can be assumed that the unreacted core is stationary while considering the concentration gradient of A in the ash layer at any time. Thus the rate of reaction of A at any instant is given by its rate of diffusion to the reaction surface, or

$$-\frac{dN_A}{dt} = 4\pi r^2 Q_A = 4\pi R_p^2 Q_{As} = 4\pi r_c^2 Q_{Ac} = \text{constant} \qquad (4.7)$$

According to Fick's law and for equimolar counterdiffusion, the flux of A is given by

$$Q_A = De \frac{dC_A}{dr} \qquad (4.8)$$

where De is the effective diffusion coefficient of gaseous reactant in the ash layer. Combining Equations 4.7 and 4.8, for any r,

$$-\frac{dN_A}{dt} = 4\pi r^2 \, De \, \frac{dC_A}{dr} = \text{constant} \qquad (4.9)$$

Integrating across the ash layer from R_p to r_c, and C_{Ag} to C_{Ac}, Equation 4.9 becomes

$$-\frac{dN_A}{dt}\left[\frac{1}{r_c} - \frac{1}{R_p}\right] = 4\pi DeC_{Ag} \qquad (4.10)$$

Equation 4.10 could be further treated following the same procedure as for the film diffusion (Levenspiel, 55). The final result will be:

$$t = \frac{\rho_B R_p^2}{6DeC_{Ag}}\left[1 - 3\left(\frac{r_c}{R_p}\right)^2 + 2\left(\frac{r_c}{R_p}\right)^3\right] \qquad (4.11)$$

In terms of fractional conversion of B, Equation 4.11 becomes

$$t = \frac{\rho_B R_p^2}{6\ DeC_{Ag}}\left[1-3(1-X)^{2/3}+2(1-X)\right] \qquad (4.12)$$

Wen (32) has shown that by defining De based on the surface area of the unreacted core, Equation 4.12 becomes

$$t = \frac{\rho_B R_p^2}{6\ DeC_{Ag}}\left[1-(1-X)^{1/3}\right]^2 \qquad (4.13)$$

iii) Chemical Reaction Controls

The progress of the reaction is unaffected by the presence of ash, thus the quantity of material reacting

is proportional to the available surface of unreacted core. Based on unit surface of unreacted core, the rate of reaction is given by:

$$-\frac{1}{4\pi r_c^2}\frac{dN_B}{dt} = -\frac{1}{4\pi r_c^2}\frac{dN_A}{dt} = k_s C_{Ag} \qquad (4.14)$$

where ks is the first-order rate constant. Substituting for N_B from Equation 4.2, Equation 4.14 becomes

$$-\rho_B \frac{dr_c}{dt} = k_s C_{Ag} \qquad (4.15)$$

Integrating equation 4.15 from R_p to r_c

$$t = \frac{\rho_B}{k_s C_{Ag}} (R_p - r_c) \qquad (4.16)$$

In terms of fractional conversion of B, Equation 4.16 becomes

$$t = \frac{\rho_B R_p}{k_s C_{Ag}} \left[1-(1-X)^{1/3}\right] \qquad (4.17)$$

The three resistances to the reaction rate can also be combined in one equation.

CHAPTER 5

EXPERIMENTAL RESULTS

By the time the reactor was brought to the desired temperature, moisture and all other volatile matter were driven off. All that remained was essentially carbon, ash and catalyst. The gasification of the chars is expressed as fractional conversion based on the amount of carbon present at the start of the reaction.

$$X = \frac{W_i - W}{W_C}$$

where W_i and W are weights of char initially and at time t respectively, and W_C is the weight of carbon at the start of the reaction.

Experiments conducted can be divided into two groups. Uncatalyzed gasification of chars, and catalyzed gasification of chars. The experimental and calculated data are given in Appendix C. A summary of experimental runs is given in Table 5.1.

TABLE 5.1

SUMMARY OF EXPERIMENTAL RUNS

Run No	Description	Parameter studied
1-9, 14-21	uncatalyzed	CO_2 flow rate, particle size
10-13, 22-25, 50-55	uncatalyzed	temperature, CO_2 partial pressure
26-35	catalyzed (Ni)	temperature, catalyst concentration
36-49	catalyzed (K_2CO_3 or K_2CO_3+Ni)	temperature, catalyst concentration
56-65		Replicates

5.1 Uncatalyzed Gasification

The chars were gasified in a stream of CO_2 at atmospheric pressure, and a temperature range of 728-875°C. The weight of the char sample used in each run was 80 mg. The parameters studied were the particle size, carbon dioxide flow rate, and temperature.

The carbon dioxide flow rate in all experiments was 150 ml/min except when the effect of the flow rate was studied. Char particle size of 0.354-0.420 mm was used when the CO_2 flow rate effect was studied, and particle size of 0.500-0.595 mm when the temperature effect was studied. All levels of conversion were obtained in the temperature range of investigation. As expected conversion increased with temperature.

To test the first order dependency of the reaction, experiments were carried out by introducing CO_2-N_2 mixtures at a total inlet flow rate of 150 ml /min and atmospheric pressure.

5.1.1 Effect of CO_2 Flow Rate

Char samples of particle size 0.354-0.420 mm were gasified at 821°C (sub-bituminous) or 823°C (lignite char) at different CO_2 flow rates. The plots of carbon conversion vs. time are shown in Figure 6 for the sub-bituminous char and Figure 7 for the lignite char. In the case of sub-bituminous char conversion remained unchanged for flow rates of CO_2 higher than 80 ml /min. However, for the lignite char it was about 110 ml/min. It could be inferred that at high CO_2 flow rates, diffusion through the gas film surrounding the char particle had insignificant effect on the rate of carbon gasification. For subsequent experiments the flow rate of CO_2 used was 150 ml/min.

5.1.2 Effect of Particle Size

Four particle sizes of char were gasified at 823°C. The plots of conversion vs. reaction time are shown in Figure 8 for the sub-bituminous char and Figure 9 for the lignite char. It can be seen from these plots that conversion remains essentially the same when the particle size is changed. A particle

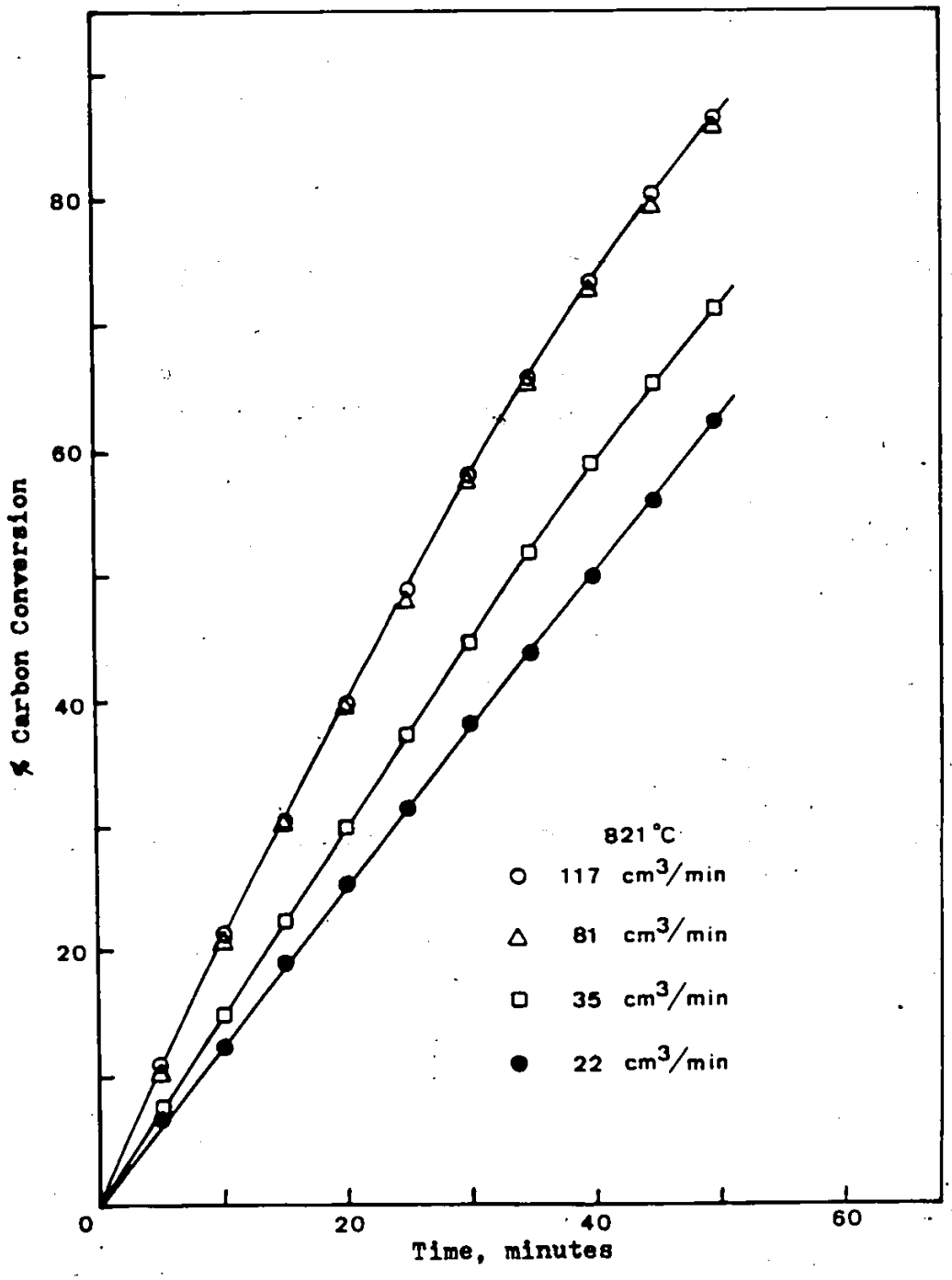

Figure 6. Effect of CO_2 Flow Rate on Carbon Conversion. Sub-bituminous Char.

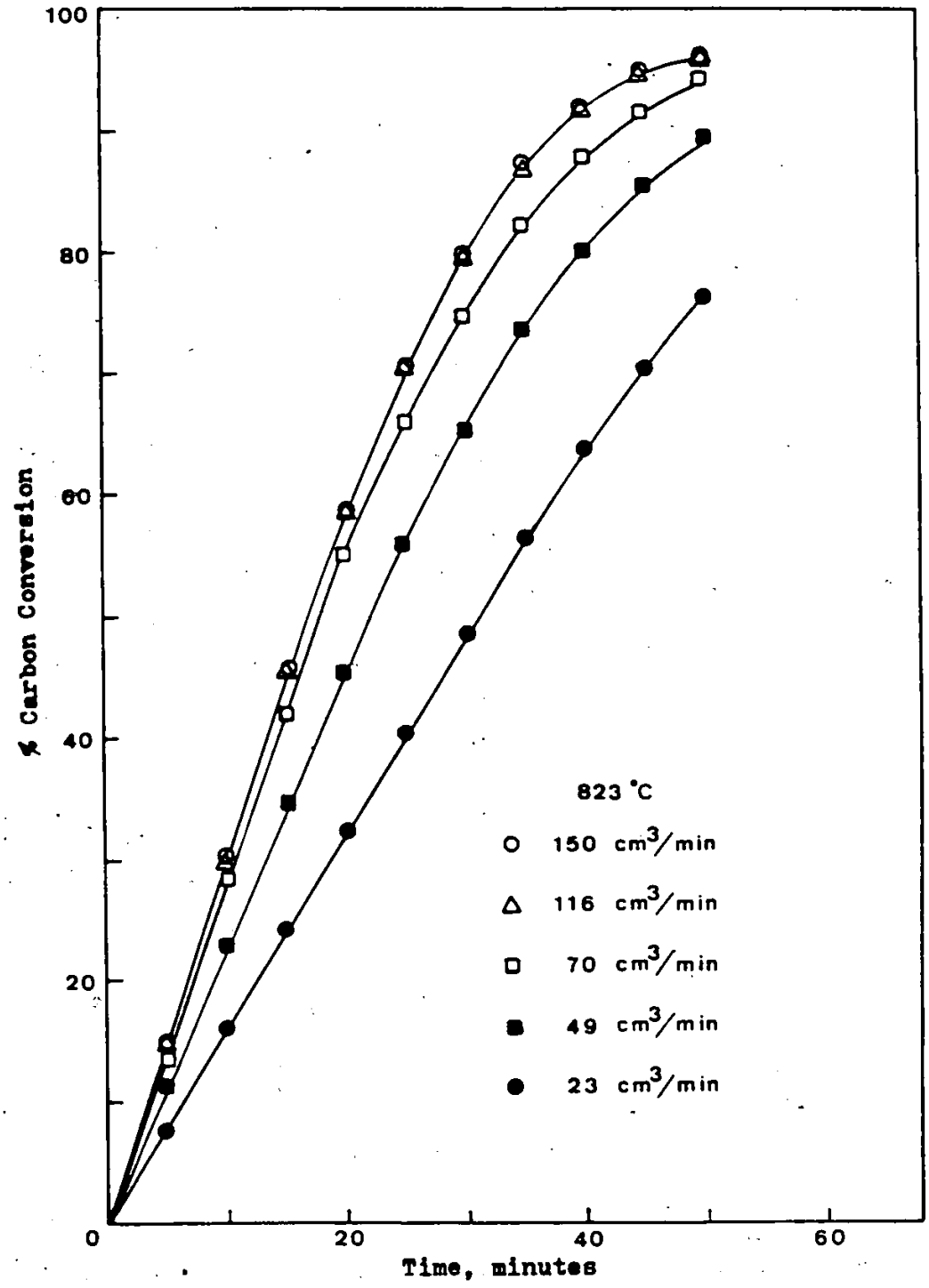

Figure 7. Effect of CO_2 Flow Rate on Carbon Conversion. Lignite Char.

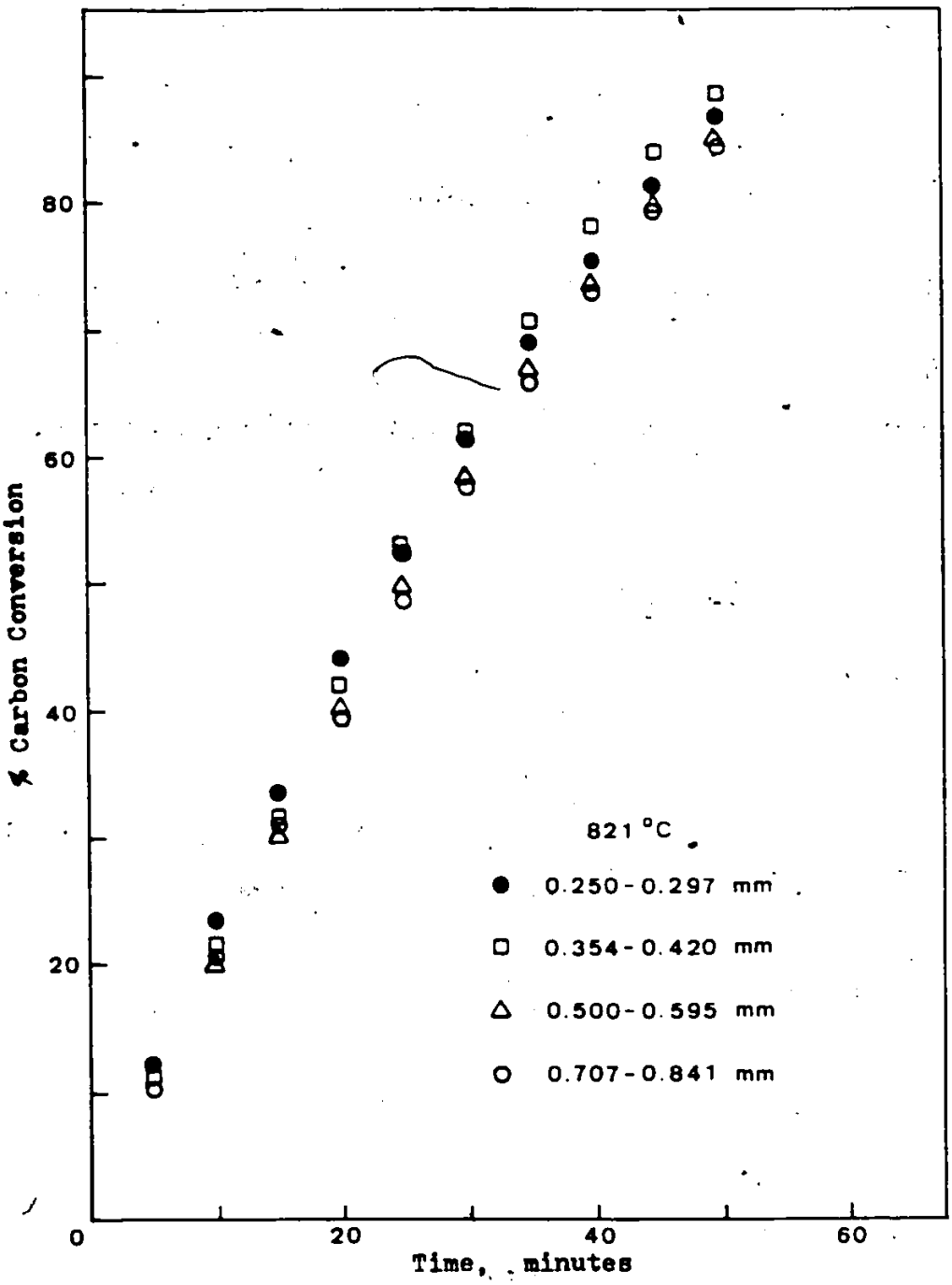

Figure 8. Effect of Particle size on Carbon Conversion. Sub-bituminous Char.

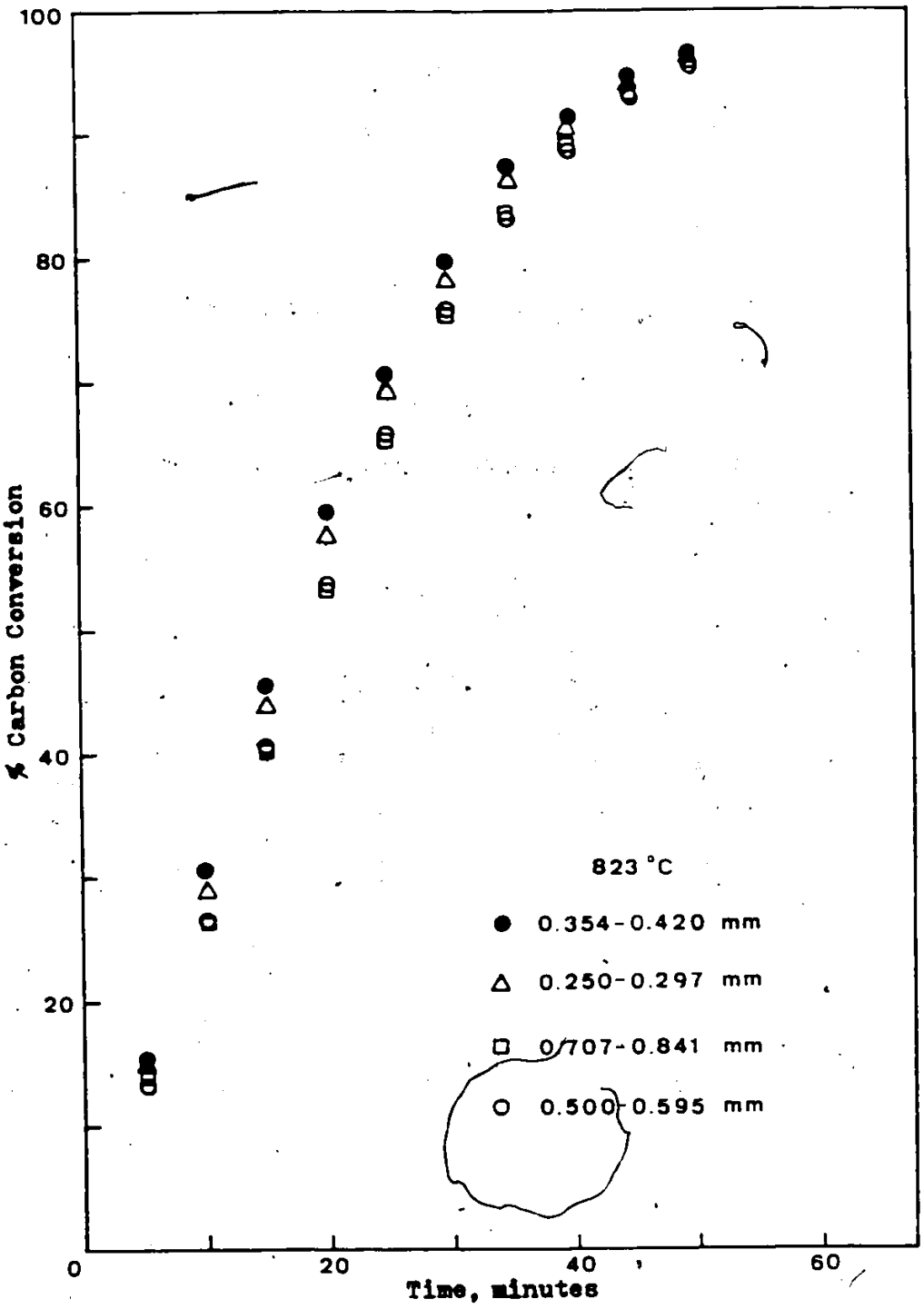

Figure 9. Effect of Particle Size on Carbon Conversion. Lignite Char.

size of 0.500 - 0.595 mm was selected for subsequent runs.

5.1.3. Effect of Temperature

The conversion of Saskatchewan lignite and Forestburg chars with respect to time at various temperatures is given in Figures 10 and 11. Reaction temperature was varied to evaluate the kinetics of reaction. The experiments were carried out with CO_2 flow rate of 150 ml/min and particle size of 0.500-0.595 mm. It can be seen from these figures that at the same temperature and for the same period of time the conversion was higher for the lignite char as compared to sub-bituminous char. Hence, lignite char is more reactive.

5.1.4 Kinetics of Gasification

Based on the observation that the chars were essentially non-porous, it was attempted to use the unreacted-core model for the kinetics of gasification.

The mathematical expressions involved in the unreacted-core model have been derived in chapter 4. It was assumed that the overall reaction is first order. To test the first order dependency, experiments were carried out by introducing CO_2-N_2 mixtures at atmospheric pressure. The total flow rate of the two gases was kept at 150 ml/min. The plots of conversion vs. time are shown in Figure 12 for the sub-bituminous

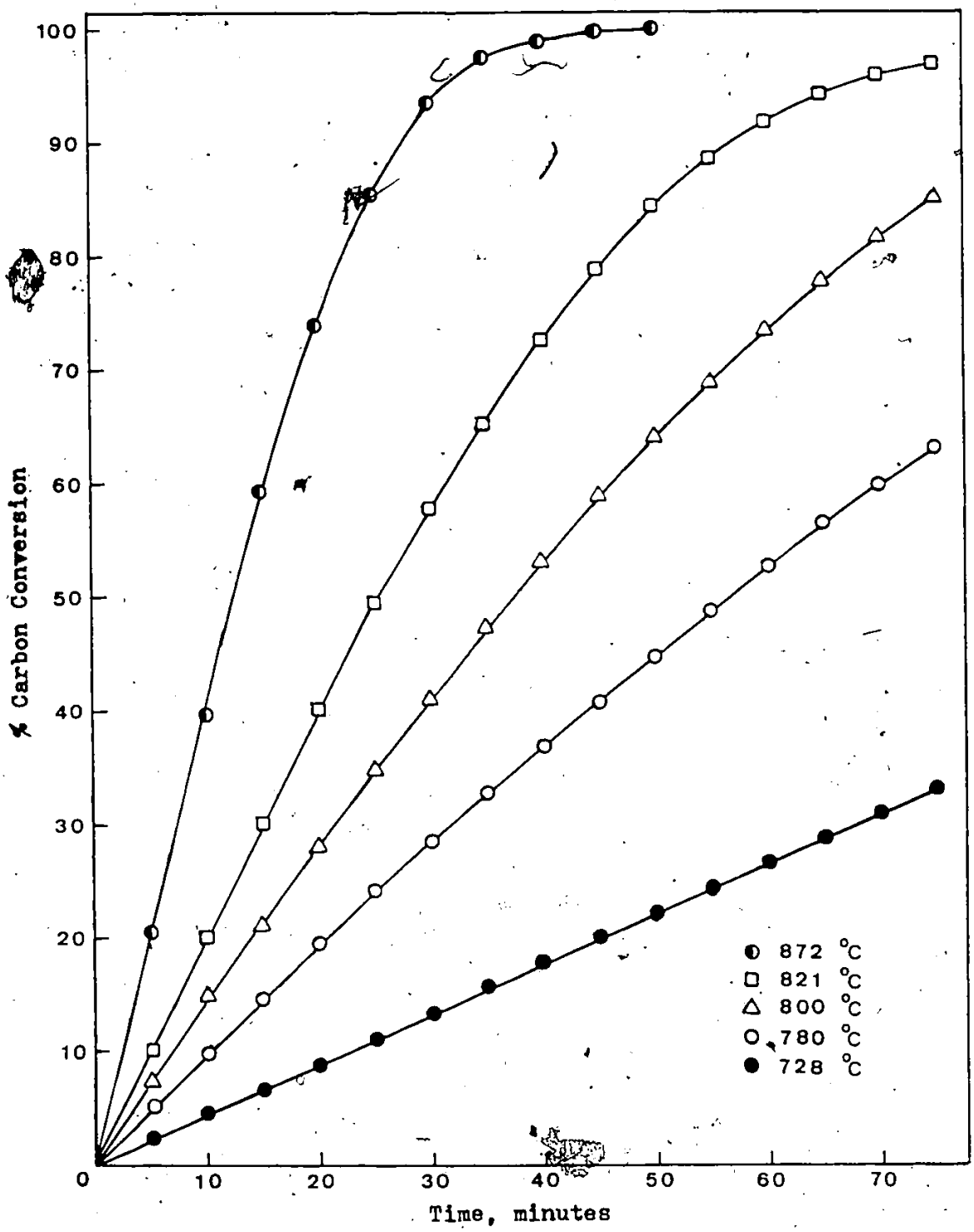

Figure 10. Carbon Conversion vs. Reaction Time. Sub-bituminous Char.

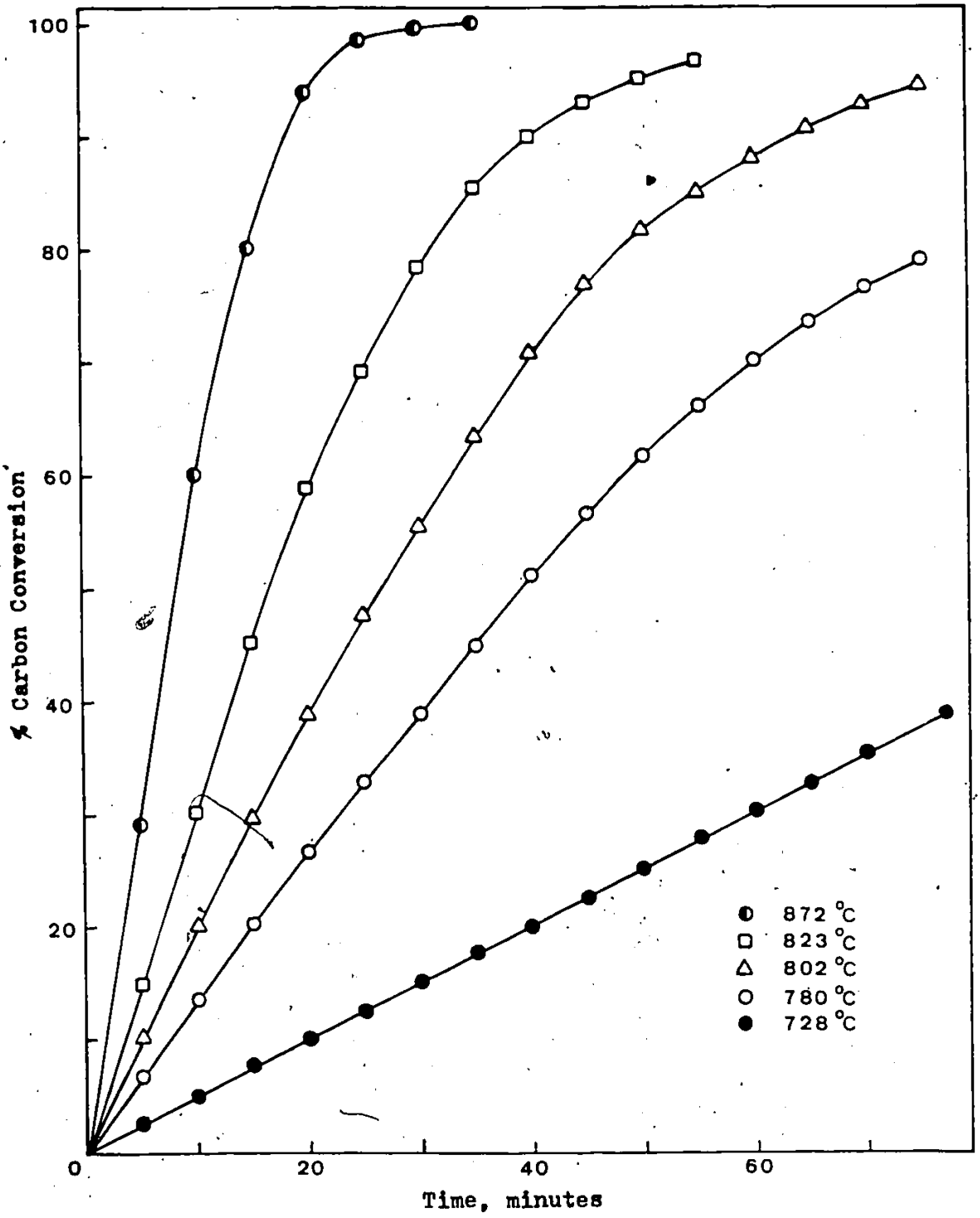

Figure 11. Carbon Conversion vs. Reaction Time. Lignite Char.

char and in Figure 13 for the lignite char. The initial rates $\left(\frac{dx}{dt}\right)_{x=0}$ were then plotted as a function of concentration of CO_2 (Figure 14).

For both of the chars the slopes of the curves were equal to one, indicating that the reaction is first order.

The equations derived in chapter 4 for the unreacted-core model are reproduced here. That is

$$t = \frac{\rho_B R_p X}{3k_g C_{Ag}} \qquad (5.1)$$

when film diffusion is controlling.

$$t = \frac{\rho_B R_p^2}{6DeC_{Ag}} \left[1-(1-X)^{1/3}\right]^2 \qquad (5.2)$$

when ash diffusion is controlling

$$t = \frac{\rho_B R_p}{k_s C_{Ag}} \left[1-(1-X)^{1/3}\right] \qquad (5.3)$$

when chemical reaction is controlling.

The results of the experiments with varying carbon dioxide flow rate and theoretical calculations (Appendix B) showed that the reaction was not film diffusion controlled. To test whether ash diffusion or chemical reaction controlled, plots of $\left[1-(1-x)^{1/3}\right]$ vs. time were made on a log-log graph and for the runs in Figures 10 and 11. These plots are shown in

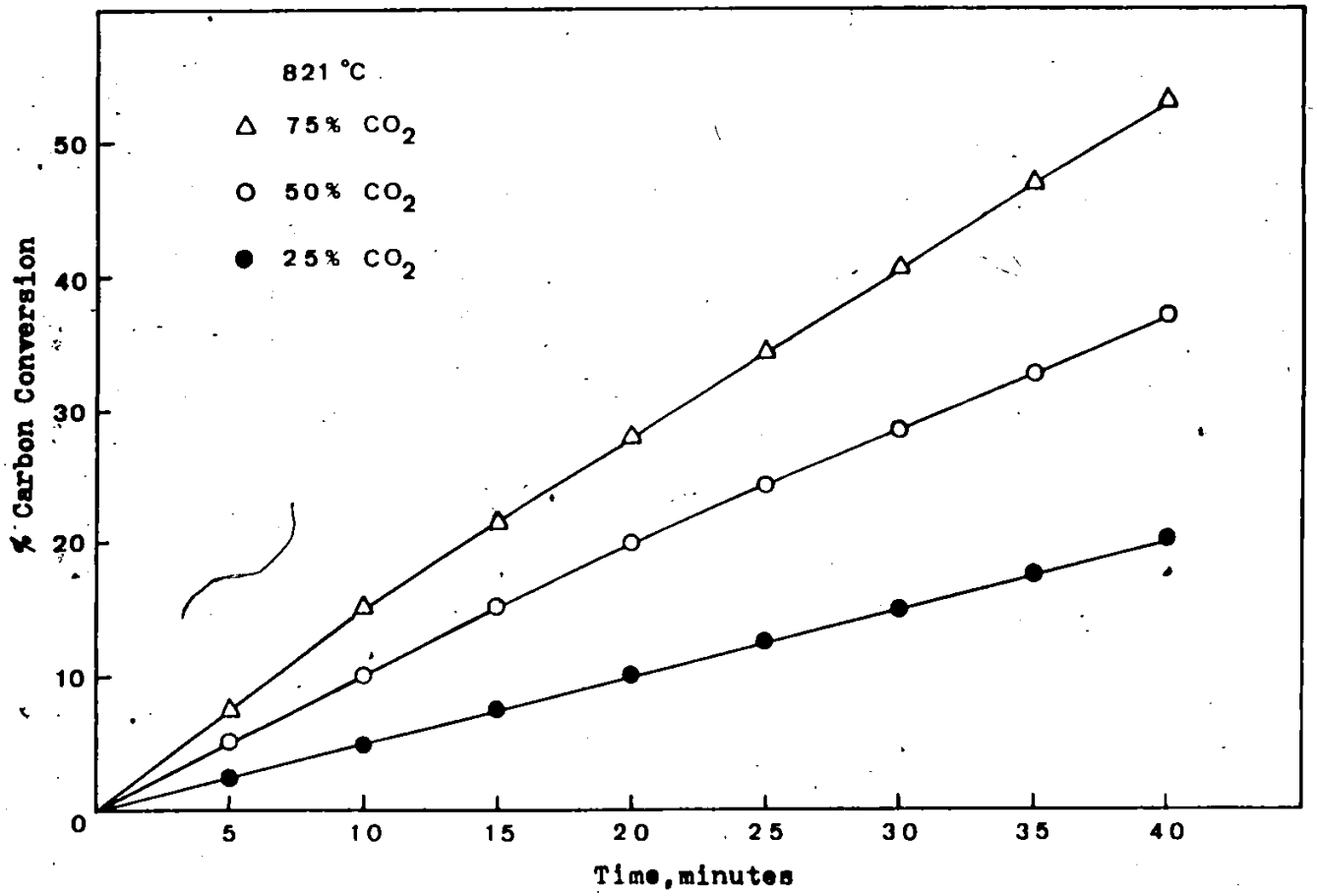

Figure 12. Carbon Conversion vs. Time for Different Composisions of CO_2-N_2 Mixtures. Sub-bituminous Char.

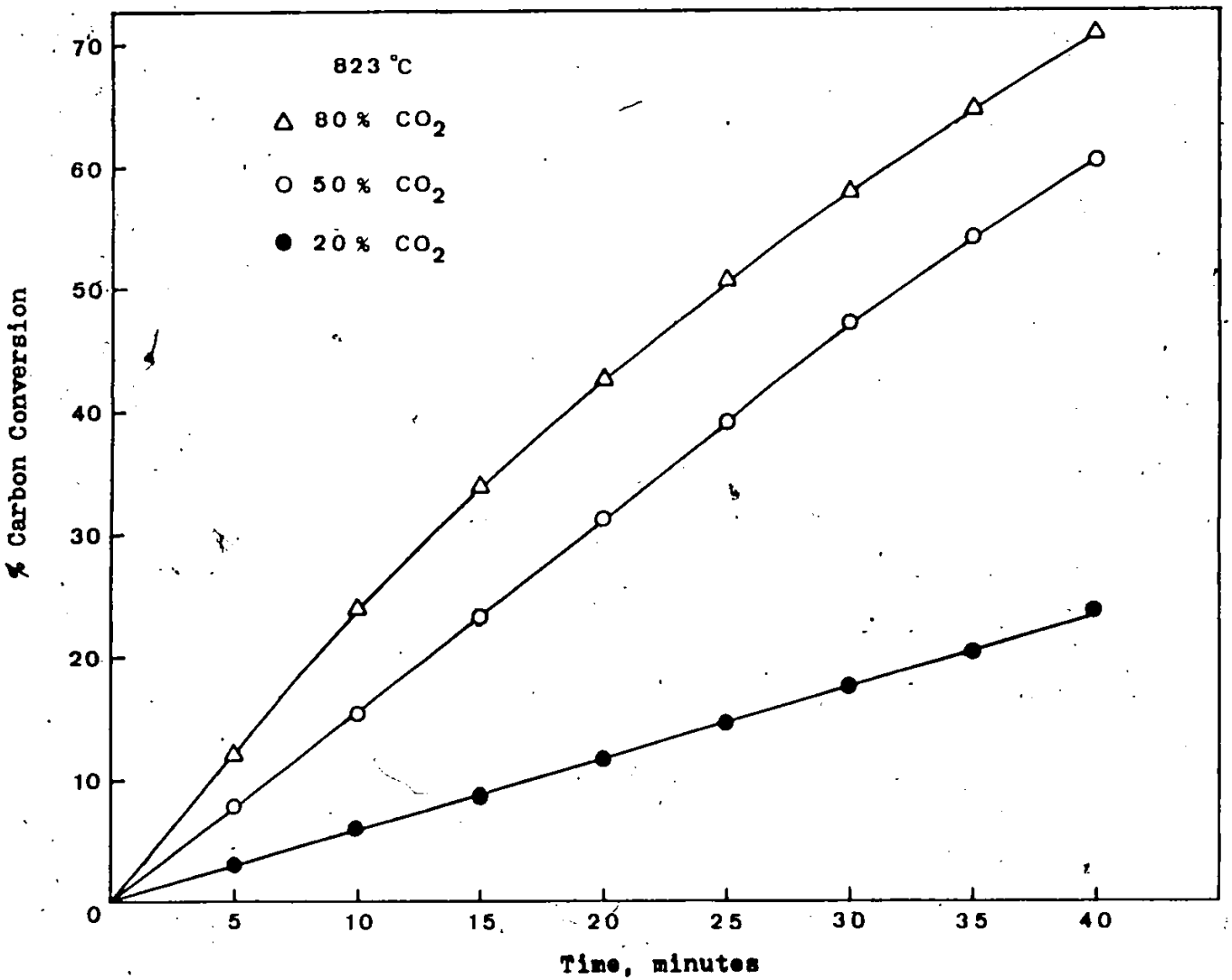

Figure 13. Carbon Conversion vs. Time for Different Compositions of CO_2-N_2 Mixtures.. Lignite Char.

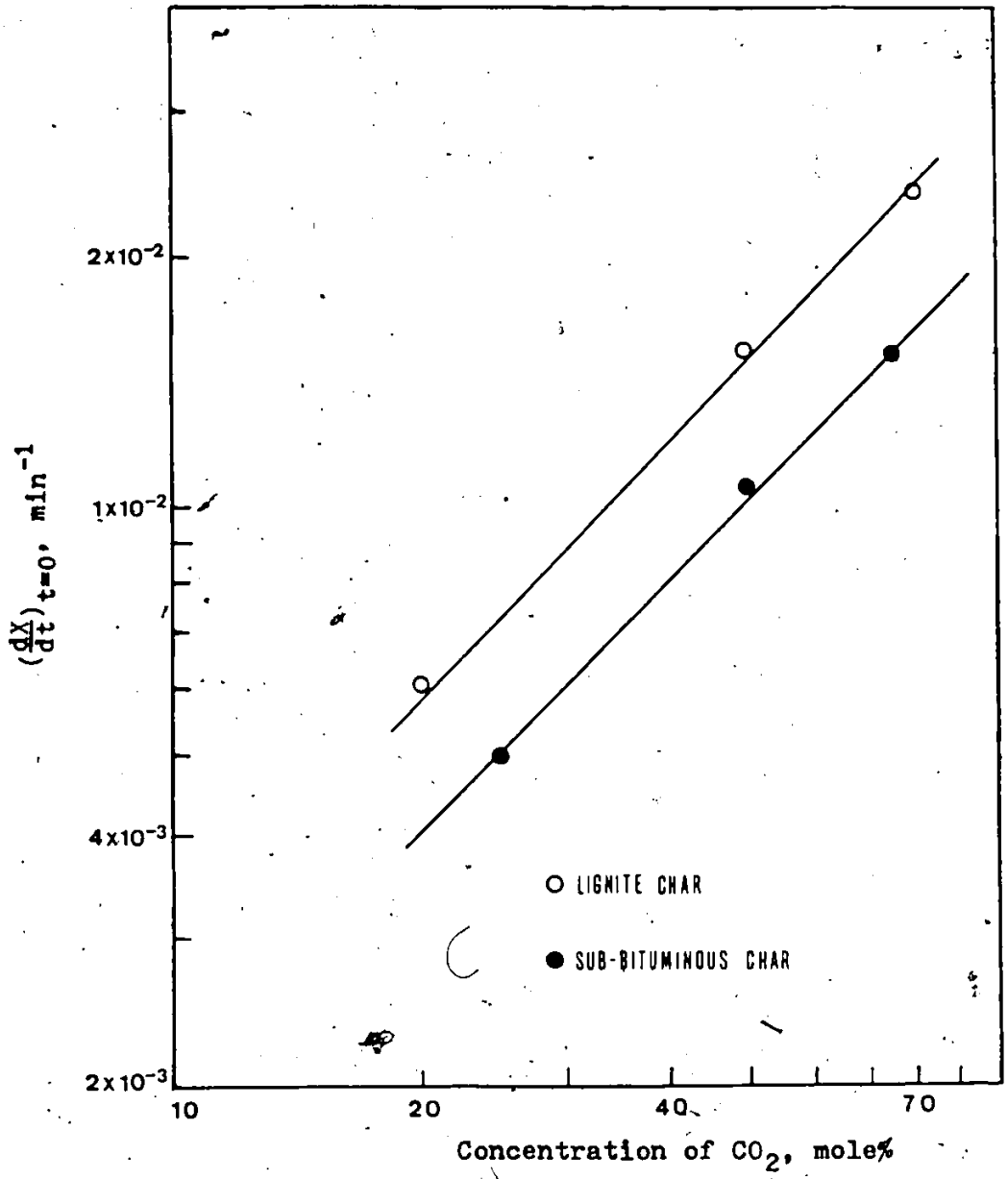

Figure 14. Initial Rates for Varying Concentrations of CO_2

Figure 15 for the lignite char and Figure 16 for the Forestburg char. It is seen from these figures that the results are well represented by straight lines whose slopes are between 0.85 and 1.0. According to Equation 5.3, a slope of 1 means that chemical reaction was controlling where from equation 5.2, a slope of 2 means ash diffusion was controlling. Therefore, the C-CO_2 reaction was chemical reaction controlled, and Equation 5.3 is applicable. Equation 5.3 in its differential form is as follows:

$$\frac{dX}{dt} = \frac{3k_s C_{Ag}}{\rho_B R_p} (1-X)^{2/3} \qquad (5.4)$$

Differential rates were obtained from the conversion-time data using a computer program. The program was DGT3 available in the Scientific Subroutine Package of IBM. Equation 5.4 was tested for its fit using a non-linear least square computer program available in the Computer Centre Library.

The condition for the applicability of a model is the rate constants to be positive. Although Equation 5.4 gave positive rate constants, the residual values obtained from predicted and experimental reaction rates were high. The next step was to further clarify the model. For this purpose Wen (32) suggested the use of an effectiveness factor which is given as:

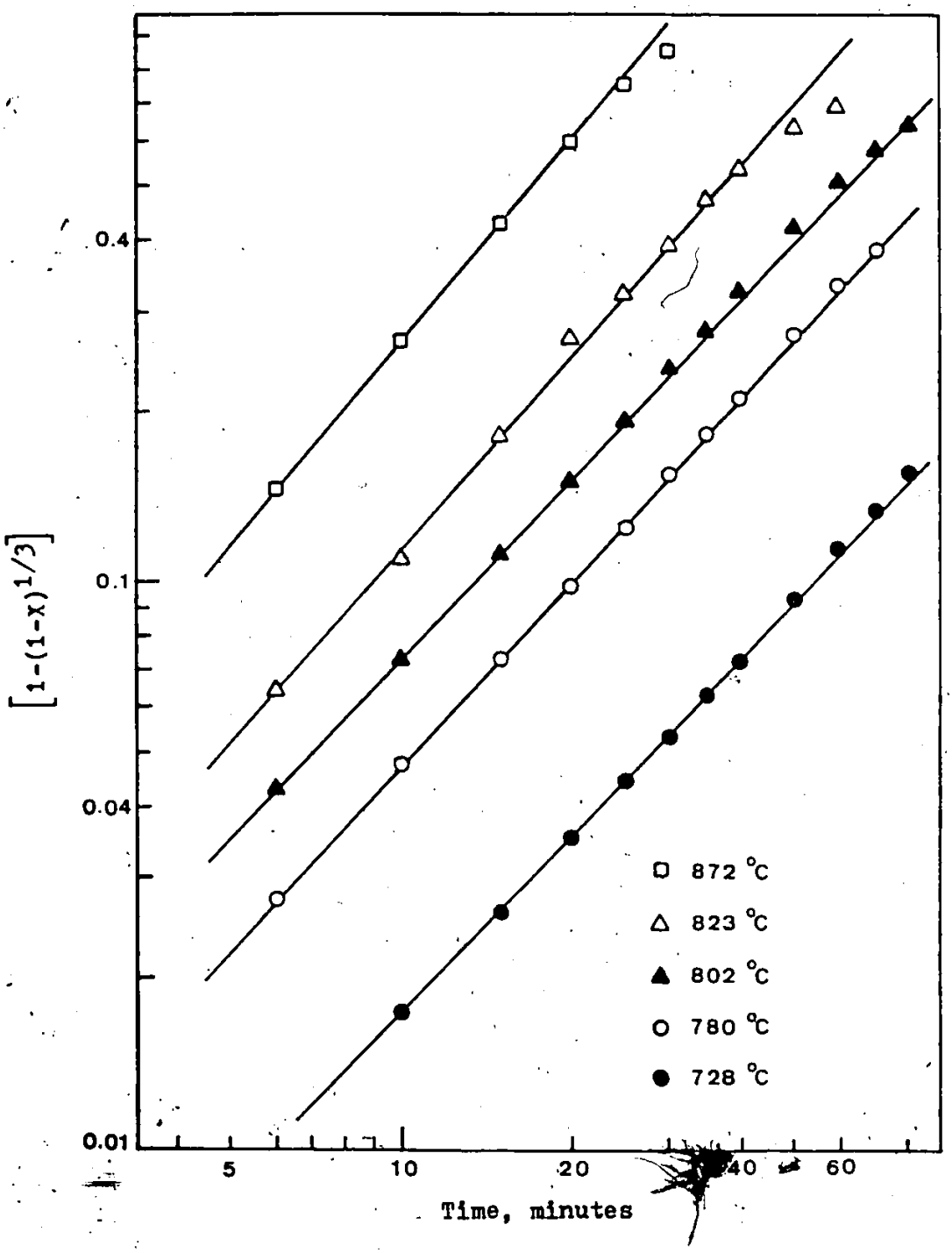

Figure 15. Plots for Unreacted-Core Model. Lignite Char.

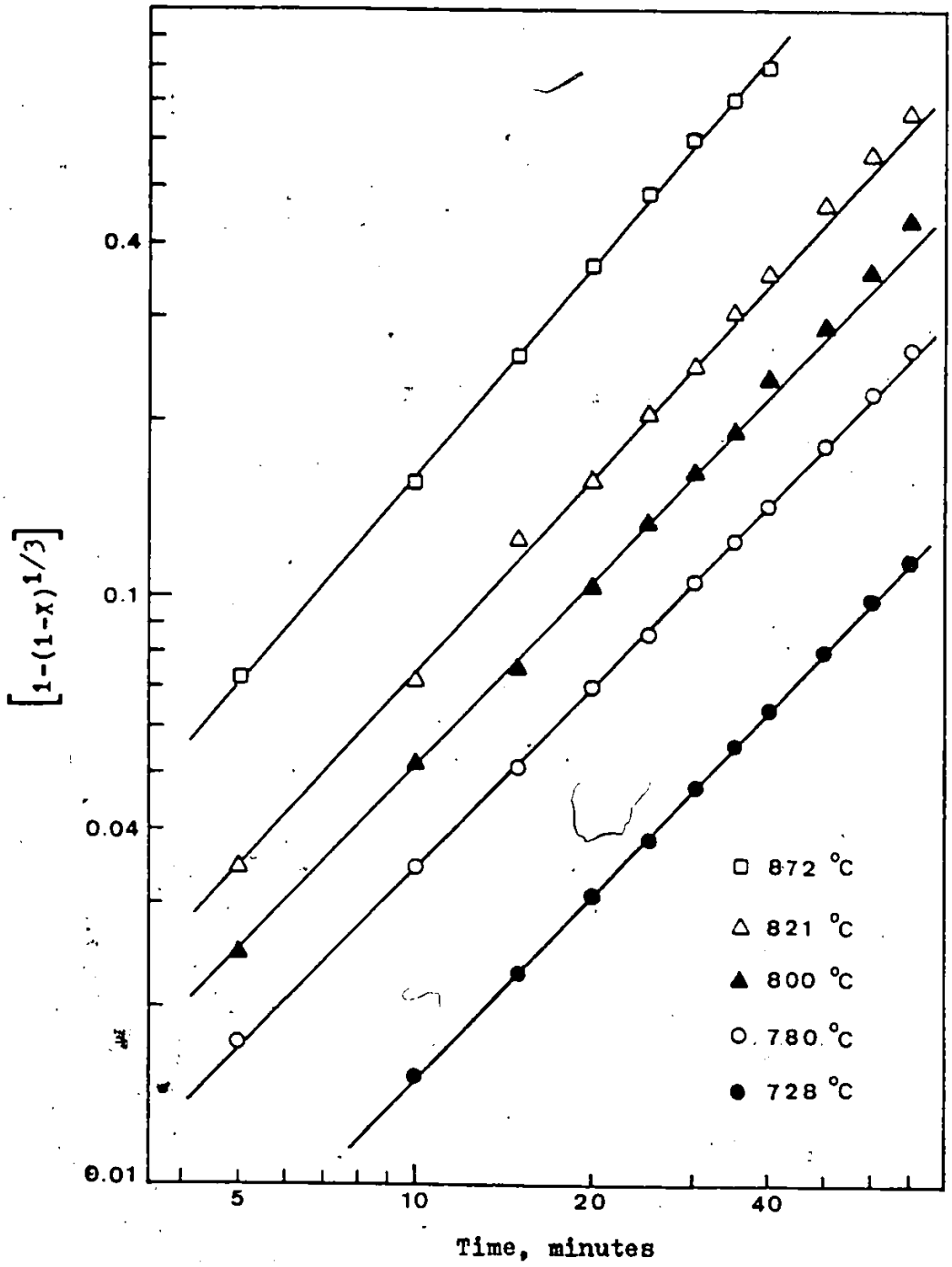

Figure 16. Plots for Unreacted-Core Model. Sub-bituminous Char.

$$\eta_s = \frac{\text{actual reaction rate}}{\text{reaction rate obtainable at the concentration and temperature of the bulk phase}} \quad (5.5)$$

The effectiveness factor relates the reaction rate at any time to the initial rate and permits the examination of the effect of diffusion. For the unreacted -core model the effectiveness factor is proportional to the reaction rate per unit reaction surface area. Reaction rate per unit surface area is defined as

$$(\eta_s) \propto \frac{M}{4r_c^2} \quad (5.6)$$

where r_c is defined as

$$4\pi r_c^2 = 4\pi R_p^2 (r_c/R_p)^2 = 4\pi R_p^2 (1-X)^{2/3} \quad (5.7)$$

M is the total reaction rate of carbon gasification.

Normalizing by dividing the reaction rate per unit reaction surface area at x=0, unit reaction rates were calculated and plotted in Figure 17 for the lignite char and Figure 18 for the sub-bituminous char.

From these figures it can be seen that reaction rate per unit surface area increased with carbon conversion. This leads to the conclusion that diffusion was not controlling. When there is no diffusion, the unreacted-core model predicts that η_s is equal to 1 for all levels of conversion. The

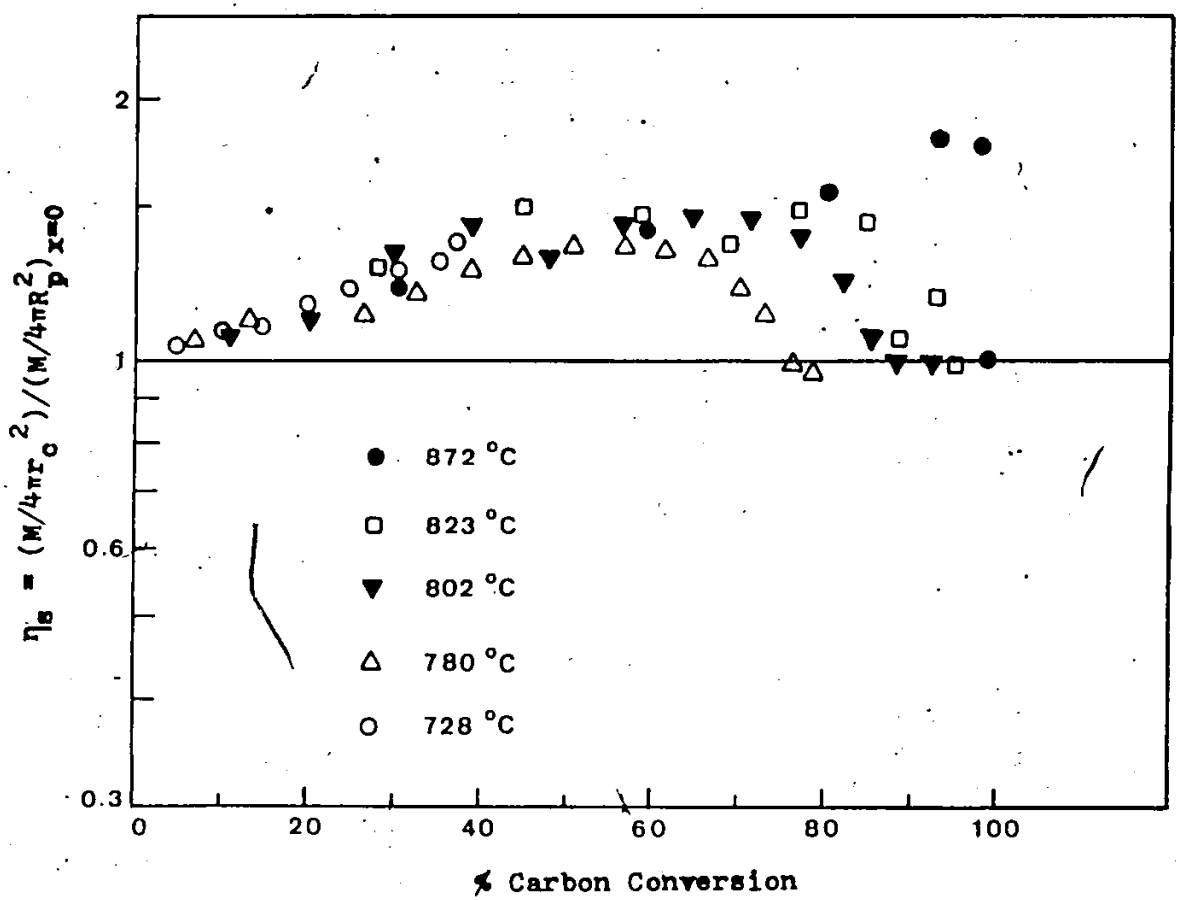

Figure 17. Normalized Reaction Rate per Unit Surface Area vs. Carbon Conversion. Lignite Char.

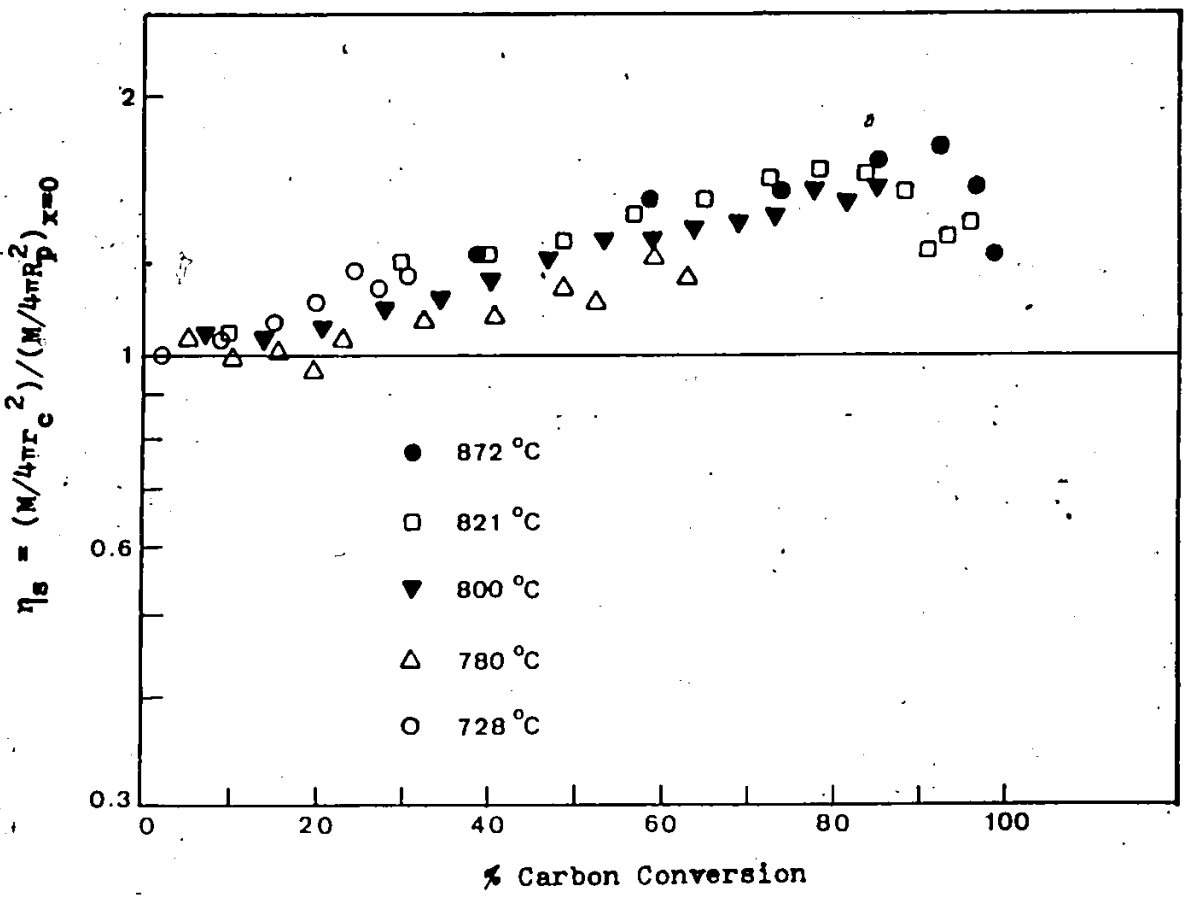

Figure 18. Normalized Reaction Rate per Unit Surface Area vs. Carbon Conversion. Sub-bituminous Char.

deviations in Figures 17 and 18 are explained by the concept of geometrical instability first pointed out by Cannon and Denbigh (56). When the rate per unit area decreases as the conversion becomes greater, the structure nonuniformity will tend to be smoothed out because the rate of reaction is less at a point of deeper penetration. On the other hand, when the rate of reaction per unit area increases as conversion increases, greater unevenness of the reaction surface will result.

Since for both chars the reaction rate per unit surface area increased, the reaction surface unevenness became greater with conversion. However for the lignite char there was a tendency towards the end of the reaction for the structure nonuniformity to be smoothed out.

As the unevenness of the reaction surface increases, there is greater penetration of the char particle by reactant gas and the reaction is not limited only to the outer surface of the particle. The above explains the high residual values obtained when Equation 5.4 was used to fit the results, and also the deviations from the value of 1.0 for the slopes in Figures 15 and 16.

The next step was to modify the unreacted-core model in order to account for the changes in the available reaction surface area due to geometrical instability. The following

modified unreacted-core models were developed:

i) In the plots of $\left[1-(1-X)^{1/3}\right]$ vs. t the results were well represented by straight lines whose slopes were different but close to 1. Equation 5.3 can be written as

$$t = \frac{\rho_B R_p}{k_s C_{Ag}} \left[1-(1-X)^{1/3}\right]^a \qquad (5.8)$$

where a is the value of the slope. After differentiation, Equation 5.8 becomes

$$\frac{dX}{dt} = \frac{3k_s C_{Ag}}{\rho_B R_p a} (1-X)^{2/3} \left[1-(1-X)^{1/3}\right]^{1-a} \qquad (5.9)$$

Equation 5.9 is the modified unreacted-core model.

ii)

To the unreacted-core model, a term x^b was added to account for the geometrical instability. That is

$$\frac{dX}{dt} = \frac{3k_s C_{Ag}}{\rho_B R_p} (1-X)^{2/3} X^b \qquad (5.10)$$

where b is a constant and has different value at different temperatures.

iii)

Dutta et al. (15) studied the gasification of 6 coals and chars of high porosity (0.65-0.86). To account for the structural changes and thus changes of the available reaction

surface area, a term A was introduced and a volumetric model was used to describe gasification. Although in the present investigation reaction takes place at the outer surface of the particle, geometrical instability results in changes of the available reaction surface. Consequently the term A was introduced here, and is defined as

$$A = 1 \pm 100 X^{\alpha} e^{-\beta X} \qquad (5.11)$$

where α and β are constants.

The value of A varies with temperature and conversion, and according to Equation 5.11 it may increase, decrease, or may show a maximum or minimum as the reaction proceeds, according to the sign (+ or -).

Since for both chars the reaction rate per unit surface area increases, the unreacted-core model becomes

$$\frac{dX}{dt} = \frac{3 k_S C_{Ag}}{\rho_B R_p} (1-X)^{2/3} (1+100\ X^{\alpha} e^{-\beta X}) \qquad (5.12)$$

iv)

In the unreacted-core model, the term $k_S C_{Ag}$ can be replaced by a function F(C) involving the reaction rate and concentration of reactive species in gas phase. F(C) can be the Langmuir-Hinshelwood mechanism for the C-CO_2 reaction in which the reaction is hindered by the product CO.

$$F(C) = \frac{K_1 pCO_2}{1+K_2 pCO+K_3 pCO_2} \qquad (5.13)$$

where K_1, K_2, K_3 are kinetic parameters.

v)

With pure CO_2 entering the reactor at a rate of 150 ml/min, the concentration of CO can be assumed to be negligible. Hence the inhibiting effect of the product CO is insignificant. Then F(C) can be written as

$$F(C) = \frac{K_1 pCO_2}{1+K_2 pCO_2} \qquad (5.14)$$

where K_1, K_2 are kinetic parameters.

All the models are summarized in Table 5.2

TABLE 5.2

REACTION MODEL FORMS

Model 1	$\frac{dX}{dt} = \frac{3k_S C_{Ag}}{\rho_B R_p}(1-X)^{2/3}$
Model 2	$\frac{dX}{dt} = \frac{3k_S C_{Ag}}{\rho_B R_p^{\ a}}(1-X)^{2/3}\left[1-(1-X)^{1/3}\right]^{1-a}$
Model 3	$\frac{dX}{dt} = \frac{3k_S C_{Ag}}{\rho_B R_p}(1-X)^{2/3}\ X^b$
Model 4	$\frac{dX}{dt} = \frac{3k_S C_{Ag}}{\rho_B R_p}(1-X)^{2/3}(1+100X^{\alpha}e^{-\beta X})$
Model 5	$\frac{dX}{dt} = \frac{3}{\rho_B R_p}(1-X)^{2/3}\ \frac{K_1 pCO_2}{1+K_2 pCO+K_3 pCO_2}$
Model 6	$\frac{dX}{dt} = \frac{3}{\rho_B R_p}(1-X)^{2/3}\ \frac{K_1 pCO_2}{1+K_2 pCO_2}$

Using the non-linear least square computer program the different models were tested for the best fit. Models 5 and 6 (Table 5.2) gave negative reaction rate constants and they were rejected. Models 1 to 4 gave positive rate constants. These models were discriminated by comparison of residuals. As shown in Figure 19, model 4 gave the lowest values of residuals. Therefore Equation 5.12 was considered to represent the data of char gasification best.

The reaction rate constants and the constants α, β are

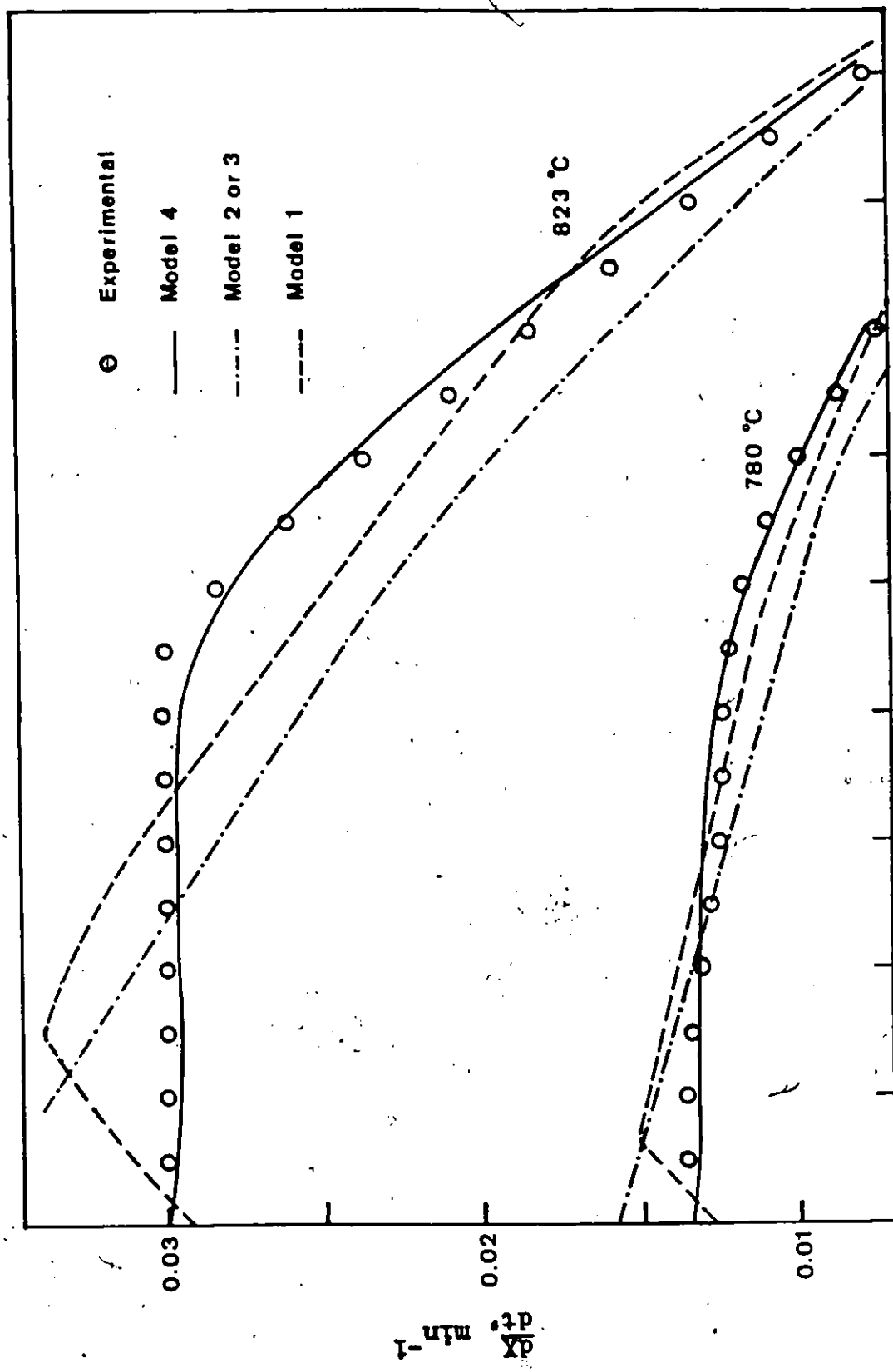

Figure 19. Experimental and Calculated Reaction Rates for the Different Models. Lignite Char.

given in table 5.3

TABLE 5.3

REACTION CONSTANTS

LIGNITE CHAR

Temp. (°C)	$k_s x 10^2$ (cm/s)	α	β
728	0.65	3.5	5.4
780	1.79	3.4	6.8
802	2.76	3.8	5.8
823	4.11	3.5	5.9
872	9.08	4.2	5.2
	SUB-BITUMINOUS CHAR		
728	0.50	2.6	9.7
780	1.18	3.8	6.9
800	1.75	4.1	5.6
821	2.52	3.9	5.4
872	5.47	4.0	5.3

Variation of k_s with temperature is shown by Arrhenius plots in Figure 20 for both chars. From the least square fit of the plots, the following equations for k_s were obtained: For the lignite char

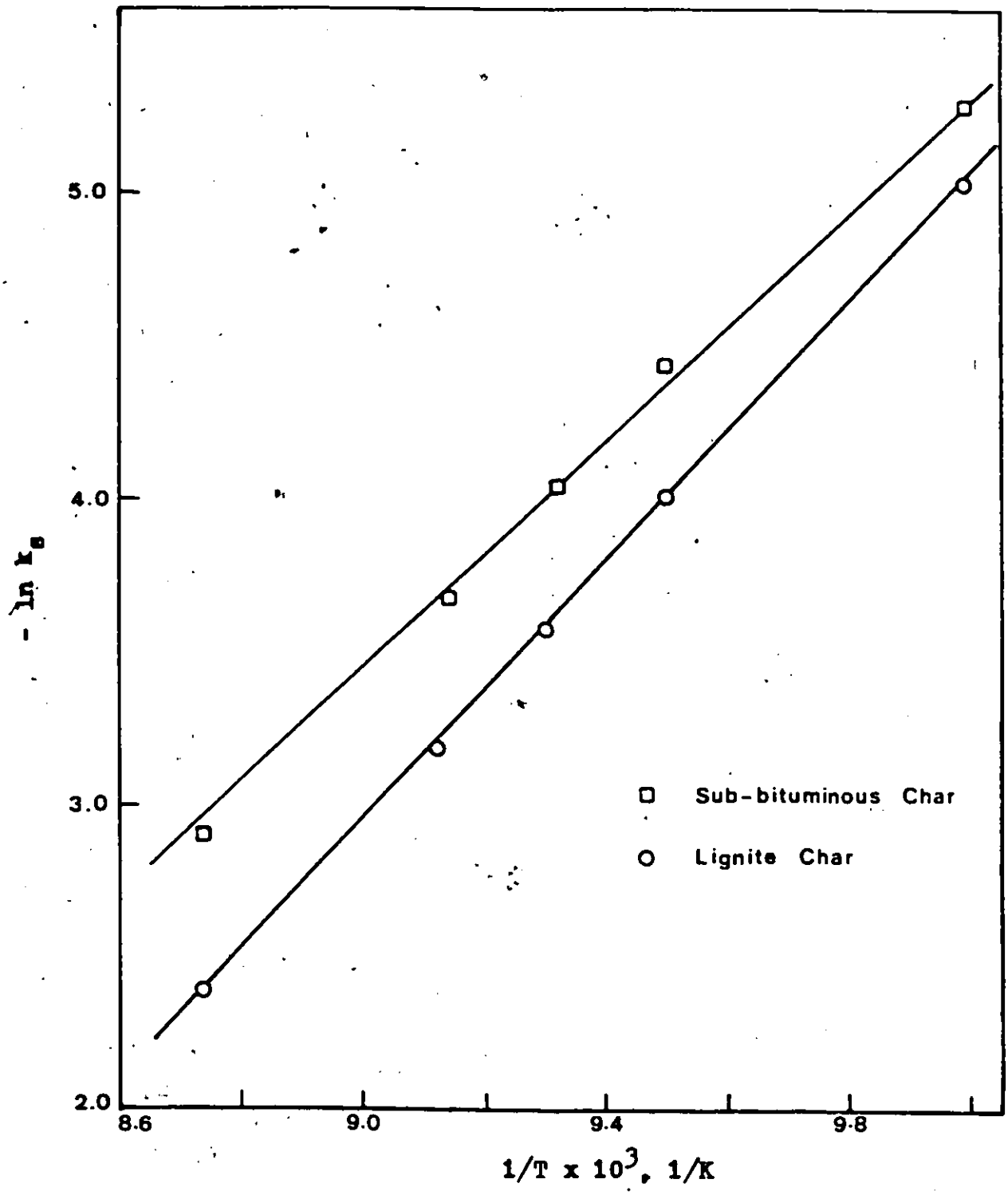

Figure 20. Arrhenious Plots for Reaction Rate Constant

$$k_s = 9.34 \times 10^6 \exp(-176{,}000/RT) \qquad (5.15)$$

For the sub-bituminous char

$$k_s = 5.9 \times 10^5 \exp(-155{,}000/RT) \qquad (5.16)$$

where R is the universal gas constant in J/mole -K.

In Figure 21 the experimental and calculated reaction rates of gasification for the lignite char are shown, and in Figure 22 for the sub-bituminous char. From these figures it can be seen that agreement between experimental and calculated values is very good.

5.2 Catalytic Gasification

The effect of two catalysts, K_2CO_3 and Ni (added in the form of $Ni(NO_3)_2$) on rates of gasificiation and conversion of chars was studied. The effect of varying concentration of catalyst was also studied. The conversion vs. time for the lignite char containing 5% Ni is shown in Figure 23, and with 10% K_2CO_3 is shown in Figure 24. Figure 25 shows the conversion vs. time for the sub-bituminous char containing 10% K_2CO_3. In all catalytic gasification runs, the particle size of chars was 0.500-0.595 mm and the CO_2 flow rate was 150 ml /min.

5.2.1 Catalyst Type and Concentration

The concentration of Ni catalyst in both chars was 5%

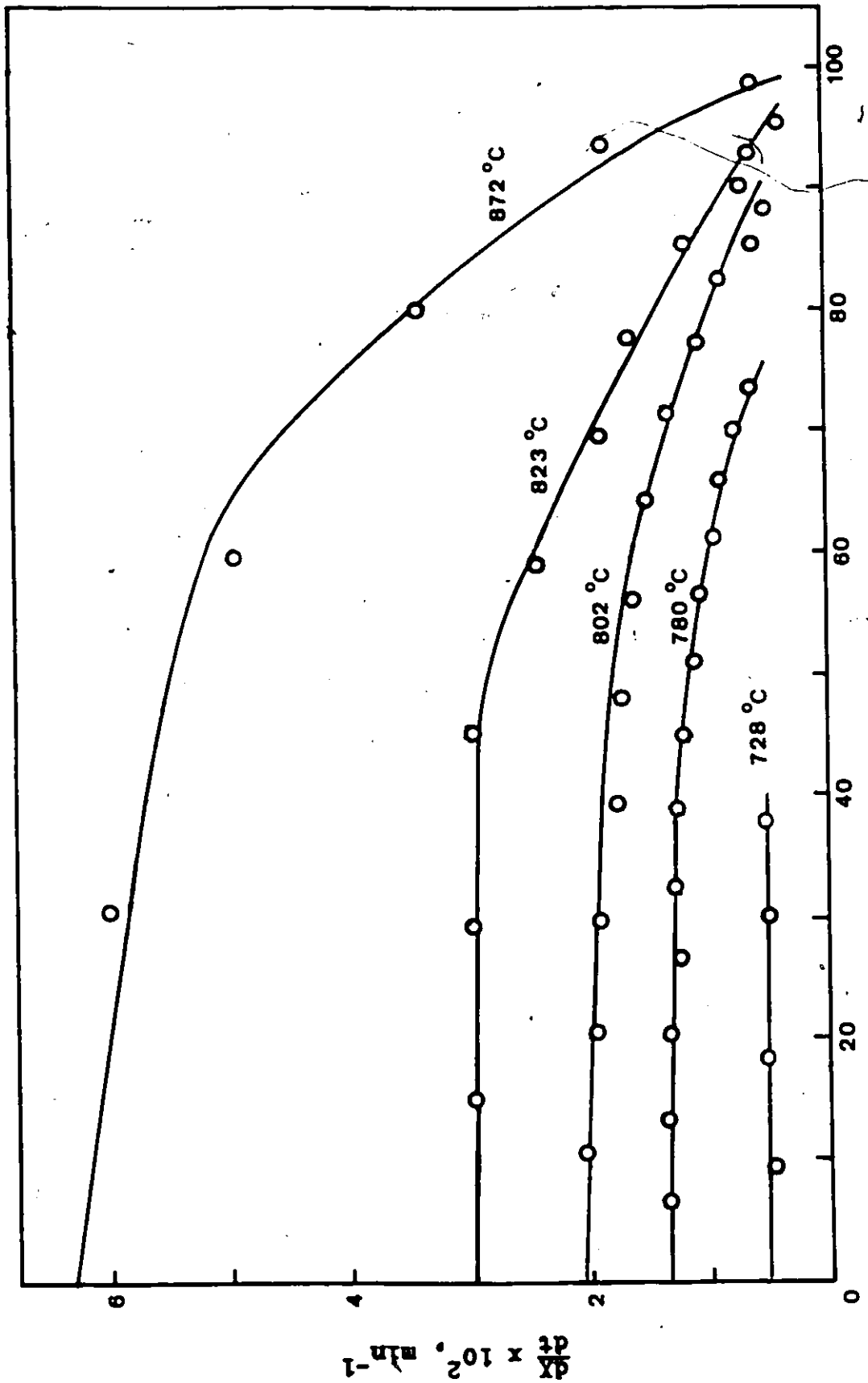

Figure 21. Predicted(solid line) and Experimental(points) Rates. Lignite Char

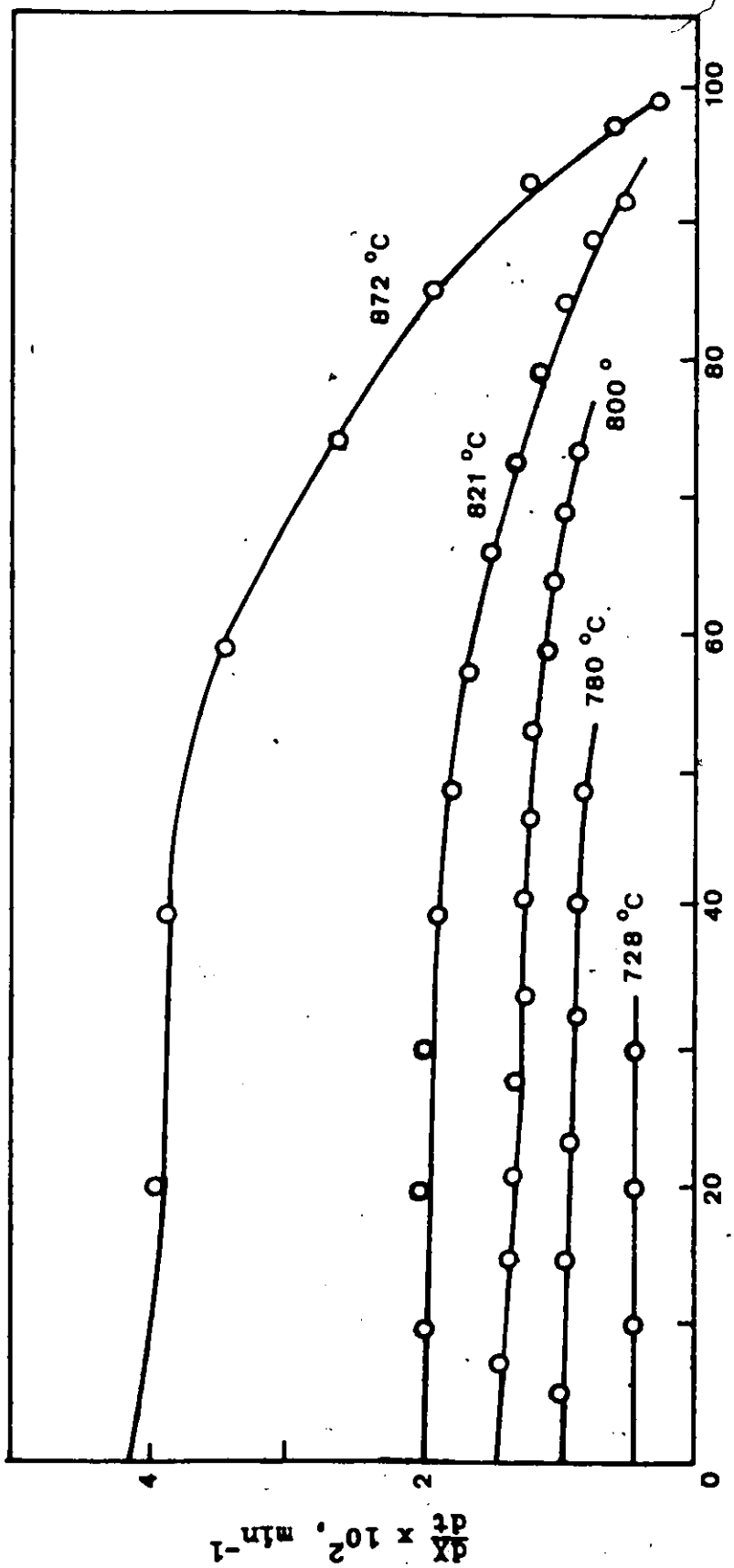

Figure 22. Predicted(solid lines) and Experimental(points) Rates. Sub-bituminous Char.

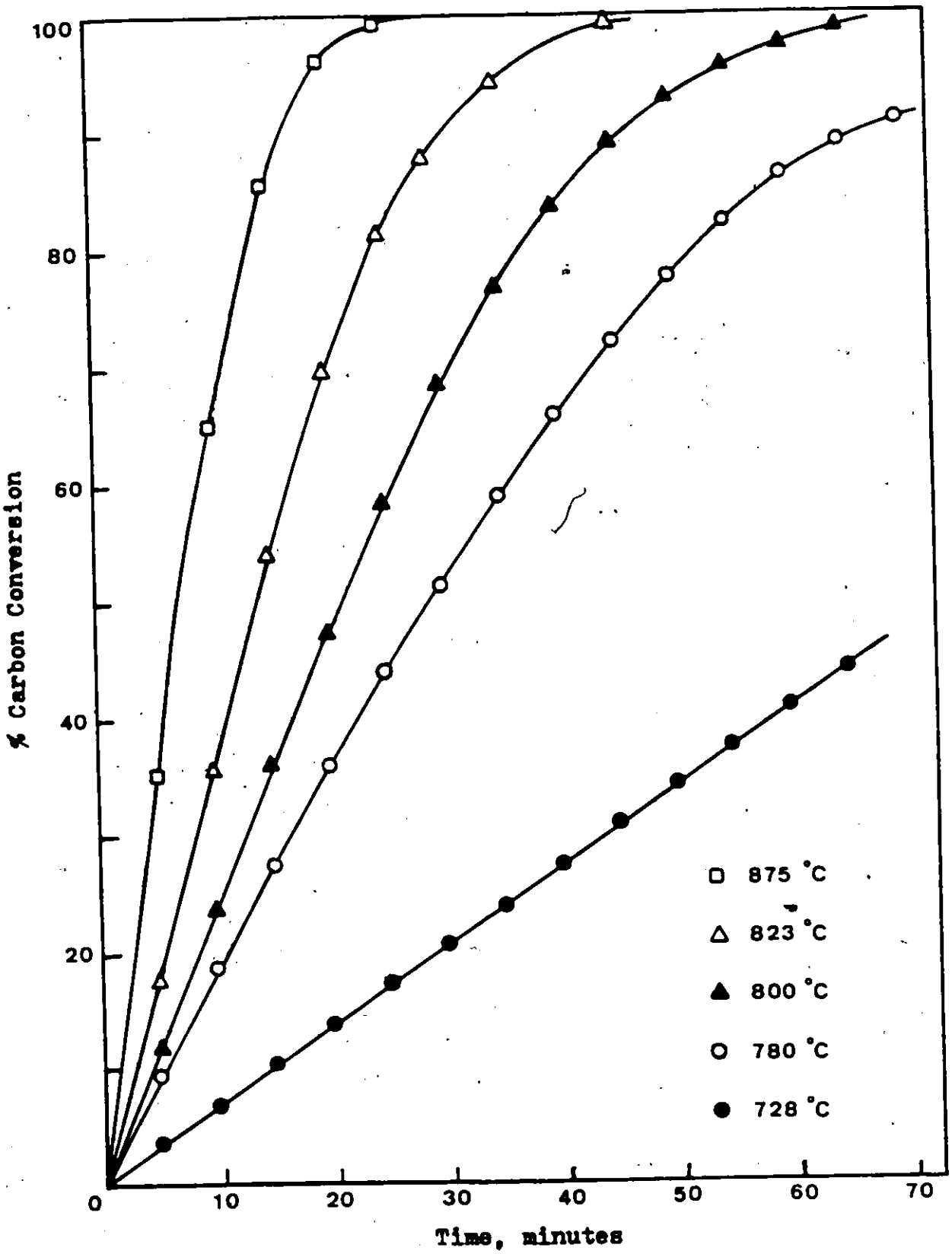

Figure 23. Effect of Nickel (5%) on Carbon Conversion. Lignite Char.

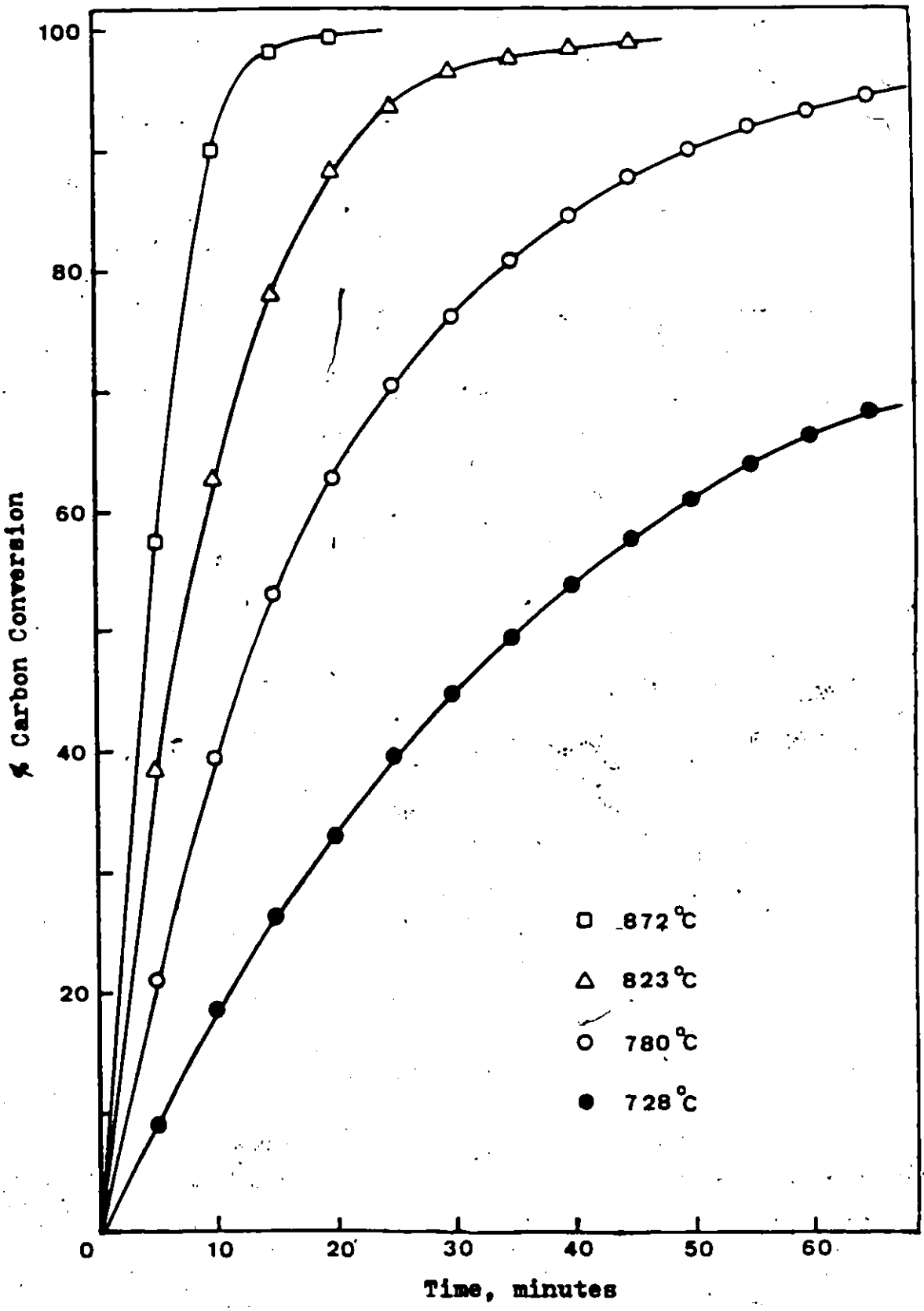

Figure 24. Effect of Potassium Carbonate (10%) on Carbon Conversion. Lignite Char.

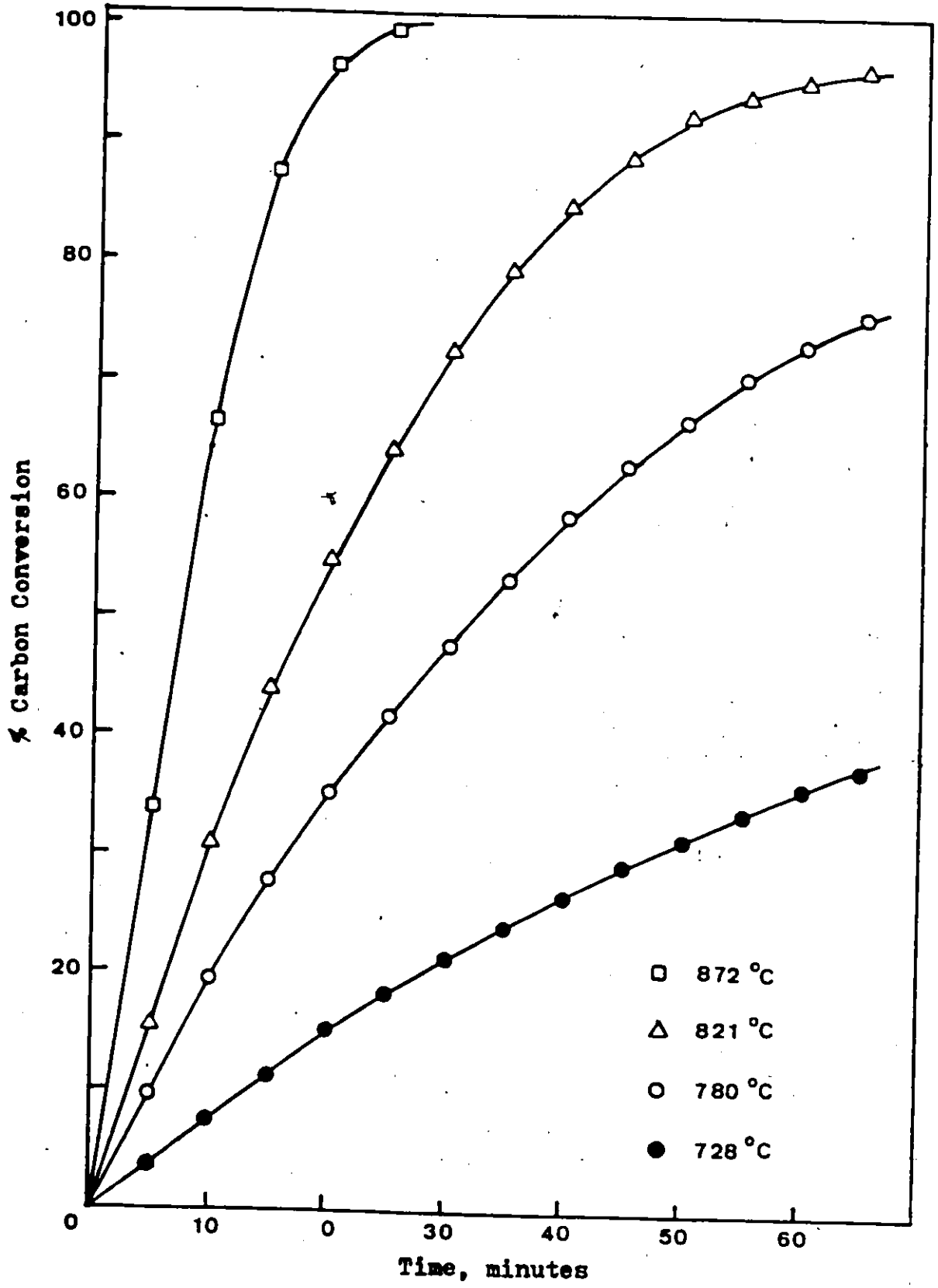

Figure 25. Effect of Potassium Carbonate (10%) On Carbon Conversion. Sub-bituminous Char.

and 10% by weight, while that of K_2CO_3 was 10% and 20%. The results obtained with lignite char are summarized in Table 5.4. The effect of catalyst for the lignite char gasification at 728°C is also shown in Figure 26.

From Table 5.4 it can be seen that at all temperatures, K_2CO_3 was much more effective than Ni. For example at 728°C and 40 minutes reaction time, the conversion for uncatalyzed gasification was 20.1%, for 5% Ni it was 27.3%, and 54.0% for 10% K_2CO_3. The conversion at lower temperatures increased by about 35% for the char containing 5% Ni, while it fell to about 15% at higher reaction temperatures. When the Ni concentration was increased to 10%, conversion remained essentially the same as for 5% Ni. It is indicated that optimum Ni concentration required is about 5%. The catalyst K_2CO_3 was more effective. At 728°C, and 15 minutes reaction time for the char containing 10% K_2CO_3 conversion increased from 7.6% to 26.3% corresponding to a reaction rate $\frac{dx}{dt}$ increase of about 4 times. In the case of this catalyst even at higher temperatures, reaction rates were doubled. When char containing 20% K_2CO_3 was used the conversion was more than that with 10% K_2CO_3. However, the catalytic effect per unit mass of the catalyst was higher for the 10% K_2CO_3. The effect of the dual catalyst (10% K_2CO_3+5% Ni) was nearly the same as for 10% K_2CO_3 at 823°C, whereas at 728°C an increased catalytic activity was noticed at reaction times greater than 15 minutes.

TABLE 5.4

COMPARISON OF CATALYSTS FOR THE LIGNITE CHAR

% Conversion

Reaction Time (min)	Temperature (°C)	None	5% Ni	10% Ni	10% K_2CO_3	20% K_2CO_3	10% K_2CO_3+5%Ni
15	728	7.6	10.2	10.2	26.3	35.7	26.3
	780	20.2	27.3	-	53.0	-	-
	802	30.2	35.7	-	-	-	-
	823	45.2	53.7	55.5	78.0	78.5	76.5
	872	80.2	85.3	-	98.0	-	-
40	728	20.1	27.3	27.3	54.0	58.4	56.2
	780	51.1	65.8	-	84.3	-	-
	802	71.5	83.6	-	-	-	-
	823	90.0	97.7	97.7	98.5	97.3	94.8

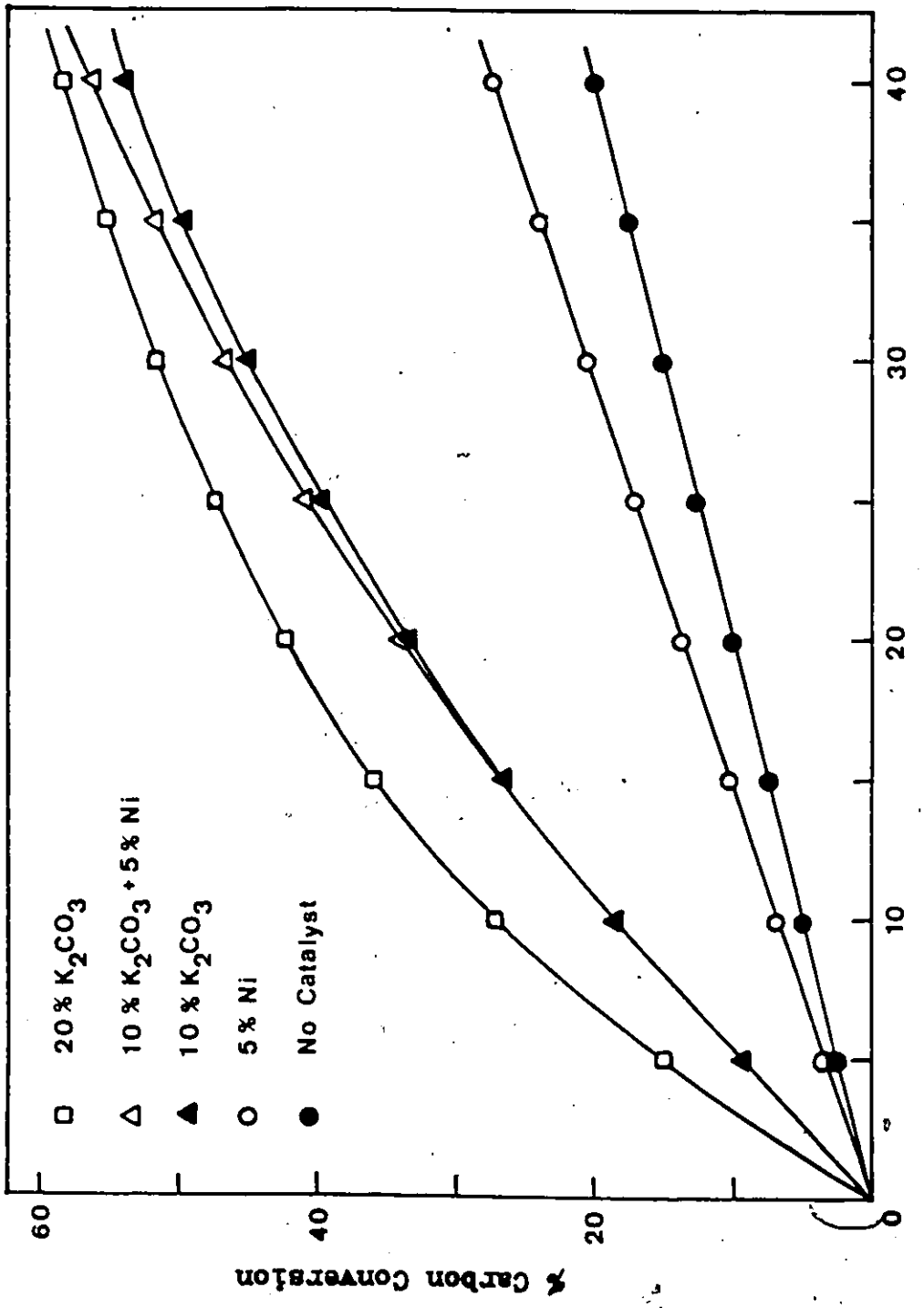

Figure 26. Effect of Catalyst on Carbon Conversion for the Lignite Char at 728°C

From Figure 26 it can be seen that 20% K_2CO_3 shows a higher catalytic effect at the beginning of the reaction and, tends to approach that of 10% K_2CO_3 as the reaction time increases. The dual catalyst tends to show an additive catalytic effect with increasing reaction time. Again it can be seen from the figure that K_2CO_3 is more effective than Ni. It can be concluded that for lignite char 10% K_2CO_3 was most effective catalyst.

The effect of varying concentration of the catalyst on the char conversion for the sub-bituminous char is given in Table 5.5. Addition of Ni (5% or 10%) did not affect the reactivity of char. 10% and 20% K_2CO_3 increased the gasification rates. However, the increase was not as much as in the case of lignite char. The catalytic effect per unit mass of catalyst was higher for 10% K_2CO_3 as compared to 20% K_2CO_3. The highest increase of gasification rates was about 2.5 times with 20% K_2CO_3 at 728°C.

5.2.2 Kinetics of Catalytic Gasification

In the previous section it was concluded that 10% K_2CO_3 was the most effective catalyst for both chars. Consequently it was selected for further study. Also the 5% Ni catalyst in lignite char was selected. Runs were conducted in the temperature range of 728-872°C. The conversion vs. time plots

TABLE 5.5

COMPARISON OF CATALYSTS FOR THE SUB-BITUMINOUS CHAR

Reaction time (min)	Temperature (°C)	% Conversion None	10% K_2CO_3	20% K_2CO_3	Ni
15	728	6.6	11.5	14.4	No effect
	780	14.7	27.5	-	
	800	21.0	-	-	
	821	30.1	44.0	42.5	
	872	59.2	87.7	-	
40	728	17.7	26.9	32.0	
	780	36.7	58.6	-	
	800	53.2	-	-	
	821	72.7	84.7	87.3	

are shown in Figures 23, 24, 25.

The approach used to find a suitable model was similar to that used for uncatalyzed gasification. Calculations (Appendix B) showed that film diffusion was not controlling. The unreacted core model of Equation 5.3 was applied to the results. Plots of $\left[1-(1-X)^{1/3}\right]$ vs. t are shown in Figures 27, 28, 29. The experimental data were well represented by straight lines whose slopes ranged from 0.85 to 1.1. Thus catalytic gasification was chemically controlled similar to uncatalyzed gasification.

Normalized reaction rates were again calculated and plotted in Figures 30, 31, 32. It can be seen from Figure 30 (lignite char with 5% Ni) that reaction rate per unit surface area increased with conversion similar to uncatalyzed gasification. Hence diffusion was not controlling. However for the case of K_2CO_3 added to chars, and as shown in Figures 31 and 32, at higher temperatures reaction rate per unit surface area increased with conversion indicating no diffusion, whereas at lower temperatures unit reaction rates decreased ($\eta_s<1$) with conversion. This could not be explained by diffusion which is a function of increasing temperature. However it was observed that the char particles before and after the reaction tended to stick to each other. Hence the reaction rate per unit surface area was reduced due to fusion. This

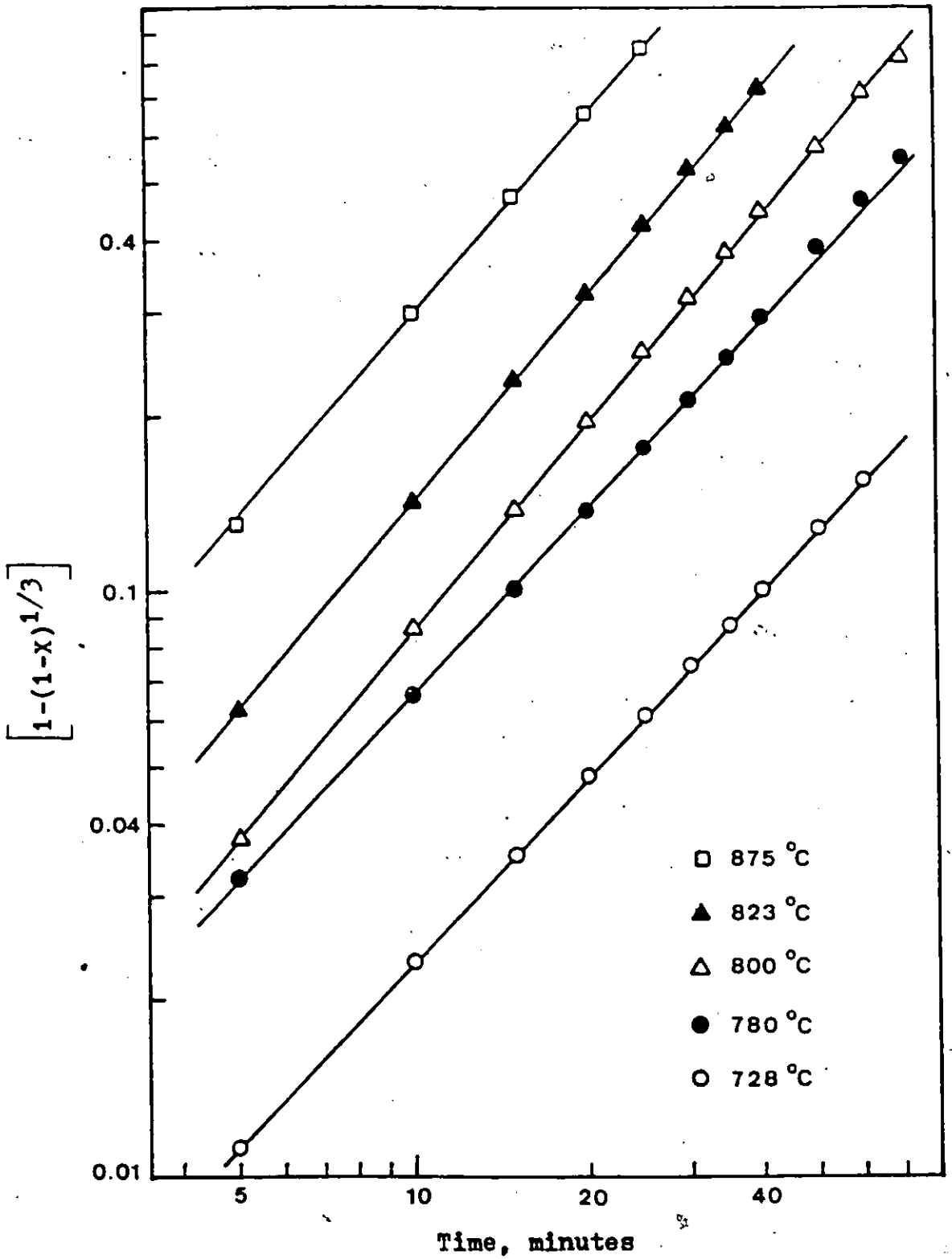

Figure 27. Plots for Unrected-Core Model. Lignite Char + 5% Ni.

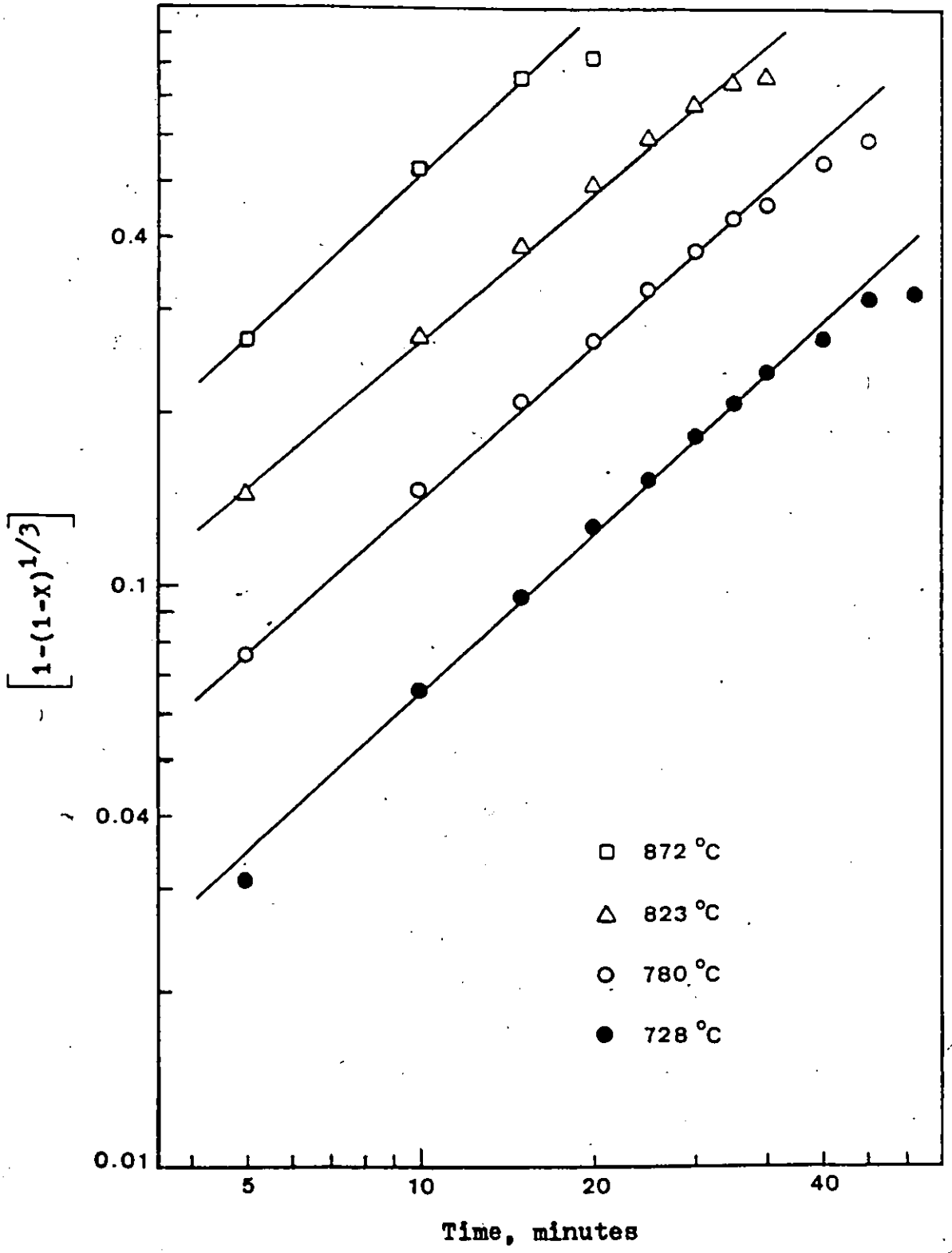

Figure 28. Plots for Unreacted-Core Model. Lignite Char + 10% K_2CO_3.

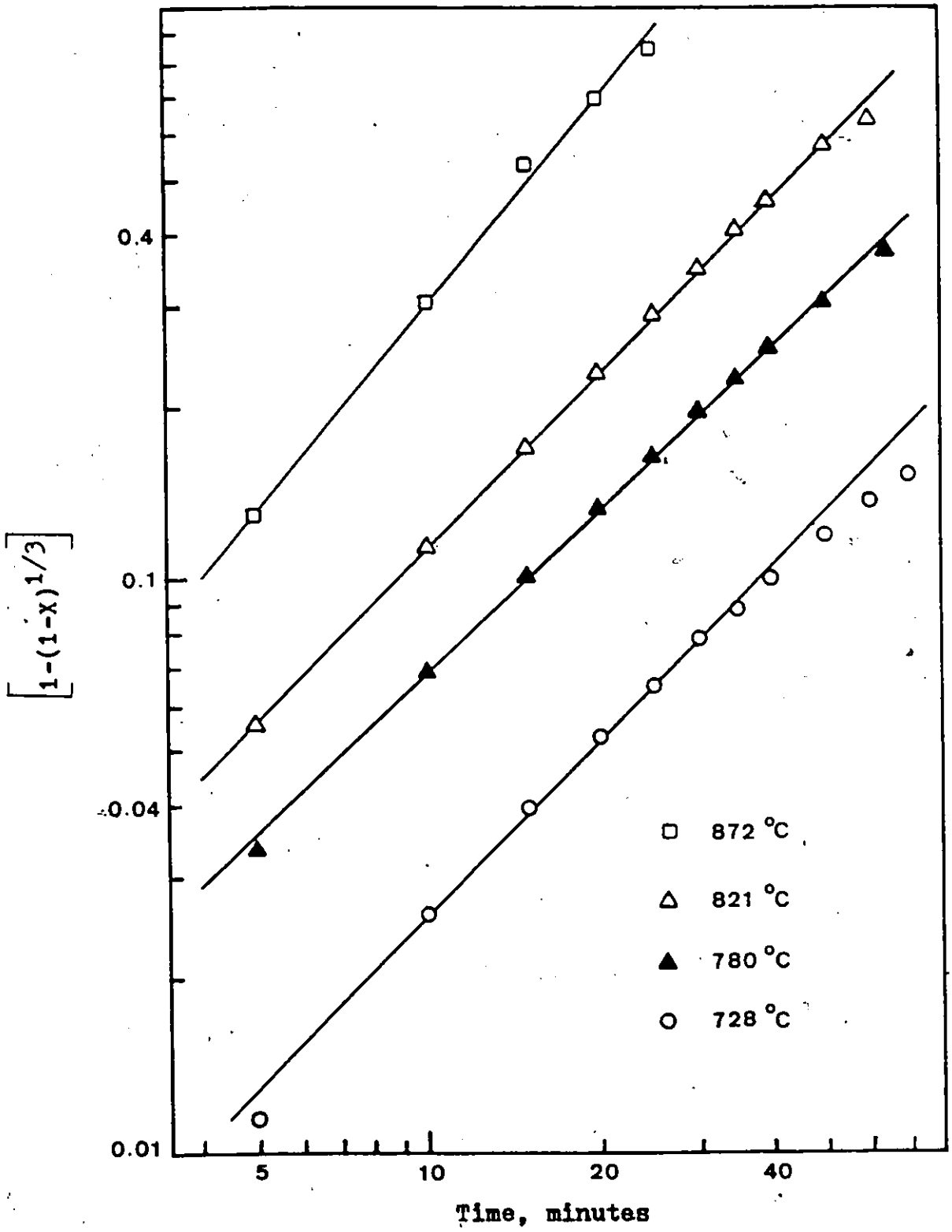

Figure 29. Plots for Unreacted-Core Model. Sub-bituminous Char + 10% K_2CO_3.

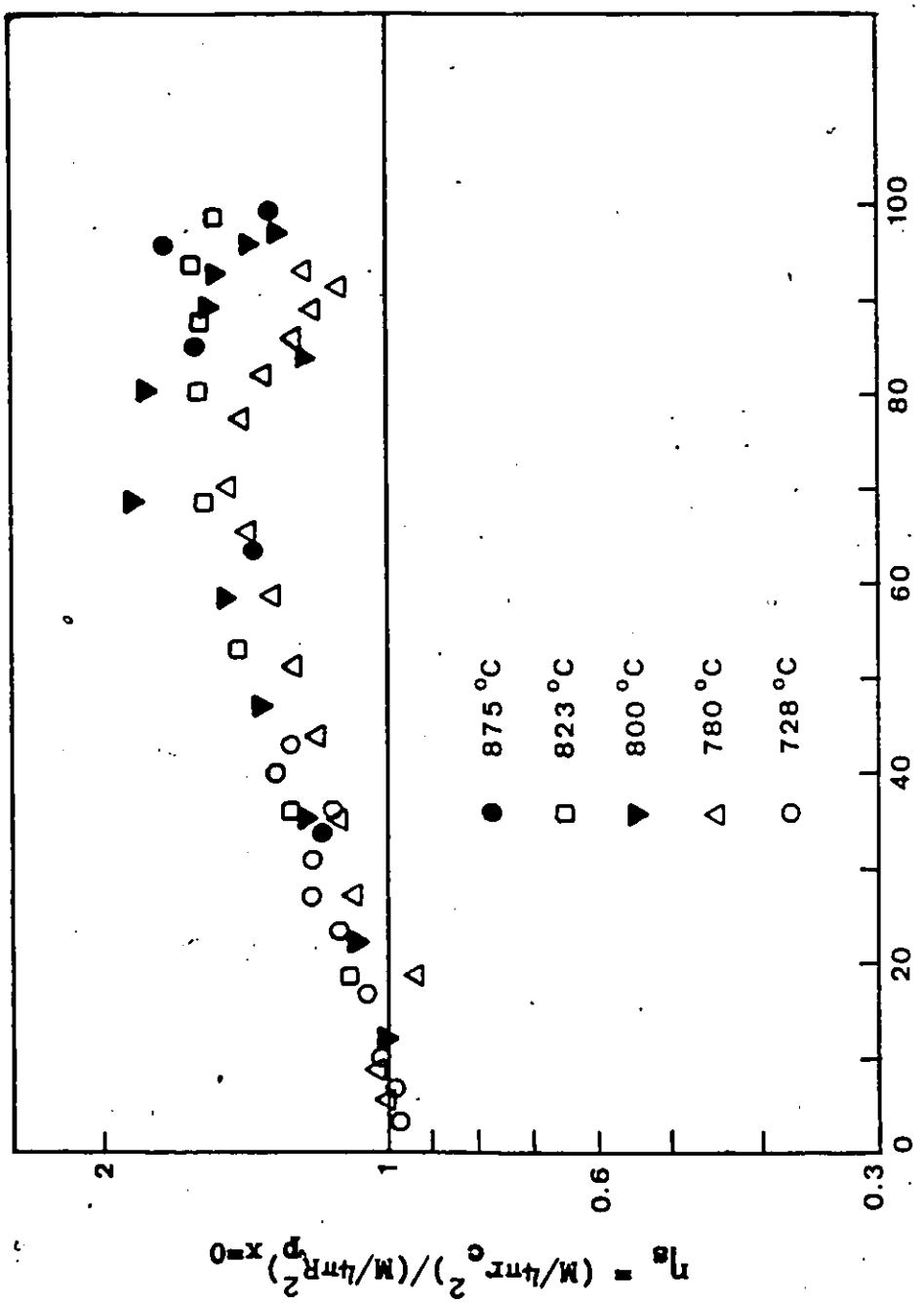

Figure 30. Normalized Reaction Rates per Unit Surface Area vs. Carbon Conversion. Lignite Char + 5% Ni.

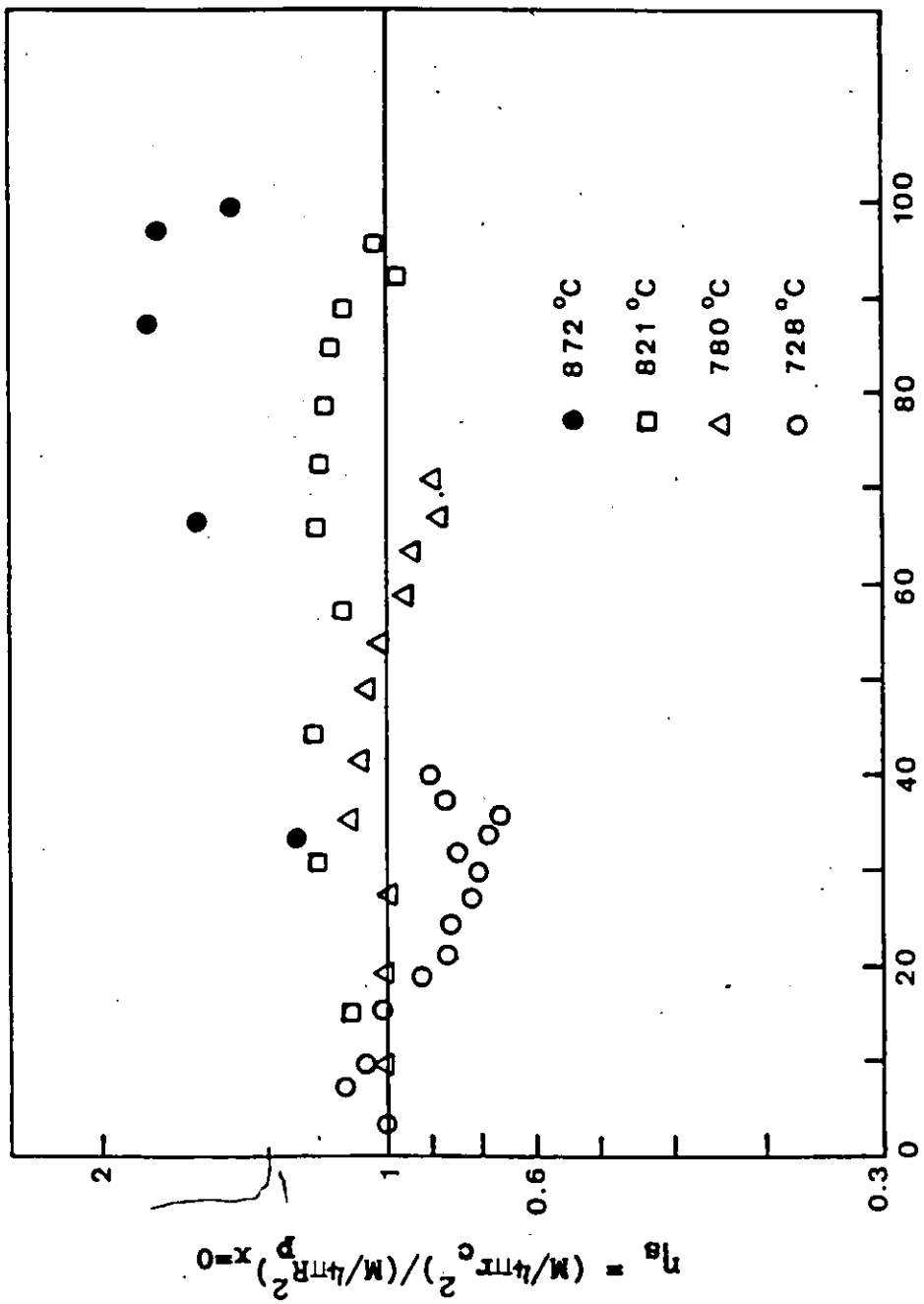

Figure 31. Normalized Reaction Rates per Unit Surface Area vs. Carbon Conversion. Sub-bituminous Char + 10% K_2CO_3.

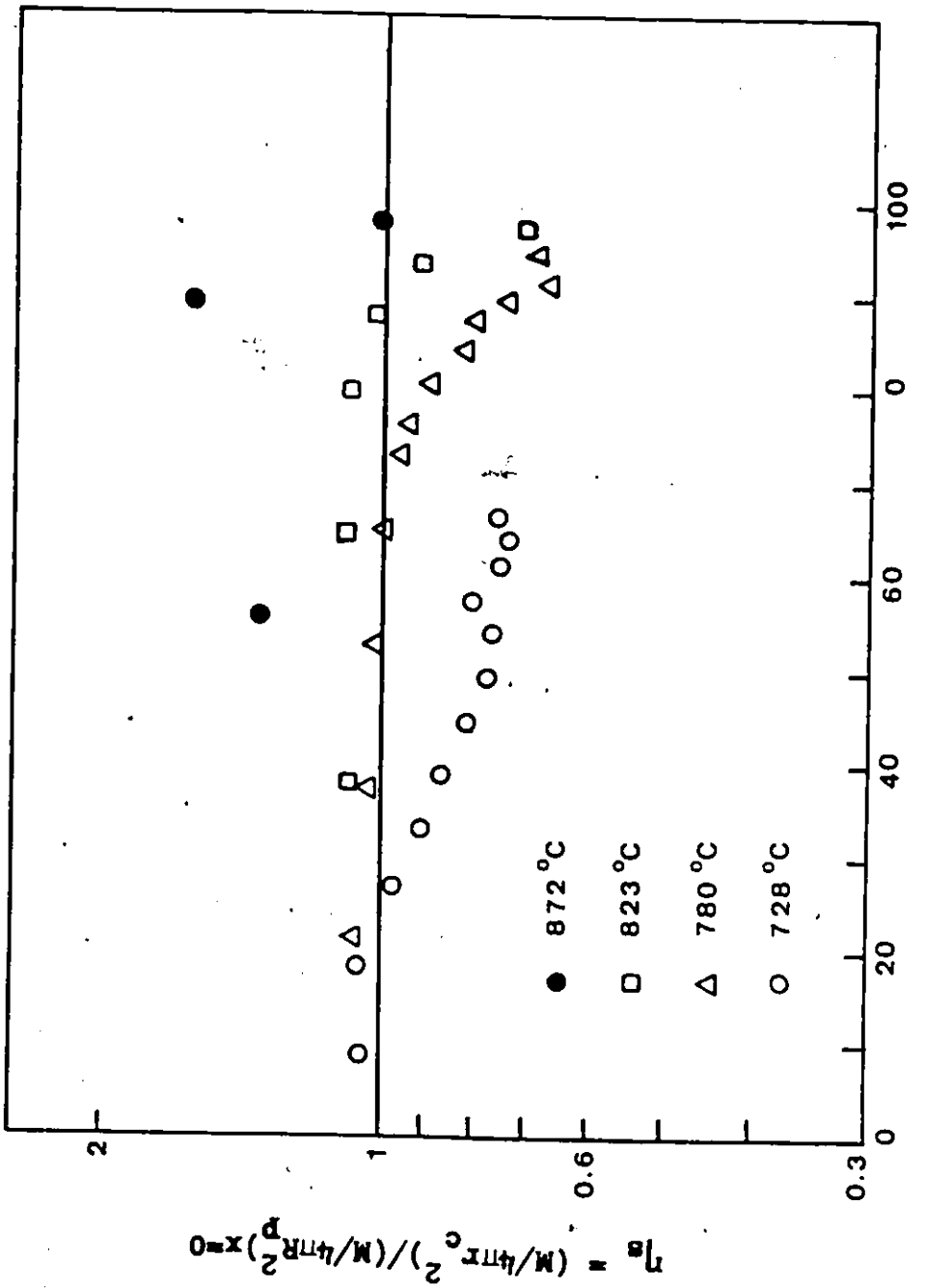

Figure 32. Normalized Reaction Rates per Unit Surface Area vs. Carbon Conversion. Lignite Char + 10% K_2CO_3.

effect was more pronounced in the case of lignite char.

The models given in Table 5.2 were tested for the best fit using the non-linear least squares computer program. As for the uncatalyzed gasification, model 4 represented the data best.

That is

$$\frac{dX}{dt} = \frac{3k_s C_{Ag}}{\rho_B R_p}(1-X)^{2/3}(1\pm 100X^{\alpha}e^{-\beta X}) \qquad (5.17)$$

A plus or minus sign in Equation 5.17 indicates that both were used. The minus was used in the case in which K_2CO_3 was added to the chars and at lower temperatures in which unit reaction rates decreased with conversion ($\eta_s<1$).

The constants are given in Table 5.6

Variation of k_s with temperature is shown by Arrhenius plots in Figure 33. From the least square fit of the plots, the following equations for k_s were obtained:

For the lignite char with 5% Ni

$$k_s = 2.10\times10^{6}\exp(-159{,}000/RT) \qquad (5.18)$$

For the lignite char with 10% K_2CO_3

$$k_s = 5.29\times10^{5}\exp(-141{,}000/RT) \qquad (5.19)$$

For the sub-bituminous char with 10% K_2CO_3

$$k_s = 7.92\times10^{5}\exp(-152{,}000/RT) \qquad (5.20)$$

TABLE 5.6

REACTION CONSTANTS FOR CATALYTIC GASIFICATION

Temp. (°C)	$k_s \times 10^2$ (cm/s)	α	β
	LIGNITE CHAR (5% Ni)		
728	0.998	3.3	8.2
780	2.83	4.3	5.8
800	3.57	3.8	5.2
823	5.70	4.2	5.2
875	11.6	4.5	5.2
	LIGNITE CHAR (10% K_2CO_3)		
728	2.13	5.0	5.0
780	5.04	5.7	5.7
823	10.0	6.1	6.1
872	17.7	6.0	6.5
	SUB-BITUMINOUS CHAR (10% K_2CO_3)		
728	0.90	4.0	4.0
780	2.48	5.5	6.0
821	3.97	2.9	9.0
872	9.45	4.0	5.1

In Figures 34, 35, 36 the experimental and calculated reaction rates are shown. From these figures it can be seen that there is a very good agreement between calculated and experimental rates.

5.3 Replicates

Some runs were repeated in order to determine the reproducibility of the measured data. Two replicates were conducted for each char, with and without catalyst, at one temperature in the range 728-875°C. The temperatures at which runs were repeated were chosen randomly. In Figure 37 plots of weight loss vs. reaction time for some of the replicates are shown; one set for sub-bituminous char at 800°C and the other for the same char containing 10% K_2CO_3 at 872°C. It can be seen from the plots that reproducibility was good, and was found to be within 5%. This variation was possibly due to the differences in the weight at the start of the reaction. Similar plots were obtained for the other cases and reproducibility was again within 5% whatever the reaction temperature was.

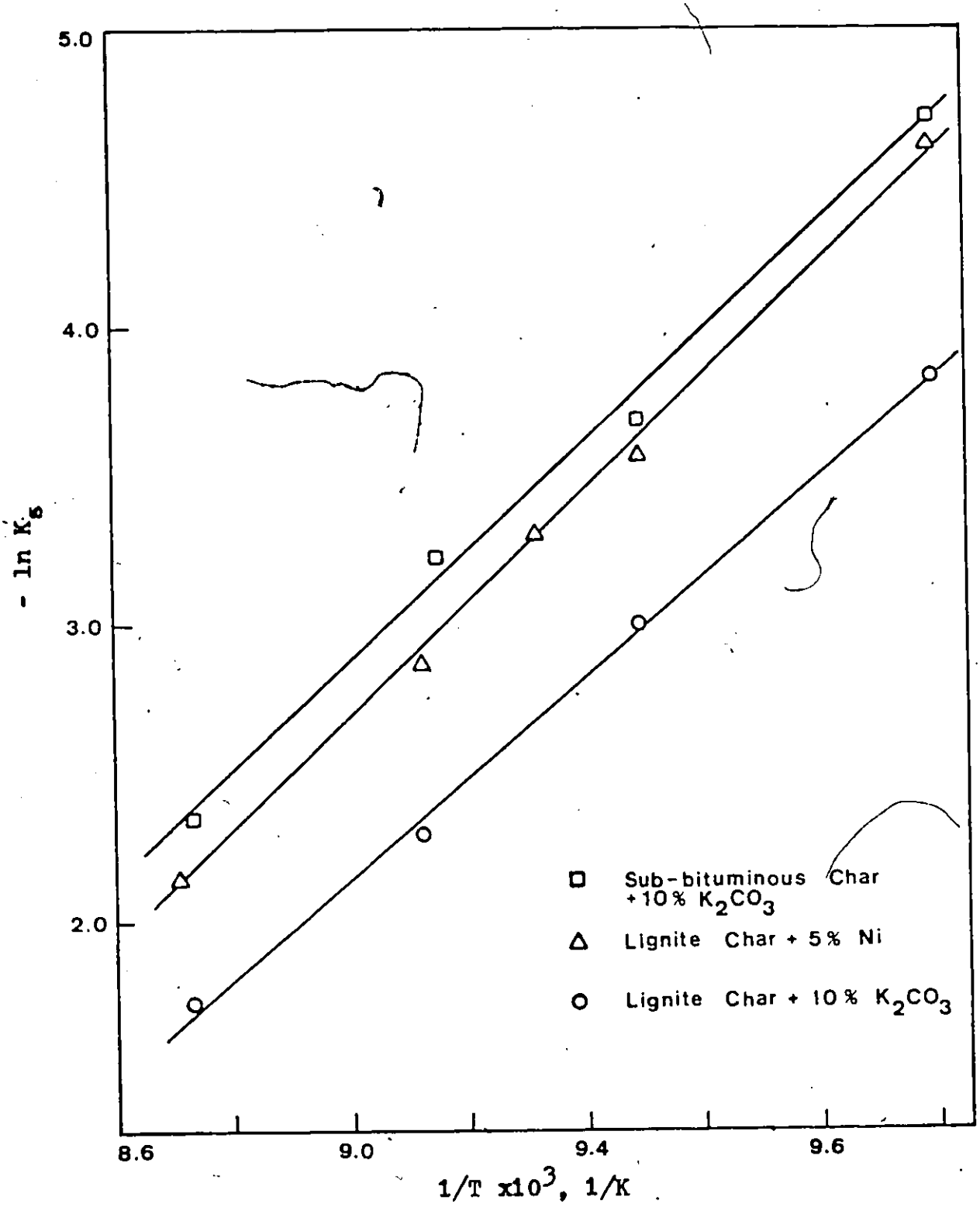

Figure 33. Arrhenious Plots for Reaction Rate Constant

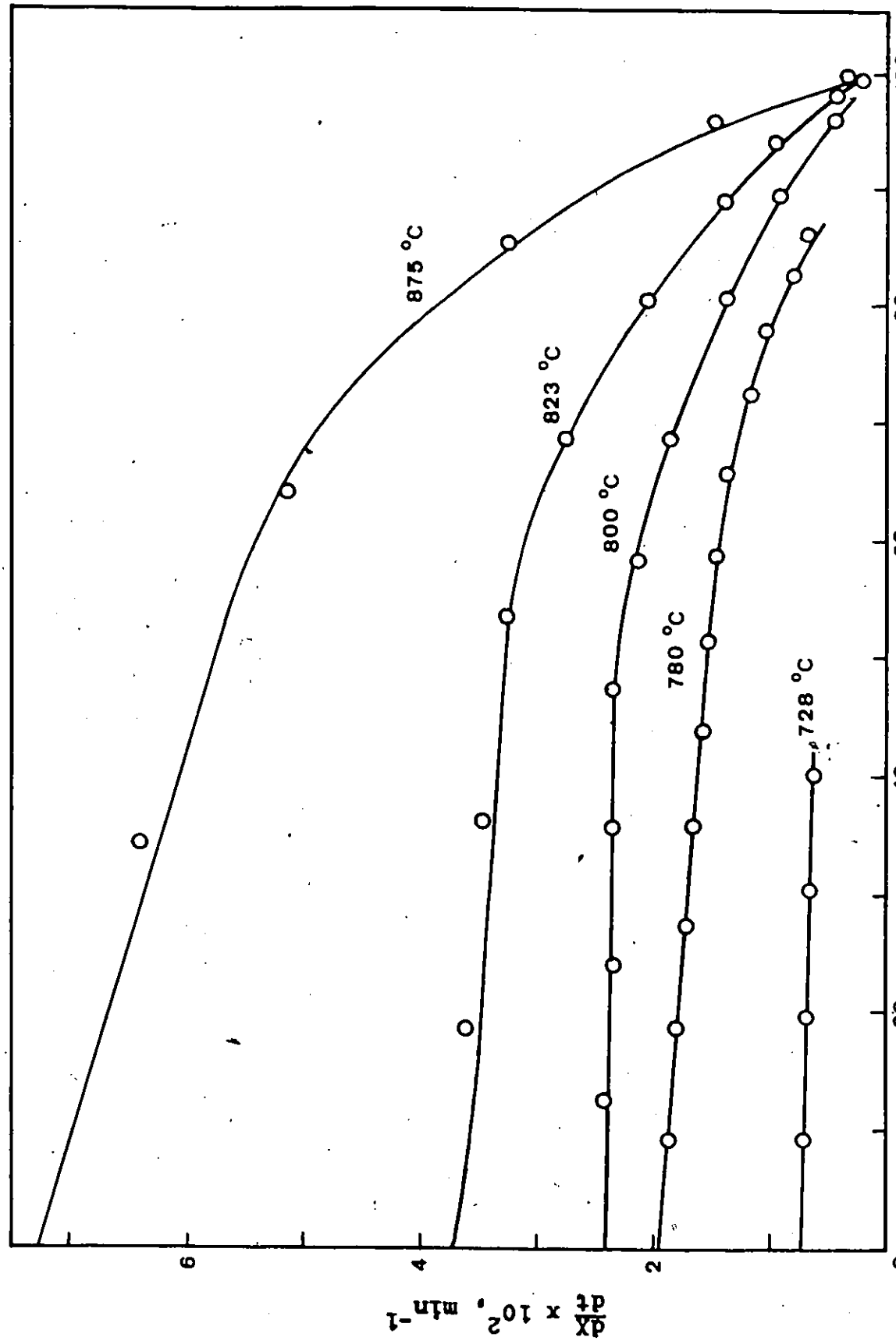

Figure 34. Predicted(solid lines) and Experimental(points) Rates. Lignite Char+5% Ni.

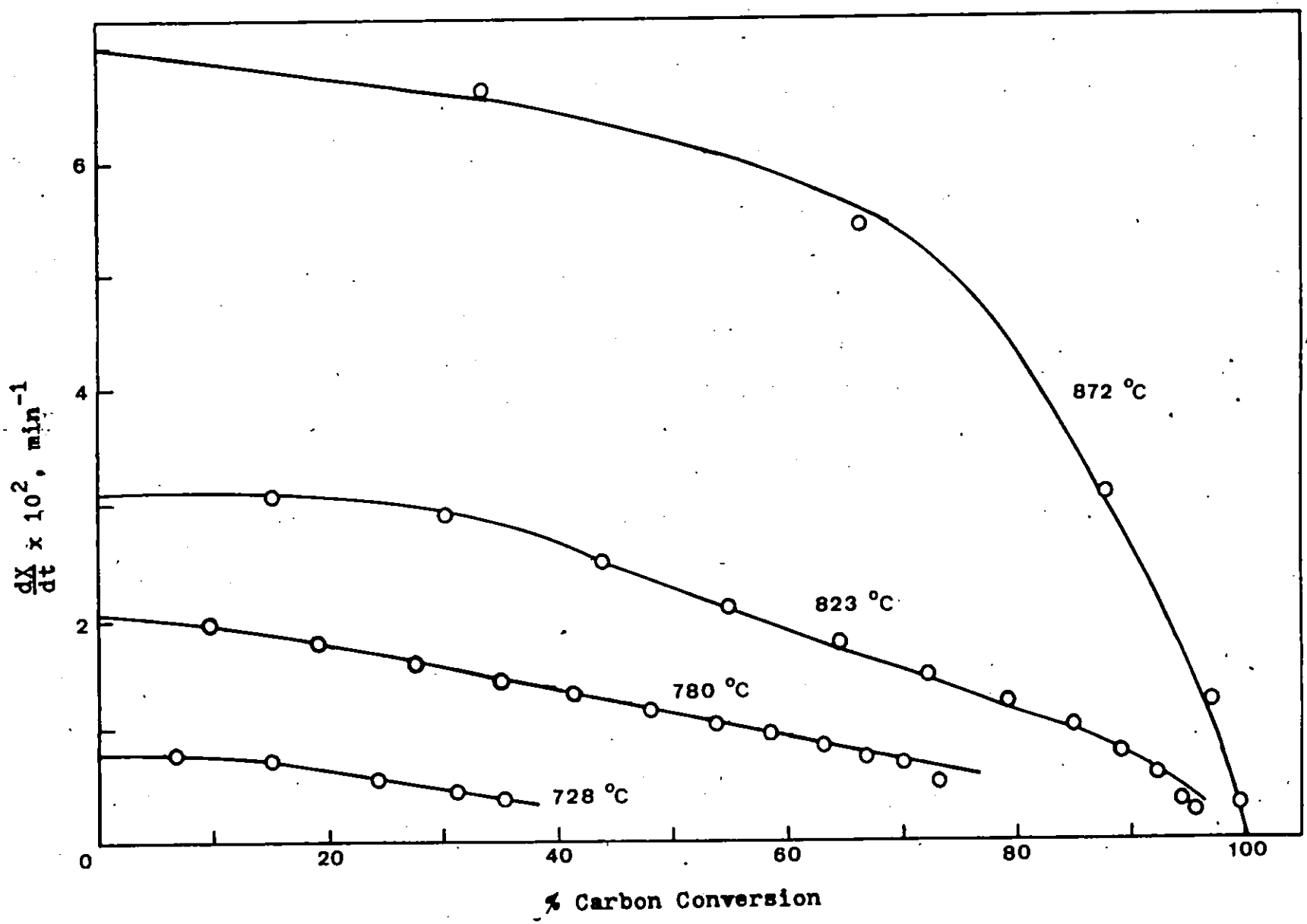

Figure 35. Predicted(solid lines) and Experimental(points) Rates. Sub-bituminous Char + 10% K_2CO_3.

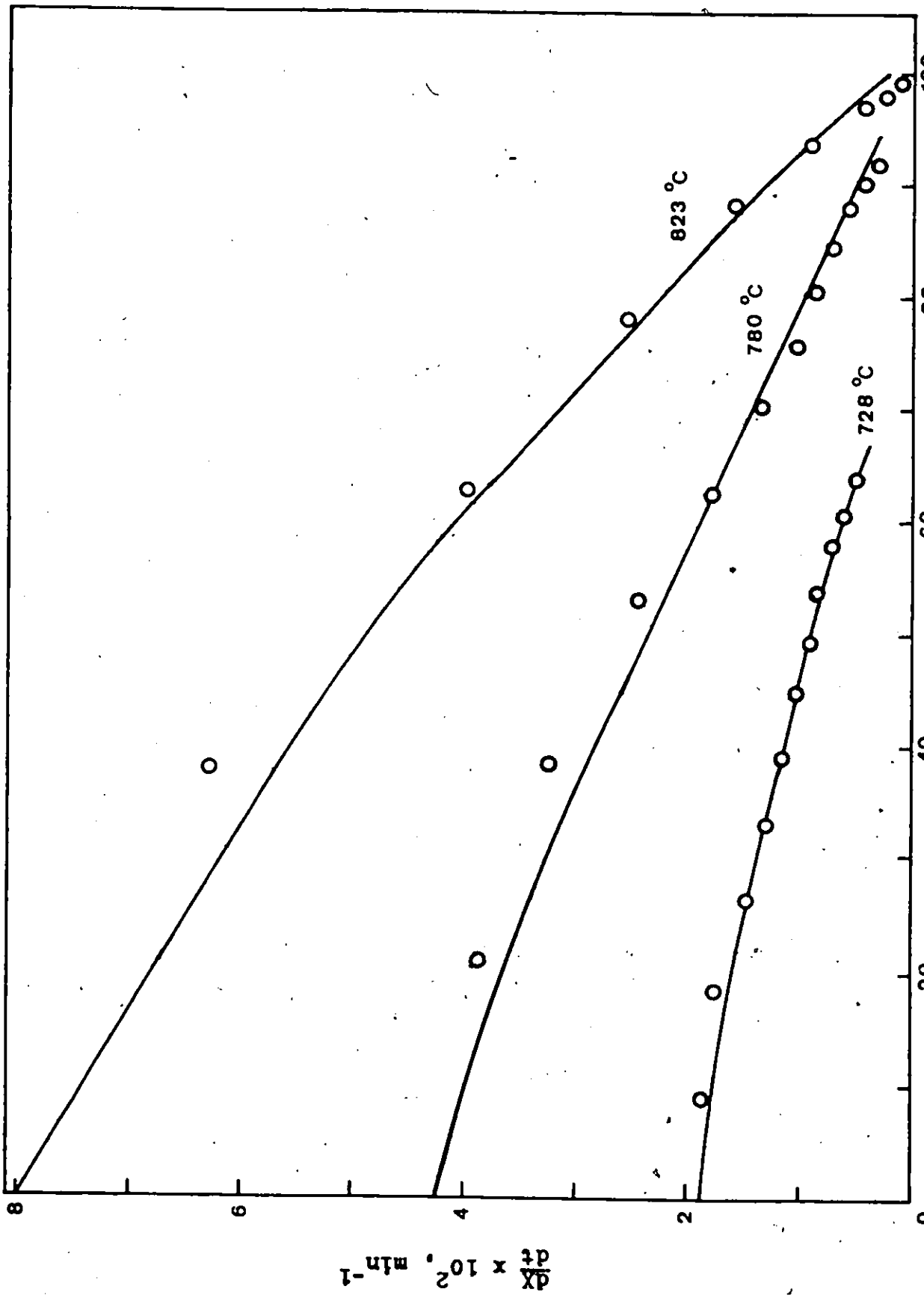

Figure 36. Predicted(solid lines) and Experimental(points) Rates. Lignite Char + 10% K_2CO_3.

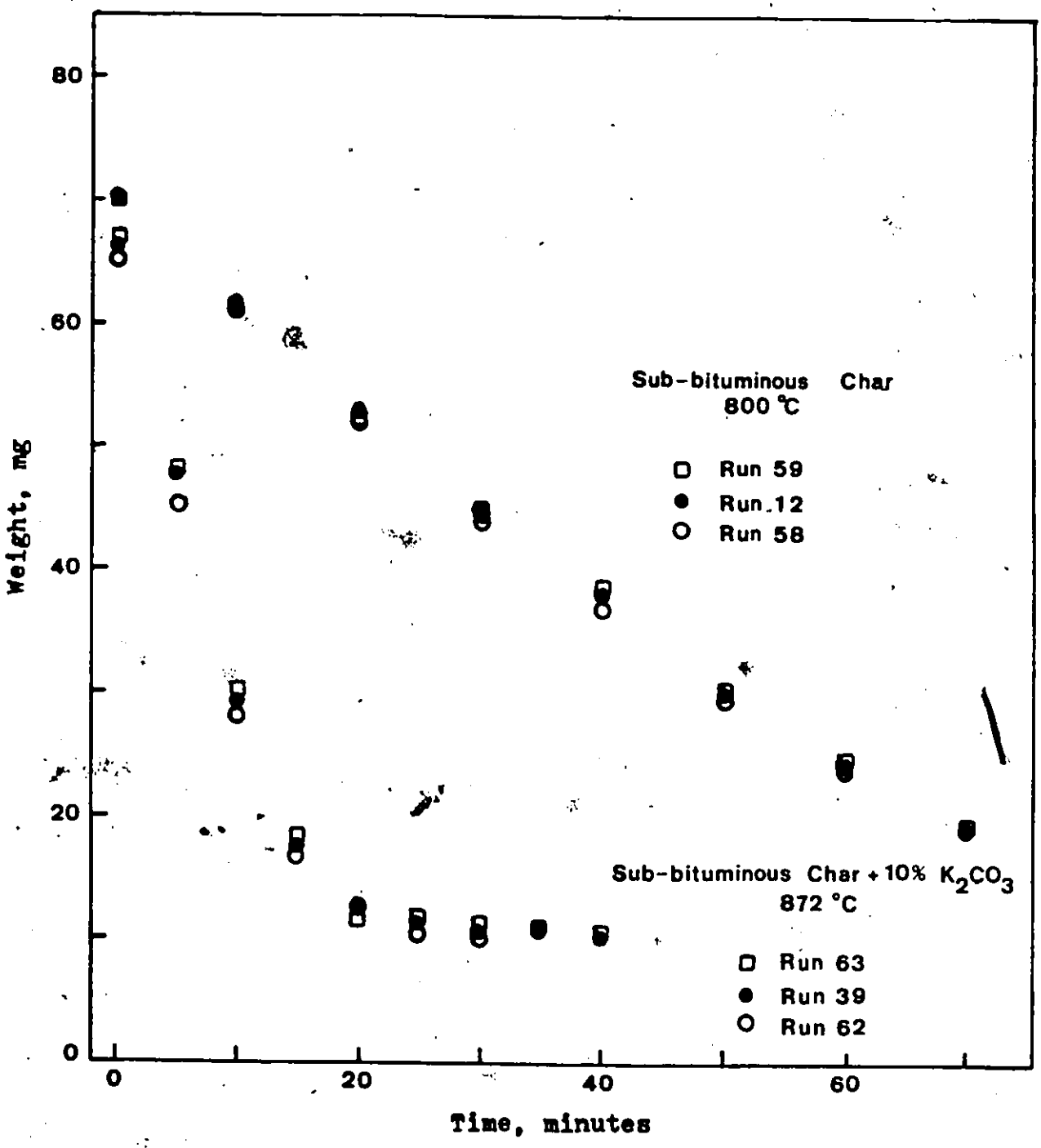

Figure 37. Weight loss vs. Time for Two Sets of Replicates

CHAPTER 6

DISCUSSION

In this chapter, the reactivities of the chars, the effectiveness of the catalysts used, and the kinetics of gasification will be discussed. In addition, the mechanism of catalytic gasification will be considered.

6.1 Kinetics of Gasification

Under the experimental conditions of this study the carbon-carbon dioxide reaction was chemical reaction controlled, and a modified unreacted-core model was found to represent the experimental data best. The rate expression is as follows:

$$\frac{dX}{dt} = \frac{3k_s C_{Ag}}{\rho_B R_p} (1-X)^{2/3} (1\pm 100X^{\alpha} e^{-\beta X}) \qquad (6.1)$$

The rate expression is applicable for both catalyzed and uncatalyzed gasification. The plus and minus sign indicates an increase (+) or decrease (-) of reaction rate per unit surface area with respect to conversion. The plus sign (increase in rate) was used for all runs except when chars contained K_2CO_3 and at lower temperatures. The rate expression is empirical and does not reveal information about the mechanism of the reaction. However it has physical significance and expresses reaction rates at any conversion level.

The last term $(1+100X^{\alpha}e^{-\beta X})$ was introduced to account for

the geometrical instability of the reacting solid surface, and was firstly proposed by Dutta et al. (15) who used a modified volume reaction model to describe the gasification of a number of coals and chars with carbon dioxide.

Jensen (57) used the unreacted-core model to interpret his results of carbon-steam reaction. Nand (58) proposed a modified unreacted-core model for both catalyzed and non-catalyzed reaction of a lignite char with steam.

As far as the mechanism of the carbon-carbon dioxide reaction is concerned, numerous studies have been conducted so far. Most of the evidence supported a two step mechanism. In the first step, CO_2 dissociates on a carbon site producing a CO molecule and an oxygen-carbon complex which gasifies to produce CO molecule. The product carbon monixide is known to inhibit the reaction, however in the present study with pure carbon dioxide as the feed gas, the carbon monoxide production is only a few percent and therefore its inhibiting effect is insignificant.

The values of the rate constant K_s obtained for both catalyzed and uncatalyzed gasification are shown in Table 6.1.

TABLE 6.1

COMPARISON OF THE RATE CONSTANT VALUES

	$k_s x 10^2$ (cm/s)		
Lignite char	None	10% K_2CO_3	5% Ni
728°C	0.65	2.13	1.00
823°C	4.11	10.0	5.70
Sub-bituminous char			
728°C	0.50	0.90	—
821°C	2.52	3.97	—

The rate constant, k_s, increased with the addition of catalyst which is consistent with the increase of gasification rates. From the Table it can also be seen that addition of K_2CO_3 to the chars resulted in a higher increase of k_s than nickel, thus K_2CO_3 is a better catalyst. Also K_2CO_3 in lignite char was more effective than in the sub-bituminous char.

In Table 6.2 the values of the activation energies are given.

TABLE 6.2

COMPARISON OF ACTIVATION ENERGIES

	E (kJ /mole)		
	None	10% K_2CO_3	5% Ni
Lignite char	176	141	159
Sub-bituminous char	155	152	—

For the uncatalyzed gasification, Spiro et al. (44) reported an activation energy of 214 kJ /mole for a North Dakota lignite, and 239 kJ /mole for a Navajo sub-bituminous char. Dutta et al. (15) found an activation energy of 247 kJ /mole for a number of coals and chars. Knight and Sergeant (31) reported activation energies in the range 219 to 233 kJ /mole for four coal chars.

Nand (58) studied the gasification of lignite char with steam. From his results he obtained an activation energy of 117 kJ /mole for the carbon-carbon dioxide reaction.

Lowry (59) in 1963, reviewed the kinetics of gasification of coals, chars, cokes or graphite. The activation energies for the C-CO_2 reaction were in the range 100 to 259 kJ /mole.

The activation energies of 176 kJ /mole for the lignite char and 155 kJ/mole for the sub-bituminous char obtained in the present study are comparable with those reported in literature. However they fall in the lower range of those

obtained by other investigators (see Table 2.1). This indicates that the reactions were catalyzed by the impurities present in the chars. This inherent catalytic effect has been pointed out by several investigators but little systematic study has been conducted (3, 10, 18, 20, 23, 26).

Since the structural disorders and the amount of impurities present increase with decreasing coal rank, it would be expected that the activation energy of the lignite char would be lower than that of the sub-bituminous char. Instead it is higher by 20.9 kJ/mole, although lignite char is more reactive. It can be said then that the degree of inherent catalysis is greater for the sub-bituminous char. The chemical composition of the ash for both chars should be known to substantiate this. It can be seen from Table 6.2 that the activation energies decreased in the presence of catalyst for the lignite whereas for the sub-bituminous char the decrease was insignificant. Thus the catalytic effect for the sub-bituminous char was mainly to increase the number of active sites. Unfortunately very few kinetic studies in catalytic gasification have been reported in the literature.

Nand (59) investigated the carbon-carbon dioxide reaction (lignite char) and reported an activation energy increase from 117 to 150 kJ /mole for 10% K_2CO_3 and a decrease to 83.7 kJ /mole for 10% Na_2CO_3.

Walker et al. (7) found an activation energy decrease from 87 kcal/mole (pure graphite) to 318 kJ /mole when Ni was present at 300 ppm. McKee (48) pointed out that activation energies are relatively insensitive to the presence of catalysts.

For the lignite char containing 10% K_2CO_3, the activation energy decreased from 176 to 141 kJ /mole. This decrease was much larger than in the case of lignite containing Ni. However for the other char containing K_2CO_3, there was no activation energy decrease. The activation energies found in the present study for catalytic gasification agree well with those reported by Nand (58).

From Figures 17, 18, 30 and Tables 5.3, 5.6, it is seen that for uncatalyzed gasification and for lignite char containing Ni, the degree of change of reaction rate per unit surface area with respect to conversion is relatively independent of temperature. Thus average values of α and β can be used for the whole temperature range, and reaction rates can be predicted at any temperature and conversion level. Dutta et al. (15) similarly found the constants α, β to be independent of temperature for most of the coals and chars used. However for the case of the chars containing K_2CO_3, the change of rate per unit surface area with conversion was a function of temperature (Figures 31, 32).

6.2 Gasification Rates and Catalyst Effectiveness

In uncatalyzed gasification, the reactivity of lignite char was found to be 0.0634 min^{-1} at 872°C and that of sub-bituminous char, 0.0415 min^{-1} at the same temperature. Lignite was more reactive which is in accordance with the reactivity increasing with decreasing rank of the parent coal (4, 10, 11, 12, 15, 23).

Johnson (5), from the studies of different investigators, calculated the reactivities of several coal chars. These, at 900°C, 1 atm and in pure CO_2, ranged from 0.0002 min^{-1} for Ceylon graphite to 0.093 min^{-1} for North Dakota lignite. The reactivities were 0.020 to 0.195 min^{-1} for four different lignites, and 0.022 to 0.077 min^{-1} for two sub-bituminous chars. Also, Spiro et al. (44) reported a reactivity of 0.05 min^{-1} for a North Dakota lignite char, and 0.025 min^{-1} for a Navajo sub-bituminous char at 900°C. Thus the reactivities of the chars found in the present study agree well with those reported by other workers.

It should be pointed out that lignites and to a lesser extent sub-bituminous chars, exhibit a wide range of reactivities which cannot be attributed to different experimental setups and methods of data evaluations alone. It is rather due to the different chemical and physical characteristics of the chars (3, 5, 10, 15, 18, 44).

Both chars were prepared by pyrolysis of the respective coals at 927°C in a stream of He. The effect of pretreatment temperatures has been discussed by Blackwood and Ingeme (21). They heated E. Marginata char in nitrogen at different temperatures from 650 to 950°C. The subsequent reactivity of the char samples in CO_2, at 1.2 atm and 650°C decreased drastically up to 900°C (preparation temperature) and then levelled-off with increasing temperature. McKee (52) reported that the reactivities of several coal chars decreased when the charring temperature was increased from 700° to 1000°C. They attributed the decrease in reactivity to the loss of surface area. According to Walker and Hippo (18, 60) increase in pretreatment temperature results in improved alignment of the crystalline planes with loss of porosity.

In the present study, the pore volumes of the chars, determined by the method described by Benesi et al. (61), were 0.035 cm^3/g for lignite and 0.011 cm^3/g for sub-bituminous char. Thus the porosities were 0.053 and 0.016 respectively. These values indicate that the chars were essentially non-porous, mainly due to the high charring temperatures (927°C). However the parent coals could not be very porous themselves. This absence of porosity led to the use of the unreacted-core model. Moreover it would be expected the chars to be more reactive if the charring temperature was lower.

It can be seen from Table 3.3 that addition of nickel nitrate to lignite char increased the porosity to about 0.07,

whereas the addition of K_2CO_3 further decreased the porosities of both chars.

It would be interesting to know the pore size distribution and surface area of both pure and catalyzed chars before and during the reaction and to correlate these structural changes with the reactivity.

As discussed previously, Ni had no effect on the reactivity of the sub-bituminous char whereas the presence of the dual catalyst (10% K_2CO_3+5% Ni) in lignite char gave almost the same results as 10% K_2CO_3. In Table 6.3 the ratios of catalyzed to non catalyzed reaction rates are shown.

TABLE 6.3

RATIOS OF CATALYZED TO NON CATALYZED REACTION RATES

Lignite char	10% K_2CO_3	20% K_2CO_3	5% Ni	10% Ni
728°C	3.60	6.29	1.38	1.35
823°C	2.68	3.21	1.25	1.24
Sub-bituminous char				
728°C	1.75	2.58	-	-
821°C	1.53	1.58	-	-

It can be seen from the Table 6.3 that increasing the concentration of nickel from 5 to 10% had no effect on the reactivity of lignite char. Thus the optimum concentration

of Ni had been reached already. Comparing ratios of the rates for the two catalysts, K_2CO_3 gave higher values, therefore it is a better catalyst. Also, although the ratio of rates increased with the increase of the K_2CO_3 concentration from 10 to 20 wt%, the effectiveness of the catalyst (increase in rate divided by the amount of catalyst) decreased. Hence, K_2CO_3 at a concentration of 10 wt% is more effective.

The conclusions on catalyst effectiveness from the present study agree with the notion that generally catalyst effectiveness increases to some optimum concentration and then either levels-off or decreases (51).

McKee et al. (43) reported a rate ratio of 3.0 for 10% K_2CO_3 in a lignite char at 700°C. In the present study, for the same concentration of K_2CO_3 in lignite and at 728°C the ratio was 3.6, in good agreement with that found by McKee et al. From these authors' results the rate ratio was 4,000 for graphite, 110 for anthracite and 7.5 for a sub-bituminous char. Obviously, the catalyst effectiveness decreased with decreasing rank of parent coal. This is due to the fact that with decreasing rank, reactivity of chars increases considerably even without the presence of a catalyst. However in the present study, for both catalysts (Ni or K_2CO_3, their effectiveness was lower for the sub-bituminous char while the opposite was expected according to the above reasoning.

Walker et al. (7), found that for graphite containing Ni

at a concentration of 300 ppm, the reaction rate increased by a factor of 160 at 900°C. Reaction rates increased by a factor of 1.4 for Ni in the present study. These results cannot be compared with those of Walker et al. since different carbon solids were used.

The high catalytic activity of alkali metal carbonates has been stressed by several investigators not only for the $C-CO_2$ reaction but also for other gasification reactions. There is a very good agreement on catalyst activity for the alkali-metal carbonates and for other catalysts in the carbon-steam and carbon-carbon dioxide reaction.

A final point to be made is that catalyst effectiveness decreased with increasing temperature for both catalysts and at all the concentrations used. Similar results were obtained by other investigators (45, 46, 51).

6.3 Mechanism of Catalytic Gasification

To this date, the mechanism of catalytic gasification is not well understood due to the lack of comprehensive studies. Out of the different mechanisms that have been proposed, the oxygen-transfer seems to be the most plausible.

The catalytic activity of alkali metal carbonates was ascribed by McKee and Chatterji (42) and other investigators (43, 44, 45, 52) to the following sequence of steps (oxygen-transfer mechanism):

$$M_2CO_3 + 2C = 2M + 3CO \quad (6.2)$$

$$2M + CO_2 = M_2O + CO \quad (6.3)$$

$$M_2O + CO_2 = M_2CO_3 \quad (6.4)$$

In this oxidation-reduction cycle, the first step is considered to be the rate determining whereas the other two steps occur rapidly. Overall reaction rates are functions of the extent of catalyst-char surface contact. Rates are accelerated above the melting point of the carbonates since the molten phase provides a better contact with the char surface. However no anomaly was observed in Arrhenius plots for temperatures above and below the melting points (43, 44, 46).

Walker et al. (7) supported an oxygen transfer mechanism for the catalytic effect of Fe, Ni, and Co for the gasification of graphite.

Although this oxidation-reduction mechanism has been supported by most of the investigators, doubts have been expressed repeatedly (6, 7, 8, 46, 58).

Wen (8) in his recent review proposed an electron-transfer mechanism and pointed out that a large number of simple and compound substances can penetrate the carbon layers, separating them and forming intermediate layers with the transfer of electrons from the inserted compound to the carbon layers or vice-versa. Thus the intercalation compounds formed are EDA (Electron-Donor-Acceptor) complexes. In the case of K_2CO_3 catalyst these

intercalates can be

$$C_8K,\ C_{24}K,\ C_{36}K,\ C_{60}K$$

and they are good electron donors. They are formed by the direct heating in the temperature range of 250 to 700°C. Potassium atoms per carbon atom decrease with increase in temperature from 250 to above 500°C. Thus at gasification temperatures intercalates of the form $C_{60}K$ would be expected.

Wen (8) proposed the following reaction steps for the catalytic action of alkali metals.

$$M_2CO_3 + 2C = 2M + 3CO \quad (6.5)$$

$$2M + 2nC = 2C_nM \quad (6.6)$$

$$2C_nM + CO_2 = (2nM).OCO = (2nC).M_2O+CO \quad (6.7)$$

$$(2nC).M_2O+CO_2 = (2nC).M_2CO_3 = 2nC+M_2CO_3 \quad (6.8)$$

Also the alkali metals may penetrate between the carbon layers resulting in the opening of the carbon structure to further attack.

McKee (52) in a review of the possible mechanisms in catalytic gasification pointed out that there is little direct evidence for the formation of intercalation compounds.

Recently Kapteijn et al. (54) heated activated carbon and coal with K_2CO_3 in nitrogen up to 827°C. X-ray analysis of the treated samples showed formation of intercalates.

Nand (58) argued that if the electron-transfer mechanism is applicable then the char samples doped with catalysts

would have unpaired electrons. He studied electron spin resonance (ESR) of lignite char and char-catalyst samples, and found the free radical relative intensity (thus the number of unpaired electrons) to increase with increasing catalytic activity.

It is obvious from the above discussion that one cannot make definite conclusions about the mechanism of catalytic gasification without further detailed research.

CHAPTER 7

CONCLUSIONS

The gasification of two chars, Saskatchewan lignite and Forestburg sub-bituminous, in carbon dioxide was studied in the temperature range 728-875°C and at atmospheric pressure. Experiments were carried out using a thermogravimetric balance. The effect of carbon dioxide flow rate, concentration, char particle size and temperature on conversion of char were investigated. Catalytic gasification was also studied with various amounts of Ni (in the form of $Ni(NO_3)_2$) and K_2CO_3 added to the chars. Carbon conversions up to 100 percent were obtained.

The following conclusions were derived.

1. A modified unreacted-core model was developed to represent reaction rates of both catalyzed and uncatalyzed gasification. The model is represented as follows:

$$\frac{dX}{dt} = \frac{3k_s C_{Ag}}{\rho_B R_p} (1-x)^{2/3} (1 \pm 100X^{\alpha} e^{-\beta X})$$

   Reaction rate is a function of carbon conversion.
2. The gas-solid reaction was chemically controlled under the experimental conditions.
3. Lignite char was more reactive than the sub-bituminous char in accordance with reactivity increasing with decreasing rank of parent coal.

4. For the uncatalyzed gasification, an activation energy of 176 kJ /mole was obtained for the lignite char and 155 kJ /mole for the sub-bituminous char indicating inherent catalytic effect.
5. For the catalyzed gasification, the activation energies were found to be 159 kJ /mole for lignite containing 5 wt% Ni, 141 kJ/mole for lignite with 10 wt% K_2CO_3 and 152 kJ /mole for the sub-bituminous char with 10 wt% K_2CO_3.
6. Nickel catalyst at a concentration of either 5 or 10 wt% in sub-bituminous char did not show any catalytic activity whereas at the same concentration levels in lignite char gasification rates increased.
7. Potassium carbonate added to both chars at 10 and 20 wt% concentrations enhanced gasification rates.
8. Catalyst effectiveness decreased with increasing catalyst concentration and reaction temperature.
9. K_2CO_3 was a better catalyst than Ni. It was most effective at a concentration of 10 wt%.
10. Due to the lack of experimental evidence no conclusion was derived regarding the mechanism of catalytic gasification.

CHAPTER 8

RECOMMENDATIONS

It became apparent from the results of the present study that some aspects needed further investigation. The following recommendations are made:

1. The catalytic effect of the impurities present in the the chars should be investigated separately from the other factors affecting char reactivity.
2. The effect of charification conditions on the reactivities should also be investigated.
3. Pore volume, pore size distribution, surface area should be determined during conversion and related to reaction rates.
4. The conditions and method of catalyst addition needs further research because it is a very important factor in determining catalyst effectiveness and has been systematically overlooked.
5. There is still a great need for research about the catalytic activity of various materials and the kinetics and mechanism of catalytic gasification. The need for this is apparent not only for the carbon-carbon dioxide reaction but for all other gasification reactions.

REFERENCES

1. Reif, A.E., J. Phys. Chem., 56, 785 (1952).

2. Von Fredstroff, G.G. and Elliot, M.A., Chemistry of Coal Utilization, Ed. H.H. Lowry, Supplementary Volume, p. 892, Willey, New York, 1963.

3. Walker, P.L., Jr., Ruskino, F., Jr. and Austin, L.G., Advances in Catalysis, Vol. 11, p. 134, Academic Press, Inc., New York, 1959.

4. Mentser, M. and Ergun, S., U.S. Bur. Mines Bull. (664), 42 pp. (1973).

5. Johnson, J.L., Chemistry of Coal Utilization, Ed. H.H. Lowry, Supplementary Volume, p. 1566, Willey, New York, 1981.

6. Taylor, H.S. and Neville, H.A., J. Am. Chem. Soc., 43, 2055 (1921).

7. Walker, P.L. Jr., Shelef, M. and Anderson, R.A., Chemistry amd Physics of Carbon, Vol. 4, p. 287, Marcel Dekker, New York, 1968.

8. Wen, W.Y., Catal. Rev.-Sci. Eng. 22(1), 1 (1980).

9. Schilling, H.D., Bonn, B. and Krauss, U., "Coal Gasification", Graham and Trotman, London, 1981.

10. Katta, S. and Keairns, D.L., Ind. Eng. Chem. Fundam., 20, 6 (1981).

11. Gadsby, J., Long, F.J., Sleightholm, P. and Sykes, K.W., Proc. Roy. Soc. (London), A193, 357 (1948).

12. Walker, P.L., Jr., Foresti, R.J., Jr. and Wright, C.C., Ind. Eng. Chem., 45, 1703 (1953).

13. Walker, P.L., Jr. and Raats, E., J. Phys. Chem., 60, 370 (1956).

14. Rao, Y.K. and Jalan, B.P., Metall. Trans., 3, 2405 (1972).

15. Dutta, S., Wen, C.Y. and Belt, R.J., Ind. Eng. Chem. Process Des. Dev., 16, 20 (1977).

16. Peterson, E.E. and Wright, C.C., Ind. Eng. Chem., 47, 1624 (1955).

17. Turkdogan, E.T. and Vinters, J.V., Carbon, 7, 101 (1969).

18. Walker, P.L., Jr. and Hippo, E.J., Prepr. Pap. Natl. Meet., Div. Fuel Chem., Am. Chem. Soc., 20(3), 45 (1975).

19. Ergun, S.J., Phys. Chem., 60, 480 (1956).

20. Ergun, S., U.S. Bur. Mines Bull., (598), 38 pp. (1962).

21. Blackwood, J.D. and Ingeme, A.J., Aust. J. Chem., 13, 194 (1960).

22. Turkdogan, E.T. and Vinters, J.V., Carbon, 8, 39 (1970).

23. Fuchs, W. and Yavorsky, P.M., Prepr. Pap. Natl. Meet., Div. Fuel Chem., Am. Chem. Soc., 20 (3), 115 (1975).

24. Rao, P.V.N.R. and Petersen, E.E., Ind. Eng. Chem., 50, 331 (1958).

25. Walker, P.L., Jr. and Rusinko, F., Jr., J. Phys. Chem., 59, 241 (1955).

26. Sakawa, M., Sakurai, Y. and Hara, Y., Fuel 61, 717 (1982).

27. Walker, P.L., Jr. and Raats, E., J. Phys. Chem., 60, 364 (1956).

28. Smith, J.M., "Chemical Engineering Kinetics", 2nd Ed., McGraw-Hill Book Co., New York, 1981.

29. Lewis, W.K., Gilliland, E.R, and McBride, G.T., Jr., Ind. Eng. Chem., 41, 1213 (1949).

30. Wen, C.Y. and Wu, N.T., AIChE J., 22, 1012 (1976).

31. Knight, A.T. and Sergeant, G.D., Fuel, 61, 145 (1982).

32. Wen, C.Y., Ind. Eng. Chem., 60, 34 (1968).

33. Ishida, M. and Wen, C.Y., AIChE J., 14, 311 (1968).

34. Ishida, M. and Wen, C.Y., Chem. Eng. Science, 26, 1031 (1971).

35. Wen, C.Y. and Wu, L.Y., AIChE J., 16, 848 (1970).

36. Yoshida, K. and Kunii, D., J. Chem. Eng. Japan, 2, 170 (1969).

37. Szekely, J. and Evans, J.W., Chem. Eng. Science, 25, 1091 (1970).

38. Szekely, J. and Evans, J.W., Chem. Eng. Science, 26, 1901 (1971).

39. John, H.Y. and Szekely, J., Chem. Eng. Science, 27, 763 (1972).

40. John, H.Y. and Szekely, J., Chem Eng. Science, 28, 1169 (1973).

41. Chida, T. and Tadaki, T., Int. Chem. Eng., 22, 503 (1982).

42. McKee, D.W. and Chatterji, D., Carbon, 13, 381 (1975).

43. McKee, D.W,, Spiro, C.L., Kosky, P.G. and Lamby, E.J., Fuel, 62, 217 (1983).

44. Spiro, C.L., McKee, D.W., Kosky, P.G. and Lamby, E.J., Fuel, 62, 180 (1983).

45. Fox, D.A. and White, A.H., Ind. Eng. Chem., 23, 259 (1931).

46. Jalan, B.P. and Rao, Y.K., Carbon, 16, 175 (1978).

47. Marsh, H. and Mochida, I., Fuel, 60, 231 (1981).

48. McKee, D.W., Fuel, 59, 308 (1980).

49. Tashiro, J., Takakuwa, J. and Yokoyama, S., Fuel, 55, 250 (1976).

50. Yamada, T., Tomita, A. Tamai, V. and Homma, T., Fuel, 62, 246 (1983).

51. Johnson, J.L., Chemistry of Coal Utilization, Ed. H.H. Lowry, Supplementary Volume, p. 1594, Willey, New York, 1981.

52. McKee, D.W., Fuel, 62, 170 (1983).

53. Long, F.J. and Sykes, K.W., Proc. Roy. Soc. (London), A215, 100 (1952).

54. Kapteijn, F., Jurriaans, J. and Moulijn, J.A., Fuel, 249 (1983).

55. Levenspiel, O., "Chemical Reaction Engineering", 2nd Ed., Willey, New York, 1972.

56. Cannon, K.R., Denbigh, K.G., Chem. Eng. Sci., 6, 145, 155 (1957).

57. Jensen, G.A., Ind. Eng. Chem. Process Des. Dev., 14, 308 (1975).

58. Nand, S.: Ph.D. Thesis, University of Ottawa, 1982.

59. Lowry, H.H., Chemistry of Coal Utilization, Supplementary Vol., Willey, New York, 1963.

60. Hippo, E. and Walker, P.L., Jr., Fuel, 54, 245 (1975).

61. Benesi, H.A., Bonnar, R.V. and Lee, C.F., Anal. Chem., 27, 1963 (1955).

62. Laurendeau, N.M., Prog. Energy Combust. Sc. Vol. 4, 221, Pergamon Press Ltd., Great Britain, 1978.

63. Ranz, W.E. and Marshall, W.R., Jr., Chem. Eng. Prog., 48, 141 (1952).

64. Ranz, W.E. and Marshall, W.R., Jr., Chem. Eng. Prog., 48, 173 (1952).

65. Bird, R.B., Stewart, W.E. and Lightfoot, E.N. "Transport Phenomena", Wiley, New York, 1960.

APPENDIX A

SAMPLE CALCULATIONS

A sample calculation for Run 24 is given here. It is representative of the calculations involved in every run.

In Run 24, the flow rate of CO_2 was 150 cm^3/min and the particle size was 0.500-0.595 mm . A lignite char sample of 80 mg was placed in the reactor. When the temperature reached 802°C and stabilized, the weight of the char sample, W_i, was 73.1 mg. The weight of the residual was 14.5 mg. From the carbon analysis, the residual had a carbon content of 26.9% or 3.9 mg of carbon. Thus at the start of the reaction the weight of carbon was

$$W_c = (73.1-14.5) + 3.9 = 62.5 \text{ mg}$$

From the recorder chart, the weight of the char was taken every five minutes. Subsequently the conversion, and partial pressures of CO_2 and CO were calculated. The reaction rate was determined using the DGT3 computer program.

In Table A-1 the results are shown for Run 24.

TABLE A-1

LIGNITE CHAR

t (min)	w (mg)	X (%)	dx/dt (min)	pCO_2 (atm)	pCO (atm)
0.0	73.1	0.0	0.0205	1.0	0
5.0	66.5	10.6	0.0205	0.9655	0.0345
10.0	60.3	20.5	0.0197	0.9666	0.0334
15.0	54.2	30.2	0.0189	0.9682	0.0318
20.0	48.5	39.4	0.0178	0.9703	0.0297
25.0	43.1	48.0	0.0173	0.9703	0.0297
30.0	37.7	56.6	0.0165	0.9730	0.0270
35.0	32.8	64.5	0.0149	0.9741	0.0259
40.0	28.4	71.5	0.0130	0.9784	0.0216
45.0	24.7	77.4	0.0106	0.9821	0.0179
50.0	21.8	82.1	0.0080	0.9864	0.0136
55.0	19.7	85.4	0.0061	0.9897	0.0103
60.0	18.0	88.2	0.0048	0.9919	0.0081
65.0	16.7	90.2	0.0045	0.9934	0.0066
70.0	15.2	92.6	0.0035	0.9940	0.0060
75.0	14.5	93.8	0.0010	0.9940	0.0060

The conversion was found according to the following equation:

$$X = \frac{W_i - W}{W_c}$$

For example at t = 30.0 min

$$X = \frac{73.1-37.7}{62.5} = 0.566$$

The reaction rate (dx/dt) was found to be 0.0165 min^{-1} at t=30.0 min using the DGT3 program.

The partial pressures of CO_2 and CO were calculated from the stoichiometry of the reaction and carbon gasified. That is

$$C + CO_2 = 2CO$$

At t=30.0, the partial pressures were calculated as follows: From the chart, the weight of char at 27.5 and 32.5 minutes were 40.3 and 35.3 mg respectively. The volume of CO_2 that reacted during the five minutes period is:

$$\text{Vol. } CO_2 \text{ reacted} = \frac{(40.3-35.2) \times 10^{-3} g \times 24{,}200 cm^3/mole}{12 g/mole}$$

$$= 10.28 \text{ cm}^3$$

where 24,200 is the molar volume of a gas at 22°C (room temperature) and 1 atm, and 12 the molecular weight of carbon. Then the volume of CO_2 produced is:

$$\text{Vol. CO} = 2 \times 10.28 \text{ cm}^3 = 20.56 \text{ cm}^3$$

The volume of CO_2 present in the 5 minute period is

$$\text{Vol. } CO_2 = 5 \text{ min} \times 150 \text{ cm}^3/\text{min} - 10.28 \text{ cm}^3$$

$$= 739.72 \text{ cm}^3$$

The total volume is:

$$\text{Total Vol.} = (739.72 + 20.56)\text{cm}^3 = 760.28\text{cm}^3$$

Thus

$$pCO_2 = \frac{739.72}{760.280} = 0.9730 \text{ atm}$$

$$pCO = \frac{20.56}{760.280} = 0.0270 \text{ atm}$$

APPENDIX B

GAS FILM DIFFUSION

Two methods were used to determine whether gas film diffusion was controlling or not. The one by Laurendeau (62) and the other by Ranz and Marshall (63, 64).

B-1 Uncatalyzed Gasification

a) Laurendeau (63) has derived an expression for the highest possible reactivity allowed by the gas film diffusion during a char-gas reaction and is as follows:

$$r_{m,D} = \frac{12\Lambda D_{AB} C_A}{\sigma d^2} \qquad \text{(B-1)}$$

where $r_{m,D}$ = specific gasification rate limited by diffusion, s^{-1}

r_m = specific gasification rate obtained experimentally, s^{-1}.

Λ = gravimetric stoichiometric coefficient

D_{AB} = binar diffusivity of carbon dioxide in nitrogen, cm^2/s

C_A = carbon dioxide concentration, g/cm^3

σ = particle density of char, g/cm^3

d = char particle diameter, cm

During the uncatalyzed runs, maximum gasification rates

were obtained in Run 25 for the lignite char.

The gravimetric stoichiometric coefficient is given by

$$\Lambda = \frac{M_c}{M_g} = \frac{12}{44} = 0.273$$

where M_c = molecular weight of carbon

M_g = molecular weight of CO_2

The carbon dioxide concentration is given by

$$C_A = \frac{P}{RT}$$

where P = carbon dioxide partial pressure = 1 atm

T = Reaction temperature = 872°C or 1145 K

$$C_A = \frac{1}{82(1145)} \times 44 = 4.69 \times 10^{-4} \text{ g/cm}^3$$

The diffusivity of carbon dioxide in nitrogen is calculated from Gilliland equation.

$$D_{AB} = 0.0043 \frac{T^{3/2}}{P(V_A^{1/3}+V_B^{1/3})^2} \left[\frac{1}{M_A} + \frac{1}{M_B}\right]^{-1/2}$$

Here V_A = molar volume of carbon dioxide = 34.0 cm^3/mole

V_B = molar volume of nitrogen = 31.2 cm^3/mole

M_A = molecular weight of carbon dioxide = 44

M_B = molecular weight of nitrogen = 14

Then $D_{AB} = 8.00 \text{ cm}^2/\text{s}$. For the lignite char

$\sigma = 1.6386 \text{ g/cm}^3$

$d = 0.0548$ cm

Substituting the values in equation B-1:

$$r_{m,D} = \frac{12(0.273)(4.69 \times 10^{-4})\ (8.00)}{(1.6386)(0.0548)^2} = 2.498\ s^{-1}$$

The highest reactivity during Run 25 is

$$r_m = 0.0011\ s^{-1}$$

Therefore $r_m << r_{m,D}$

Hence the $C\text{-}CO_2$ reaction is not limited by gas film diffusion.

b). The magnitude of the film resistance can also be estimated from the dimensionless correlation by Ranz and Marshall (63, 64).

That is

$$\frac{k_g d}{D_{AB}} = 2 + 0.6\left[\frac{\mu}{C_A D_{AB}}\right]^{1/3}\left[\frac{duC_A}{\mu}\right]^{1/2} \qquad \text{(B-2)}$$

From the previous section

$$d = 0.0548\ cm$$

$$D_{AB} = 8.00\ cm^2/s$$

$$C_A = 4.69 \times 10^{-4}\ g/cm^3$$

The velocity of the gas stream is given by

$$u = \frac{Q}{\frac{\pi}{4} D^2}$$

where Q = flow rate of the gas stream = 150 cm^3/min.

D = diameter of the reactor = 3.5 cm

Therefore

$$u = \frac{150}{\frac{\pi}{4}(3.5)^2\ (60)} = 0.260\ cm/s$$

The viscosity can be calculated from the critical properties of CO_2.

$$\mu_c = 7.70\ M_A^{1/2}\ P_c^{2/3} T_c^{-1/6}$$

where T_c = critical temperature = 304.2 K

P_c = critical pressure = 72.9 atm

M_A = molecular weight of CO_2 = 44

μ_c = critical viscosity of CO_2

Therefore

$$\mu_c = 7.70(44)^{1/2}\ (72.9)^{2/3}\ (304.2)^{-1/6} = 343.7\ \mu pc$$

The reduced temperature and pressure are:

$$Tr = \frac{T}{T_C} = \frac{1145}{304.2} = 3.76$$

$$P_r = \frac{1}{72.9} = 0.014$$

From Figure 1.3-1 in Bird et al (65)

$$\mu_r = 1.4\ \frac{\mu}{\mu_c}$$

Thus

$$\mu = 1.4 \times 343.7 \times 10^{-6}\ g\ cm^{-1}\ s^{-1} = 4.8 \times 10^{-4}\ g\ cm^{-1} s^{-1}$$

From Equation B-2, the mass transfer coefficient, k_g, is:

$$k_g = \frac{8.00}{0.0548}\left[2+0.6\left[\frac{4.8\times10^{-4}}{4.69\times10^{-4}\times8.00}\right]^{1/3} x \left[\frac{0.0548\times2.060\times4.69\times10^{-4}}{4.8\times10^{-4}}\right]^{1/2}\right]$$

$$k_g = 297 \text{ cm/s}$$

The reaction rate when film diffusion is controlling is:

$$r_{m,F} = \frac{dx}{dt} = \frac{3k_g D_{Ag}}{\rho_B R_p}$$

where $C_{Ag} = \frac{1}{82(1145)} = 1.06 \times 10^{-5}$ moles/cm^3

$\rho_B = 0.1001$ moles/cm^3

$R_p = 0.0274$ cm

Thus

$$r_{m,F} = \frac{3(297)(1.06 \times 10^{-5})}{(0.1001)(0.0274)} = 3.44 \text{ s}^{-1}$$

The highest reactivity for Run 25 is

$$r_m = 0.0011 \text{ s}^{-1}$$

Therefore $r_m << r_{m,F}$

Hence the C-CO_2 reaction is not limited by gas film diffusion.

B-2 Catalyzed Gasification

For catalyzed gasification, the highest reaction rate was obtained in Run 45.

a) In Run 45, the conditions were

$T = 872°C = 1145$ K

$\Lambda = 0.273$

$D_{AB} = 8.00$ cm^3/s

$C_A = 4.69 \times 10^{-4}$ g/cm^3

$d = 0.0548$ cm

$\sigma = 1.6550$ g/cm^3

From Laurendeau's expression (B-1)

$$r_{m,D} = \frac{12(0.273)(8.00)(4.69 \times 10^{-4})}{(1.6550)(0.0548)^2} = 2.473 \text{ s}^{-1}$$

Maximum reactivity obtained during Run 45 is

$$r_m = 0.00225 \text{ s}^{-1}$$

Again $r_m << r_{m,D}$, and the reaction is not limited by gas film diffusion.

b) From the correlation of Ranz and Marshall, the rate $r_{m,F}$ is:

$$r_{m,F} = 3.44 \text{ s}^{-1}$$

The observed rate is

$$r_m = 0.00225 \text{ s}^{-1}$$

Thus $r_m << r_{m,F}$ and the C-CO_2 reaction is not limited by film diffusion for both catalyzed and non-catalyzed.

APPENDIX C

GASIFICATION DATA

Experimental and calculated data for all the successful runs are given. On the top of each page, the type of char and catalyst, if present, is given. Also given are the weight of the char sample at the start of the reaction, the weight of the carbon present in the char sample, the temperature of the reaction, the particle size, and the CO_2 flow rate. In the runs where nitrogen was also fed during the reaction, its flow rate is recorded.

The weight, conversion, and differential rate with reaction time are given in the Table.

RUN NUMBER 1

SUB-BITUMINOUS CHAR

WEIGHT OF CHAR=69.8 mg

WEIGHT OF CARBON=61.7 mg

TEMPERATURE=821 °C

PARTICLE SIZE=0.354-0.420 mm

FLOW RATE OF CO_2=22 ml/min

TIME (min)	WEIGHT (mg)	CONVERSION (%)	REACTION RATE (min^{-1})
0	69.8	0.0	0.0126
5	66.1	6.0	0.0126
10	62.0	12.6	0.0126
15	58.3	18.6	0.0125
20	54.3	25.1	0.0125
25	50.6	31.1	0.0123
30	46.7	37.4	0.0123
35	43.0	43.4	0.0123
40	39.1	49.7	0.0126
45	35.2	56.0	0.0123
50	31.5	62.0	0.0117

RUN NUMBER 2

SUB-BITUMINOUS CHAR

WEIGHT OF CHAR=70.3 mg

WEIGHT OF CARBON=62.2 mg

TEMPERATURE=821 ^{o}C

PARTICLE SIZE=0.354-0.420 mm

FLOE RATE OF CO_2=35 ml/min

TIME (min)	WEIGHT (mg)	CONVERSION (%)	REACTION RATE (min^{-1})
0	70.3	0.0	0.0143
5	65.8	7.2	0.0146
10	61.2	14.6	0.0150
15	56.5	22.2	0.0151
20	51.8	29.7	0.0150
25	47.2	37.1	0.0148
30	42.6	44.5	0.0148
35	38.0	51.9	0.0143
40	33.7	58.8	0.0133
45	29.7	65.3	0.0127
50	25.8	71.5	0.0124

RUN NUMBER 3

SUB-BITUMINOUS CHAR

WEIGHT OF CHAR=70.9 mg

WEIGHT OF CARBON=62.7 mg

TEMPERATURE=821 °C

PARTICLE SIZE=0.354-0.420 mm

FLOW RATE OF CO_2=55 ml/min

TIME (min)	WEIGHT (mg)	CONVERSION (%)	REACTION RATE (min^{-1})
0	70.9	0.0	0.0204
5	64.8	9.7	0.0185
10	59.3	18.5	0.0175
15	53.8	27.3	0.0175
20	48.3	36.0	0.0166
25	43.4	43.9	0.0155
30	38.6	51.5	0.0139
35	34.7	57.7	0.0148
40	29.3	66.4	0.0152
45	25.2	72.9	0.0121
50	21.7	78.5	0.0102

RUN NUMBER 4

SUB-BITUMINOUS CHAR

WEIGHT OF CHAR=71.2 mg

WEIGHT OF CARBON=62.0 mg

TEMPERATURE=821°C

PARTICLE SIZE=0.354-0.420 mm

FLOW RATE OF CO_2=81 ml/min

TIME (min)	WEIGHT (mg)	CONVERSION (%)	REACTION RATE (min^{-1})
0	71.2	0.0	0.0224
5	64.3	10.9	0.0214
10	57.7	21.4	0.0195
15	52.0	30.5	0.0183
20	46.2	39.7	0.0183
25	40.5	48.7	0.0183
30	34.7	57.9	0.0171
35	29.7	65.9	0.0154
40	25.0	73.3	0.0143
45	20.7	80.1	0.0132
50	16.7	86.5	0.0122

RUN NUMBER 5

SUB-BITUMINOUS CHAR

WEIGHT OF CHAR=70.4 mg

WEIGHT OF CARBON=62.3 mg

TEMPERATURE=821 °C

PARTICLE SIZE=0.354-0.420 mm

FLOW RATE OF CO_2=117 ml/min

TIME (min)	WEIGHT (mg)	CONVERSION (%)	REACTION RATE (min^{-1})
0	70.4	0.0	0.0196
5	64.2	10.0	0.0202
10	57.8	20.2	0.0199
15	51.8	29.1	0.0189
20	46.0	39.2	0.0189
25	40.0	48.8	0.0189
30	34.2	58.1	0.0167
35	29.6	65.5	0.0148
40	25.0	72.9	0.0146
45	20.5	80.1	0.0136
50	16.5	86.5	0.0120

RUN NUMBER 6

SUB-BITUMINOUS CHAR

WEIGHT OF CHAR=70.9 mg

WEIGHT OF CARBON=62.7 mg

TEMPERATURE=821°C

PARTICLE SIZE=0.707-0.841 mm

FLOW RATE OF CO_2=150 ml/min

TIME (min)	WEIGHT (mg)	CONVERSION (%)	REACTION RATE (min^{-1})
0	70.9	0.0	0.0206
5	64.5	10.2	0.0203
10	58.2	20.2	0.0203
15	51.8	30.4	0.0190
20	46.3	39.2	0.0185
25	40.2	48.9	0.0185
30	34.7	57.7	0.0167
35	29.7	65.7	0.0152
40	25.2	72.8	0.0129
45	21.6	79.2	0.0105
50	18.6	83.4	0.0086

RUN NUMBER 7

SUB-BITUMINOUS CHAR

WEIGHT OF CHAR=69.1 mg

WEIGHT OF CARBON=61.2 mg

TEMPERATURE=821 °C

PARTICLE SIZE=0.500-0.595 mm

FLOW RATE OF CO_2=150 ml/min

TIME (min)	WEIGHT (mg)	CONVERSION (%)	REACTION RATE (min^{-1})
0	69.1	0.0	0.0201
5	63.0	10.0	0.0198
10	57.0	19.8	0.0200
15	50.7	30.1	0.0200
20	44.6	40.1	0.0188
25	39.2	48.9	0.0176
30	33.8	57.7	0.0167
35	29.0	66.6	0.0150
40	24.6	72.7	0.0136
45	20.7	79.1	0.0116
50	17.5	84.4	0.0095
55	14.9	88.6	0.0074
60	13.0	91.7	0.0051
65	11.8	93.7	0.0044
70	10.3	96.2	0.0033
75	9.8	97.0	0.0016

RUN NUMBER 8

SUB-BITUMINOUS CHAR

WEIGHT OF CHAR=70.8 mg

WEIGHT OF CARBON=62.7 mg

TEMPERATURE=821 °C

PARTICLE SIZE=0.354-0.420 mm

FLOW RATE OF CO_2=150 ml/min

TIME (min)	WEIGHT (mg)	CONVERSION (%)	REACTION RATE (min^{-1})
0	70.8	0.0	0.0193
5	64.5	10.0	0.0209
10	57.7	20.9	0.0211
15	51.3	31.2	0.0211
20	44.5	42.0	0.0212
25	38.0	52.3	0.0199
30	32.0	61.9	0.0182
35	26.6	70.5	0.0156
40	22.2	77.7	0.0134
45	18.2	83.9	0.0107
50	15.5	88.2	0.0065

RUN NUMBER 9

SUB-BITUMINOUS CHAR

WEIGHT OF CHAR=69.4 mg

WEIGHT OF CARBON=61.4 mg

TEMPERATURE=821 °C

PARTICLE SIZE=0.250-0.297 mm

FLOW RATE OF CO_2=150 ml/min

TIME (min)	WEIGHT (mg)	CONVERSION (%)	REACTION RATE (min^{-1})
0	69.4	0.0	0.0244
5	62.2	11.7	0.0225
10	55.6	22.5	0.0217
15	48.9	33.4	0.0217
20	42.3	44.2	0.0195
25	36.9	53.0	0.0169
30	31.9	61.0	0.0156
35	27.3	68.5	0.0138
40	23.4	75.0	0.0125
45	19.6	81.1	0.0116
50	16.3	86.5	0.0099

RUN NUMBER 10

SUB-BITUMINOUS CHAR

WEIGHT OF CHAR=71.3 mg

WEIGHT OF CARBON=63.1 mg

TEMPERATURE=728°C

PARTICLE SIZE=0.500-0.595 mm

FLOW RATE OF CO_2=150 ml/min

TIME (min)	WEIGHT (mg)	CONVERSION (%)	REACTION RATE (min^{-1})
0	71.3	0.0	0.0044
5	69.9	2.2	0.0044
10	68.5	4.5	0.0044
15	67.1	6.6	0.0046
20	65.6	9.0	0.0043
25	64.4	11.0	0.0043
30	62.9	13.3	0.0046
35	63.3	15.5	0.0043
40	61.9	17.7	0.0044
45	58.7	20.0	0.0044
50	57.4	22.0	0.0044
55	55.9	24.3	0.0046
60	54.5	26.6	0.0044
65	53.9	27.6	0.0043
70	51.8	30.9	0.0043

RUN NUMBER 11

SUB-BITUMINOUS CHAR

WEIGHT OF CHAR=70.7 mg

WEIGHT OF CARBON=62.6 mg

TEMPERATURE=780°C

PARTICLE SIZE=0.500-0.595 mm

FLOW RATE OF CO_2=150 ml/min

TIME (min)	WEIGHT (mg)	CONVERSION (%)	REACTION RATE (min^{-1})
0	70.7	0.0	0.0098
5	67.3	5.4	0.0100
10	64.4	10.0	0.0093
15	61.5	14.7	0.0094
20	58.5	19.5	0.0092
25	56.2	23.2	0.0088
30	53.0	28.3	0.0088
35	50.2	32.7	0.0082
40	47.7	36.7	0.0080
45	45.2	40.7	0.0080
50	42.7	44.7	0.0080
55	40.2	48.7	0.0078
60	37.8	52.6	0.0072
65	35.7	55.9	0.0072
70	33.3	59.7	0.0073
75	31.1	63.2	0.0067

RUN NUMBER 12

SUB-BITUMINOUS CHAR

WEIGHT OF CHAR=70.5 mg
WEIGHT OF CARBON=62.4 mg
TEMPERATURE=800°C
PARTICLE SIZE=0.500-0.595 mm
FLOW RATE OF CO_2=150 ml/min

TIME (min)	WEIGHT (mg)	CONVERSION (%)	REACTION RATE (min^{-1})
0	70.5	0.0	0.0143
5	66.0	7.2	0.0143
10	61.4	14.6	0.0138
15	57.4	21.0	0.0135
20	53.0	28.0	0.0133
25	49.1	34.3	0.0128
30	45.0	40.9	0.0127
35	41.2	47.0	0.0123
40	37.3	53.2	0.0120
45	33.7	59.0	0.0109
50	30.5	64.1	0.0103
55	27.3	69.2	0.0095
60	24.6	73.6	0.0088
65	21.8	78.0	0.0082
70	19.5	81.7	0.0071
75	17.4	85.1	0.0064

RUN NUMBER 13

SUB-BITUMINOUS CHAR

WEIGHT OF CHAR=68.9 mg

WEIGHT OF CARBON=61.0 mg

TEMPERATURE=872°C

PARTICLE SIZE=0.500-0.595 mm

FLOW RATE OF CO_2=150 ml/min

TIME (min)	WEIGHT (mg)	CONVERSION (%)	REACTION RATE (min^{-1})
0	68.9	0.0	0.0415
5	56.5	20.3	0.0398
10	44.6	39.8	0.0389
15	32.9	59.2	0.0343
20	23.7	74.1	0.0262
25	16.8	85.4	0.0192
30	12.0	93.3	0.0120
35	9.5	97.4	0.0057
40	8.5	99.0	0.0025
45	8.0	99.8	0.0010
50	7.9	100.0	-

RUN NUMBER 14

LIGNITE CHAR

WEIGHT OF CHAR=71.6 mg

WEIGHT OF CARBON=61.6 mg

TEMPERATURE=823°C

PARTICLE SIZE=0.354-0.420 mm

FLOW RATE OF CO_2=23 ml/min

TIME (min)	WEIGHT (mg)	CONVERSION (%)	REACTION RATE (min^{-1})
0	71.6	0.0	0.0157
5	66.7	8.0	0.0161
10	61.7	16.1	0.0162
15	56.7	24.2	0.0162
20	51.7	32.3	0.0157
25	47.0	40.1	0.0162
30	41.7	48.6	0.0164
35	36.9	56.4	0.0151
40	32.4	63.7	0.0140
45	28.3	70.3	0.0128
50	24.5	76.5	0.0119

RUN NUMBER 15

LIGNITE CHAR

WEIGHT OF CHAR=71.3 mg

WEIGHT OF CARBON=61.3 mg

TEMPERATURE=823°C

PARTICLE SIZE=0.354-0.420 mm

FLOW RATE OF CO_2=49 ml/min

TIME (min)	WEIGHT (mg)	CONVERSION (%)	REACTION RATE (min^{-1})
0	71.3	0.0	0.0235
5	64.2	11.6	0.0228
10	57.3	22.8	0.0227
15	50.3	34.2	0.0228
20	43.3	45.7	0.0214
25	37.2	55.6	0.0196
30	31.3	65.2	0.0178
35	26.3	73.4	0.0152
40	22.0	80.4	0.0124
45	18.7	85.8	0.0090
50	16.5	89.4	0.0054

RUN NUMBER 16

LIGNITE CHAR

WEIGHT OF CHAR=73.3 mg

WEIGHT OF CARBON=63.0 mg

TEMPERATURE=823°C

PARTICLE SIZE=0.354-0.420 mm

FLOW RATE OF CO_2=70 ml/min

TIME (min)	WEIGHT (mg)	CONVERSION (%)	REACTION RATE (min^{-1})
0	73.3	0.0	0.0300
5	64.0	14.8	0.0290
10	55.0	29.0	0.0273
15	46.8	42.0	0.0262
20	38.5	55.2	0.0240
25	31.7	66.0	0.0198
30	26.0	75.0	0.0163
35	21.4	82.3	0.0127
40	18.0	87.7	0.0094
45	15.5	91.7	0.0063
50	14.0	94.1	0.0032

RUN NUMBER 17

LIGNITE CHAR

WEIGHT OF CHAR=71.6 mg

WEIGHT OF CARBON=61.6 mg

TEMPERATURE=823°C

PARTICLE SIZE=0.354-0.420 mm

FLOW RATE OF CO_2=116 ml/min

TIME (min)	WEIGHT (mg)	CONVERSION (%)	REACTION RATE (min^{-1})
0	71.6	0.0	0.0244
5	63.2	18.4	0.0302
10	53.0	30.2	0.0318
15	43.6	45.4	0.0289
20	35.2	59.1	0.0252
25	28.1	70.6	0.0208
30	22.4	79.8	0.0167
35	17.8	87.3	0.0114
40	15.4	91.2	0.0071
45	13.4	94.4	0.0047
50	12.5	96.0	0.0011

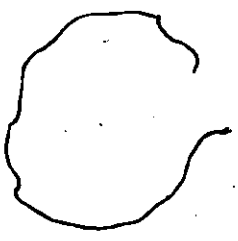

RUN NUMBER 18

LIGNITE CHAR

WEIGHT OF CHAR=71.2 mg

WEIGHT OF CARBON=61.2 mg

TEMPERATURE=823°C

PARTICLE SIZE=0.354-0.420 mm

FLOW RATE OF CO_2=150 ml/min

TIME (min)	WEIGHT (mg)	CONVERSION (%)	REACTION RATE (min^{-1})
0	71.2	0.0	0.0310
5	61.8	15.4	0.0304
10	52.6	30.4	0.0302
15	43.3	45.6	0.0289
20	34.9	59.3	0.0252
25	27.9	70.7	0.0204
30	22.4	79.7	0.0167
35	17.7	87.4	0.0116
40	15.3	91.3	0.0070
45	13.4	94.4	0.0047
50	12.4	96.0	0.0018

RUN NUMBER 19

LIGNITE CHAR

WEIGHT OF CHAR=71.0 mg

WEIGHT OF CARBON=61.1 mg

TEMPERATURE=823°C

PARTICLE SIZE=0.250-0.297 mm

FLOW RATE OF CO_2=150 ml/min

TIME (min)	WEIGHT (mg)	CONVERSION (%)	REACTION RATE (min^{-1})
0	71.0	0.0	0.0290
5	62.1	14.6	0.0293
10	53.1	29.3	0.0295
15	44.1	44.1	0.0283
20	35.8	57.6	0.0252
25	28.7	69.3	0.0208
30	23.1	78.4	0.0173
35	18.1	86.6	0.0119
40	15.8	90.4	0.0067
45	14.0	93.3	0.0051
50	12.7	95.5	0.0034

RUN NUMBER 20

LIGNITE CHAR

WEIGHT OF CHAR=70.7 mg PARTICLE SIZE=0.500-0.595 mm

WEIGHT OF CARBON=60.8 mg FLOW RATE OF CO_2=150 ml/min

TEMPERATURE=823°C

TIME (min)	WEIGHT (mg)	CONVERSION (%)	REACTION RATE (min^{-1})
0	70.7	0.0	0.0299
5	61.7	14.8	0.0299
10	52.9	29.3	0.0300
15	43.3	45.1	0.0298
20	34.8	59.0	0.0242
25	28.6	69.2	0.0186
30	23.5	77.6	0.0164
35	18.6	85.6	0.0115
40	16.5	90.0	0.0071
45	14.3	92.8	0.0061
50	12.8	95.2	0.0038
55	12.0	96.5	0.0030

RUN NUMBER 21

LIGNITE CHAR

WEIGHT OF CHAR=73.2 mg PARTICLE SIZE=0.707-0.841 mm

WEIGHT OF CARBON=62.6 mg FLOW RATE OF CO_2=150 ml/min

TEMPERATURE=823°C

TIME (min)	WEIGHT (mg)	CONVERSION (%)	REACTION RATE (min^{-1})
0	73.2	0.0	0.0251
5	65.1	12.9	0.0267
10	56.5	26.6	0.0276
15	47.8	40.6	0.0268
20	39.7	53.5	0.0251
25	32.1	65.7	0.0222
30	25.8	75.7	0.0174
35	21.2	83.1	0.0125
40	18.0	88.2	0.0096
45	15.2	92.7	0.0069
50	13.7	95.1	0.0027

RUN NUMBER 22

LIGNITE CHAR

WEIGHT OF CHAR=73.5 mg

WEIGHT OF CARBON=62.9 mg

TEMPERATURE=728°C

PARTICLE SIZE=0.500-0.595 mm

FLOW RATE OF CO_2=150 ml/min

TIME (min)	WEIGHT (mg)	CONVERSION (%)	REACTION RATE (min^{-1})
0	73.5	0.0	0.0052
5	71.9	2.6	0.0049
10	70.4	5.0	0.0049
15	68.8	7.5	0.0051
20	67.2	10.0	0.0051
25	65.6	12.6	0.0051
30	64.0	15.1	0.0051
35	62.4	17.7	0.0051
40	60.8	20.2	0.0049
45	59.3	22.6	0.0051
50	57.6	25.2	0.0052
55	56.0	27.8	0.0051
60	54.4	30.3	0.0049
65	52.9	32.7	0.0049
70	51.3	35.3	0.0051
75	49.7	37.8	0.0051

RUN NUMBER 23

LIGNITE CHAR

WEIGHT OF CHAR=70.4 mg
WEIGHT OF CARBON=60.7 mg
TEMPERATURE=780°C
PARTICLE SIZE=0.500-0.595 mm
FLOW RATE OF CO_2=150 ml/min

TIME (min)	WEIGHT (mg)	CONVERSION (%)	REACTION RATE (min^{-1})
0	70.4	0.0	0.0136
5	66.5	6.4	0.0136
10	62.3	13.3	0.0136
15	58.1	20.3	0.0133
20	54.2	26.7	0.0125
25	50.5	32.8	0.0124
30	46.7	39.0	0.0124
35	43.0	45.1	0.0120
40	39.4	51.1	0.0115
45	36.0	56.7	0.0105
50	33.0	61.6	0.0096
55	30.2	66.2	0.0086
60	27.8	70.1	0.0074
65	25.7	73.6	0.0063
70	24.0	76.5	0.0051
75	22.6	78.8	0.0041

RUN NUMBER 24

LIGNITE CHAR

WEIGHT OF CHAR=73.1 mg PARTICLE SIZE=0.500-0.595 mm

WEIGHT OF CARBON=62.5 mg FLOW RATE OF CO_2=150 ml/min

TEMPERATURE=802°C

TIME (min)	WEIGHT (mg)	CONVERSION (%)	REACTION RATE (min^{-1})
0	73.1	0.0	0.0205
5	66.5	10.6	0.0205
10	60.3	20.5	0.0197
15	54.2	30.2	0.0189
20	48.5	39.4	0.0178
25	43.1	48.0	0.0173
30	37.7	56.6	0.0165
35	32.8	64.5	0.0149
40	28.4	71.5	0.0130
45	24.7	77.4	0.0106
50	21.8	82.1	0.0080
55	19.7	85.4	0.0061
60	18.0	88.2	0.0048
65	16.7	90.2	0.0045
70	15.2	92.6	0.0035
75	14.5	93.8	0.0010

RUN NUMBER 25

LIGNITE CHAR

WEIGHT OF CHAR=71.7 mg

WEIGHT OF CARBON=61.7 mg

TEMPERATURE=872°C

PARTICLE SIZE=0.500-0.595 mm

FLOW RATE OF CO_2=150 ml/min

TIME (min)	WEIGHT (mg)	CONVERSION (%)	REACTION RATE (min^{-1})
0	71.7	0.0	0.0634
5	52.7	30.8	0.0598
10	34.8	59.8	0.0494
15	22.2	80.2	0.0337
20	14.0	93.5	0.0185
25	10.8	98.7	0.0062
30	10.2	99.7	0.0013
35	10.0	100.0	-

RUN NUMBER 26

LIGNITE CHAR
5% Ni

WEIGHT OF CHAR=75.7 mg
WEIGHT OF CARBON=60.0 mg
TEMPERATURE=728°C
PARTICLE SIZE=0.500-0.595 mm
FLOW RATE OF CO_2=150 ml/min

TIME (min)	WEIGHT (mg)	CONVERSION (%)	REACTION RATE (min^{-1})
0	75.7	0.0	0.0072
5	73.6	3.5	0.0068
10	71.6	6.8	0.0067
15	69.6	10.2	0.0068
20	67.5	13.7	0.0068
25	65.5	17.0	0.0067
30	63.5	20.3	0.0067
35	61.5	23.7	0.0070
40	59.4	27.2	0.0067
45	57.3	30.7	0.0062
50	55.4	33.8	0.0063
55	53.6	36.8	0.0060
60	51.6	40.2	0.0060
65	49.6	43.5	0.0059

RUN NUMBER 27

LIGNITE CHAR
5% Ni

WEIGHT OF CHAR=74.3 mg
WEIGHT OF CARBON=58.8 mg
TEMPERATURE=780°C
PARTICLE SIZE=0.500-0.595 mm
FLOW RATE OF CO_2=150 ml/min

TIME (min)	WEIGHT (mg)	CONVERSION (%)	REACTION RATE (min^{-1})
0	74.3	0.0	0.0194
5	68.7	9.5	0.0187
10	63.3	18.7	0.0179
15	58.2	27.4	0.0170
20	53.3	35.7	0.0165
25	48.5	43.9	0.0158
30	44.0	51.5	0.0150
35	39.7	58.8	0.0143
40	35.6	65.8	0.0134
45	31.8	72.3	0.0121
50	28.5	77.9	0.0102
55	25.8	82.5	0.0082
60	23.[illegible]	86.1	0.0066
65	21.[illegible]	89.1	0.0053
70	20.6	91.3	0.0043
75	19.4	93.4	0.0039

RUN NUMBER 28

LIGNITE CHAR
5% Ni

WEIGHT OF CHAR=74.0 mg
WEIGHT OF CARBON=58.6 mg
TEMPERATURE=800°C
PARTICLE SIZE=0.500-0.595 mm
FLOW RATE OF CO_2=150 ml/min

TIME (min)	WEIGHT (mg)	CONVERSION (%)	REACTION RATE (min^{-1})
0	74.0	0.0	0.0241
5	66.7	12.5	0.0241
10	59.9	24.1	0.0234
15	53.0	35.8	0.0234
20	46.2	47.4	0.0227
25	39.7	58.5	0.0212
30	33.8	68.6	0.0184
35	26.7	80.7	0.0136
40	24.8	84.0	0.0119
45	21.7	89.3	0.0090
50	19.5	93.0	0.0067
55	17.8	95.9	0.0043
60	17.0	97.3	0.0031
65	16.0	99.0	0.0010

RUN NUMBER 29

LIGNITE CHAR
5% Ni

WEIGHT OF CHAR=74.9 mg

WEIGHT OF CARBON=59.4 mg

TEMPERATURE=823°C

PARTICLE SIZE=0.500-0.595 mm

FLOW RATE OF CO_2=150 ml/min

TIME (min)	WEIGHT (mg)	CONVERSION (%)	REACTION RATE (min^{-1})
0	74.9	0.0	0.0374
5	64.0	18.4	0.0360
10	53.5	36.0	0.0348
15	43.3	53.2	0.0325
20	34.2	68.5	0.0273
25	27.1	80.5	0.0202
30	22.2	88.7	0.0138
35	18.9	94.3	0.0088
40	17.0	97.5	0.0054
45	15.7	99.7	0.0012
50	15.5	100.0	-

RUN NUMBER 30

LIGNITE CHAR
5% Ni

WEIGHT OF CHAR=74.4 mg
WEIGHT OF CARBON=58.4 mg
TEMPERATURE=875°C
PARTICLE SIZE=0.500-0.595 mm
FLOW RATE OF CO_2=150 ml/min

TIME (min)	WEIGHT (mg)	CONVERSION (%)	REACTION RATE (min^{-1})
0	74.4	0.0	0.0725
5	54.3	34.1	0.0640
10	36.7	64.0	0.0513
15	24.1	85.4	0.0321
20	17.8	96.1	0.0143
25	15.7	99.7	0.0020
30	15.5	100.0	

RUN NUMBER 31

LIGNITE CHAR
10% Ni

WEIGHT OF CHAR=76.6 mg
WEIGHT OF CARBON=52.4 mg
TEMPERATURE=728°C
PARTICLE SIZE=0.500-0.595 mm
FLOW RATE OF CO_2=150 ml/min

TIME (min)	WEIGHT (mg)	CONVERSION (%)	REACTION RATE (min^{-1})
0	76.6	0.0	0.0069
5	74.8	3.5	0.0069
10	73.0	6.9	0.0069
15	71.2	10.2	0.0069
20	69.4	13.7	0.0067
25	67.7	17.0	0.0067
30	65.9	20.4	0.0067
35	64.2	23.7	0.0069
40	62.3	27.3	0.0071
45	60.5	30.7	0.0067
50	58.8	33.9	0.0063
55	57.2	36.9	0.0065
60	55.4	40.5	0.0073

RUN NUMBER 32

LIGNITE CHAR
10% Ni

WEIGHT OF CHAR=73.9 mg PARTICLE SIZE=0.500-0.595 mm

WEIGHT OF CARBON=56.0 mg FLOW RATE OF CO_2=150 ml/min

TEMPERATURE=823°C

TIME (min)	WEIGHT (mg)	CONVERSION (%)	REACTION RATE (min^{-1})
0	73.9	0.0	0.0375
5	63.8	18.0	0.0375
10	52.9	37.5	0.0375
15	42.8	55.5	0.0337
20	34.0	71.3	0.0268
25	27.8	82.3	0.0189
30	23.4	90.2	0.0129
35	20.6	95.1	0.0075
40	19.2	97.7	0.0045
45	18.1	99.7	0.0021
50	18,0	99.9	0.0004
55	17.9	100.0	-

RUN NUMBER 33

SUB-BITUMINOUS CHAR
5% Ni

WEIGHT OF CHAR=76.8 mg
WEIGHT OF CARBON=64.3 mg
TEMPERATURE=728°C
PARTICLE SIZE=0.500-0.595 mm
FLOW RATE OF CO_2=150 ml/min

TIME (min)	WEIGHT (mg)	CONVERSION (%)	REACTION RATE (min^{-1})
0	76.8	0.0	0.0047
5	75.3	2.4	0.0047
10	73.8	4.6	0.0044
15	72.5	6.6	0.0044
20	71.0	9.0	0.0045
25	69.6	11.2	0.0044
30	68.2	13.4	0.0044
35	66.8	15.6	0.0047
40	65.2	18.0	0.0045
45	63.9	20.0	0.0042
50	62.5	22.3	0.0045
55	61.0	24.6	0.0048
60	59.4	27.0	0.0051

RUN NUMBER 34

SUB-BITUMINOUS CHAR
5% Ni

WEIGHT OF CHAR=74.5 mg PARTICLE SIZE=0.500-0.595 mm

WEIGHT OF CARBON=62.4 mg FLOW RATE OF CO_2=150 ml/min

TEMPERATURE=823°C

TIME (min)	WEIGHT (mg)	CONVERSION (%)	REACTION RATE (min^{-1})
0	74.5	0.0	0.0208
5	68.1	10.2	0.0202
10	61.9	20.2	0.0202
15	55.5	30.5	0.0204
20	49.2	40.5	0.0191
25	43.6	49.5	0.0175
30	38.3	58.0	0.0165
35	33.3	66.0	0.0145
40	25.8	78.0	0.0131
45	25.1	79.2	0.0069
50	21.5	85.0	0.0060

RUN NUMBER 35

SUB-BITUMINOUS CHAR
10% Ni

WEIGHT OF CHAR=75.3 mg
WEIGHT OF CARBON=64.5 mg
TEMPERATURE=728°C
PARTICLE SIZE=0.500-0.595 mm
FLOW RATE OF CO_2=150 ml/min

TIME (min)	WEIGHT (mg)	CONVERSION (%)	REACTION RATE (min^{-1})
0	75.3	0.0	0.0039
5	74.0	2.0	0.0042
10	72.6	4.2	0.0037
15	71.6	5.8	0.0034
20	70.4	7.6	0.0028
25	69.8	8.5	0.0040
30	67.8	11.8	0.0051
35	66.5	13.7	0.0040
40	65.2	15.7	0.0037
45	64.1	17.6	0.0037
50	62.8	20.4	0.0043

RUN NUMBER 36

SUB-BITUMINOUS CHAR
10% K_2CO_3

WEIGHT OF CHAR=70.0 mg
WEIGHT OF CARBON=58.1 mg
TEMPERATURE=728°C
PARTICLE SIZE=0.500-0.595 mm
FLOW RATE OF CO_2=150 ml/min

TIME (min)	WEIGHT (mg)	CONVERSION (%)	REACTION RATE (min^{-1})
0	70.0	0.0	0.0077
5	68.0	3.4	0.0076
10	65.6	7.6	0.0076
15	63.3	11.5	0.0076
20	61.2	15.2	0.0069
25	59.3	18.4	0.0062
30	57.6	21.3	0.0057
35	56.0	24.1	0.0055
40	54.4	26.9	0.0052
45	53.0	29.7	0.0046
50	51.7	31.5	0.0043
55	50.5	33.6	0.0040
60	49.4	35.5	0.0038
65	48.3	37.4	0.0038
70	47.2	39.2	0.0037

RUN NUMBER 37

SUB-BITUMINOUS CHAR
10% K_2CO_3

WEIGHT OF CHAR=70.6 mg
WEIGHT OF CARBON=60.1 mg
TEMPERATURE=780°C
PARTICLE SIZE=0.500-0.595 mm
FLOW RATE OF CO_2=150 ml/min

TIME (min)	WEIGHT (mg)	CONVERSION (%)	REACTION RATE (min^{-1})
0	70.6	0.0	0.0201
5	64.7	9.8	0.0191
10	59.1	19.1	0.0176
15	54.1	27.5	0.0160
20	49.5	35.1	0.0143
25	45.5	41.8	0.0131
30	41.6	48.3	0.0118
35	38.4	53.6	0.0103
40	35.4	58.6	0.0096
45	32.7	63.1	0.0082
50	30.5	66.7	0.0073
55	28.3	70.4	0.0065
60	26.6	73.2	0.0050
65	25.3	75.4	0.0050

RUN NUMBER 38

SUB-BITUMINOUS CHAR
10% K_2CO_3

WEIGHT OF CHAR=67.6 mg
WEIGHT OF CARBON=57.5 mg
TEMPERATURE=821°C
PARTICLE SIZE=0.500-0.595 mm
FLOW RATE OF CO_2=150 ml/min

TIME (min)	WEIGHT (mg)	CONVERSION (%)	REACTION RATE (min^{-1})
0	67.6	0.0	0.0308
5	58.8	15.3	0.0304
10	50.1	30.4	0.0287
15	42.3	44.0	0.0245
20	36.0	55.0	0.0205
25	30.5	64.5	0.0174
30	26.0	72.4	0.0146
35	22.1	79.1	0.0123
40	18.9	84.7	0.0101
45	16.3	89.2	0.0078
50	14.4	92.5	0.0054
55	13.2	94.6	0.0033
60	12.5	95.8	0.0021
65	12.0	96.7	0.0021

RUN NUMBER 39

SUB-BITUMINOUS CHAR
10% K_2CO_3

WEIGHT OF CHAR=67.1 mg
WEIGHT OF CARBON=57.1 mg
TEMPERATURE=872°C
PARTICLE SIZE=0.500-0.595 mm
FLOW RATE OF CO_2=150 ml/min

TIME (min)	WEIGHT (mg)	CONVERSION (%)	REACTION RATE (min^{-1})
0	67.1	0.0	0.0700
5	47.9	33.6	0.0664
10	29.2	66.4	0.0541
15	17.0	87.7	0.0306
20	11.7	97.0	0.0119
25	10.2	99.7	0.0026
30	10.0	100.0	-

RUN NUMBER 40

SUB-BITUMINOUS CHAR
20% K_2CO_3

WEIGHT OF CHAR=71.3 mg
WEIGHT OF CARBON=48.4 mg
TEMPERATURE=728°C
PARTICLE SIZE=0.500-0.595 mm
FLOW RATE OF CO_2=150 ml/min

TIME (min)	WEIGHT (mg)	CONVERSION (%)	REACTION RATE (min^{-1})
0	71.3	0.0	0.0103
5	69.3	4.1	0.0103
10	66.3	9.7	0.0103
15	64.3	14.4	0.0081
20	62.4	18.3	0.0079
25	60.5	22.3	0.0070
30	59.0	25.4	0.0060
35	57.6	28.2	0.0066
40	55.8	32.0	0.0048
45	55.3	33.0	0.0033
50	54.2	35.3	0.0041
55	53.9	36.1	0.0040

RUN NUMBER 41

SUB-BITUMINOUS CHAR
20% K_2CO_3

WEIGHT OF CHAR=67.3 mg
WEIGHT OF CARBON=52.9 mg
TEMPERATURE=821°C
PARTICLE SIZE=0.500-0.595 mm
FLOW RATE OF CO_2=150 ml/min

TIME (min)	WEIGHT (mg)	CONVERSION (%)	REACTION RATE (min^{-1})
0	67.3	0.0	0.0318
5	59.2	15.2	0.0295
10	51.7	29.5	0.0272
15	44.8	42.5	0.0255
20	38.2	55.0	0.0242
25	32.0	66.7	0.0212
30	27.0	76.2	0.0161
35	23.5	82.8	0.0112
40	21.1	87.3	0.0076
45	19.5	90.4	0.0049
50	18.5	92.3	0.0036
55	17.6	94.0	0.0030
60	16.9	95.3	0.0025
65	16.3	96.5	0.0021

RUN NUMBER 42

LIGNITE CHAR
10% K_2CO_3

WEIGHT OF CHAR=69.5 mg
WEIGHT OF CARBON=53.2 mg
TEMPERATURE=728°C
PARTICLE SIZE=0.500-0.595 mm
FLOW RATE OF CO_2=150 ml/min

TIME (min)	WEIGHT (mg)	CONVERSION (%)	REACTION RATE (min^{-1})
0	69.5	0.0	0.0187
5	64.7	9.0	0.0184
10	59.7	18.4	0.0173
15	55.5	26.3	0.0148
20	51.8	33.3	0.0128
25	48.7	39.1	0.0115
30	45.7	44.7	0.0102
35	43.3	49.3	0.0092
40	40.8	54.0	0.0085
45	38.8	57.7	0.0070
50	37.1	60.9	0.0060
55	35.6	63.7	0.0053
60	34.2	66.2	0.0045
65	33.2	68.2	0.0045

RUN NUMBER 43

LIGNITE CHAR
10% K_2CO_3

WEIGHT OF CHAR=69.5 mg
WEIGHT OF CARBON=53.2 mg
TEMPERATURE=780°C
PARTICLE SIZE=0.500-0.595 mm
FLOW RATE OF CO_2=150 ml/min

TIME (min)	WEIGHT (mg)	CONVERSION (%)	REACTION RATE (min^{-1})
0	69.5	0.0	0.0420
5	58.3	21.1	0.0385
10	49.0	38.5	0.0318
15	41.4	52.8	0.0242
20	36.1	62.8	0.0175
25	32.1	70.3	0.0132
30	29.1	75.9	0.0103
35	26.6	80.6	0.0083
40	24.7	84.2	0.0070
45	22.9	87.6	0.0058
50	21.6	90.0	0.0041
55	20.7	91.7	0.0032
60	19.9	93.2	0.0026
65	19.3	94.4	0.0026

RUN NUMBER 44

LIGNITE CHAR
10% K_2CO_3

WEIGHT OF CHAR=68.8 mg
WEIGHT OF CARBON=52.6 mg
TEMPERATURE=823°C
PARTICLE SIZE=0.500-0.595 mm
FLOW RATE OF CO_2=150 ml/min

TIME (min)	WEIGHT (mg)	CONVERSION (%)	REACTION RATE (min^{-1})
0	68.8	0.0	0.0800
5	48.8	38.0	0.0625
10	35.9	62.5	0.0399
15	27.8	78.0	0.0255
20	22.5	88.0	0.0158
25	19.5	93.7	0.0087
30	17.9	96.7	0.0040
35	17.4	97.7	0.0019
40	16.9	98.6	0.0011
45	16.8	98.8	0.0010

RUN NUMBER 45

LIGNITE CHAR
10% K_2CO_3

WEIGHT OF CHAR=68.9 mg
WEIGHT OF CARBON=52.7 mg
TEMPERATURE=872°C
PARTICLE SIZE=0.500-0.595 mm
FLOW RATE OF CO_2=150 ml/min

TIME (min)	WEIGHT (mg)	CONVERSION (%)	REACTION RATE (min^{-1})
0	68.9	0.0	0.1349
5	39.4	56.0	0.0890
10	22.0	89.0	0.0419
15	17.3	98.0	0.0104
20	16.5	99.5	0.0019
25	16.3	99.8	0.0006
30	16.2	100.0	-

RUN NUMBER 46

LIGNITE CHAR
20% K_2CO_3

WEIGHT OF CHAR=66.5 mg
WEIGHT OF CARBON=46.2 mg
TEMPERATURE=728°C
PARTICLE SIZE=0.500-0.595 mm
FLOW RATE OF CO_2=150 ml/min

TIME (min)	WEIGHT (mg)	CONVERSION (%)	REACTION RATE (min^{-1})
0	66.5	0.0	0.0327
5	59.6	15.0	0.0271
10	54.0	27.1	0.0208
15	50.0	35.7	0.0149
20	47.1	42.0	0.0115
25	44.7	47.2	0.0097
30	42.6	51.8	0.0080
35	41.0	55.3	0.0067
40	39.5	58.4	0.0063
45	38.1	61.5	0.0052
50	37.1	63.7	0.0041
55	36.2	65.6	0.0035
60	35.5	67.0	0.0026
65	35.0	68.2	0.0017

RUN NUMBER 47

LIGNITE CHAR
20% K_2CO_3

WEIGHT OF CHAR=66.5 mg
WEIGHT OF CARBON=46.2 mg
TEMPERATURE=823°C
PARTICLE SIZE=0.500-0.595 mm
FLOW RATE OF CO_2 150 ml/min

TIME (min)	WEIGHT (mg)	CONVERSION (%)	REACTION RATE (min^{-1})
0	66.5	0.0	0.0961
5	48.0	40.0	0.0641
10	36.9	64.0	0.0385
15	30.2	78.5	0.0232
20	26.2	87.2	0.0134
25	24.0	92.0	0.0074
30	22.8	94.5	0.0039
35	22.2	95.9	0.0028
40	21.5	97.3	0.0017
45	21.4	97.6	0.0004
50	21.3	97.8	0.0004
55	21.2	98.0	0.0003

RUN NUMBER 48

LIGNITE CHAR
10% K_2CO_3+5% Ni

WEIGHT OF CHAR=74.5 mg
WEIGHT OF CARBON=55.3 mg
TEMPERATURE=728°C
PARTICLE SIZE=0.500-0.595 mm
FLOW RATE OF CO_2=150 ml/min

TIME (min)	WEIGHT (mg)	CONVERSION (%)	REACTION RATE (min^{-1})
0	74.5	0.0	0.0177
5	69.5	9.0	0.0184
10	64.3	18.5	0.0172
15	60.0	26.2	0.0156
20	55.7	34.0	0.0148
25	51.8	41.0	0.0130
30	48.5	47.0	0.0108
35	45.8	51.8	0.0092
40	43.4	56.2	0.0081
45	41.3	60.0	0.0072
50	39.4	63.5	0.0060

RUN NUMBER 49

LIGNITE CHAR
10% K_2CO_3+5% Ni

WEIGHT OF CHAR=74.2 mg
WEIGHT OF CARBON=55.1 mg
TEMPERATURE=823°C
PARTICLE SIZE=0.500-0.595 mm
FLOW RATE OF CO_2=150 ml/min

TIME (min)	WEIGHT (mg)	CONVERSION (%)	REACTION RATE (min^{-1})
0	74.2	0.0	0.0780
5	54.9	35.0	0.0626
10	40.0	62.0	0.0416
15	32.0	76.5	0.0229
20	27.4	85.0	0.0129
25	24.9	89.5	0.0071
30	23.5	92.0	0.0040
35	22.7	93.4	0.0027
40	22.0	94.8	0.0025
45	21.3	96.0	0.0018
50	21.0	96.5	0.0010

RUN NUMBER 50

LIGNITE CHAR

WEIGHT OF CHAR=71.5 mg
WEIGHT OF CARBON=61.6 mg
TEMPERATURE=823°C
PARTICLE SIZE=0.500-0.595 mm
FLOW RATE OF CO_2=119 ml/min
FLOW RATE OF N_2=31 ml/min

TIME (min)	WEIGHT (mg)	CONVERSION (%)	REACTION RATE (min^{-1})
0	71.5	0.0	0.0240
5	64.1	12.0	0.0240
10	56.7	24.0	0.0218
15	50.7	33.7	0.0183
20	45.4	42.4	0.0169
25	40.3	50.6	0.0153
30	36.0	57.6	0.0135
35	32.0	64.1	0.0131
40	27.9	70.7	0.0115
45	24.9	75.7	0.0094
50	22.1	80.2	0.0090

RUN NUMBER 51

LIGNITE CHAR

WEIGHT OF CHAR=69.5 mg

WEIGHT OF CARBON=59.8 mg

TEMPERATURE=823°C

PARTICLE SIZE=0.500-0.595 mm

FLOW RATE OF CO_2=75 ml/min

FLOW RATE OF N_2=75 ml/min

TIME (min)	WEIGHT (mg)	CONVERSION (%)	REACTION RATE (min^{-1})
0	69.5	0.0	0.0157
5	64.8	7.6	0.0157
10	60.1	15.2	0.0159
15	55.3	23.1	0.0164
20	50.3	32.1	0.0164
25	45.5	40.1	0.0162
30	40.6	48.3	0.0152
35	47.0	55.4	0.0137
40	32.4	62.0	0.0137
45	28.2	69.1	0.0124
50	25.0	74.4	0.0097
55	22.4	76.4	0.0071

RUN NUMBER 52

LIGNITE CHAR

WEIGHT OF CHAR=70.2 mg

WEIGHT OF CARBON=60.4 mg

TEMPERATURE=823°C

PARTICLE SIZE=0.500-0.595 mm

FLOW RATE OF CO_2=32 ml/min

FLOW RATEOF N_2=118 ml/min

TIME (min)	WEIGHT (mg)	CONVERSION (%)	REACTION RATE (min^{-1})
0	70.2	0.0	0.0061
5	68.4	3.0	0.0058
10	66.7	5.8	0.0058
15	64.9	8.8	0.0058
20	63.2	11.6	0.0058
25	61.4	14.5	0.0060
30	59.6	17.5	0.0058
35	57.9	20.3	0.0058
40	56.1	23.4	0.0055
45	54.6	25.9	0.0055

RUN NUMBER 53

SUB-BITUMINOUS CHAR

WEIGHT OF CHAR=70.4 mg

WEIGHT OF CARBON=62.4 mg

TEMPERATURE=821°C

PARTICLE SIZE=0.500-0.595 mm

FLOW RATE OF CO_2=112 ml/min

FLOW RATE OF N_2=37 ml/min

TIME (min)	WEIGHT (mg)	CONVERSION (%)	REACTION RATE (min^{-1})
0	70.4	0.0	0.0151
5	65.7	7.5	0.0151
10	61.0	15.1	0.0141
15	56.9	21.6	0.0127
20	53.1	27.8	0.0125
25	49.1	34.2	0.0128
30	45.1	40.5	0.0125
35	41.3	46.7	0.0125
40	37.3	53.0	0.0123
45	33.6	59.0	0.0096

RUN NUMBER 54

SUB-BITUMINOUS CHAR

WEIGHT OF CHAR=69.6 mg

WEIGHT OF CARBON=61.6 mg

TEMPERATURE=821°C

PARTICLE SIZE=0.500-0.595 mm

FLOW RATE OF CO_2=75 ml/min

FLOW RATE OF N_2=75 ml/min

TIME (min)	WEIGHT (mg)	CONVERSION (%)	REACTION RATE (min^{-1})
0	69.6	0.0	0.0107
5	66.4	5.1	0.0101
10	63.4	10.1	0.0101
15	60.2	15.2	0.0097
20	57.4	19.8	0.0089
25	54.7	24.2	0.0084
30	52.2	28.3	0.0084
35	49.5	32.7	0.0086
40	46.9	36.8	0.0082

RUN NUMBER 55

SUB-BITUMINOUS CHAR

WEIGHT OF CHAR=70.1 mg

WEIGHT OF CARBON=62.0 mg

TEMPERATURE=821 °C

PARTICLE SIZE=0.500-0.595 mm

FLOW RATE OF CO_2=37 ml/min

FLOW RATE OF N_2=112 ml/min

TIME (min)	WEIGHT (mg)	CONVERSION (%)	REACTION RATE (min^{-1})
0	70.1	0.0	0.0042
5	68.7	2.3	0.0048
10	67.1	4.9	0.0053
15	65.4	7.5	0.0053
20	63.8	10.1	0.0050
25	62.3	12.6	0.0048
30	60.8	15.0	0.0048
35	59.3	17.4	0.0052
40	57.6	20.1	0.0052
45	56.1	22.6	0.0052
50	54.4	25.3	0.0050

RUN NUMBER 56

LIGNITE CHAR

WEIGHT OF CHAR=71.9 mg

WEIGHT OF CARBON=61.8 mg

TEMPERATURE=823°C

PARTICLE SIZE=0.500-0.595 mm

FLOW RATE OF CO_2=150 ml/min

TIME (min)	WEIGHT (mg)	CONVERSION (%)	REACTION RATE (min^{-1})
0	71.9	0.0	0.0304
5	62.5	15.2	0.0301
10	52.8	30.9	0.0299
15	44.0	45.1	0.0282
20	35.4	59.1	0.0267
25	27.5	71.8	0.0217
30	22.0	80.7	0.0154
35	18.0	87.2	0.0108
40	15.3	91.6	0.0071
45	13.6	94.3	0.0049
50	12.3	96.4	0.0029
55	11.8	97.3	0.0020

RUN NUMBER 57

LIGNITE CHAR

WEIGHT OF CHAR=68.7 mg
WEIGHT OF CARBON=59.1 mg
TEMPERATURE=823°C
PARTICLE SIZE=0.500-0.595 mm
FLOW RATE OF CO_2=150 ml/min

TIME (min)	WEIGHT (mg)	CONVERSION (%)	REACTION RATE (min^{-1})
0	68.7	0.0	0.0280
5	60.8	13.4	0.0279
10	52.2	27.9	0.0286
15	43.9	42.0	0.0269
20	36.3	54.8	0.0242
25	29.6	66.2	0.0203
30	24.3	75.1	0.0156
35	20.4	81.7	0.0115
40	17.5	86.6	0.0083
45	15.5	90.0	0.0052

RUN NUMBER 58

SUB-BITUMINOUS CHAR

WEIGHT OF CHAR=70.6 mg PARTICLE SIZE=0.500-0.595 mm

WEIGHT OF CARBON=62.5 mg FLOW RATE OF CO_2=150 ml/min

TEMPERATURE=800°C

TIME (min)	WEIGHT (mg)	CONVERSION (%)	REACTION RATE (min^{-1})
0	70.6	0.0	0.0155
5	65.8	7.7	0.0152
10	61.1	15.2	0.0149
15	56.5	22.6	0.0146
20	52.0	29.8	0.0136
25	48.0	36.2	0.0128
30	44.0	42.6	0.0126
35	40.1	48.8	0.0118
40	36.6	54.4	0.0114
45	33.0	60.2	0.0112
50	29.6	65.6	0.0102
55	26.6	70.4	0.0090
60	24.0	74.6	0.0085
65	21.3	78.9	0.0077
70	19.2	82.2	0.0060
75	17.4	85.1	0.0055

RUN NUMBER 59

SUB-BITUMINOUS CHAR

WEIGHT OF CHAR=69.8 mg

WEIGHT OF CARBON=61.8 mg

TEMPERATURE=800°C

PARTICLE SIZE=0.500-0.595 mm

FLOW RATE OF CO_2=150 ml/min

TIME (min)	WEIGHT (mg)	CONVERSION (%)	REACTION RATE (min^{-1})
0	69.8	0.0	0.0146
5	65.4	7.1	0.0139
10	61.2	13.9	0.0141
15	56.7	21.2	0.0136
20	52.8	27.5	0.0129
25	48.7	34.1	0.0133
30	44.6	40.8	0.0131
35	40.6	47.3	0.0094
40	38.8	50.2	0.0115
45	33.5	58.7	0.0138
50	30.3	62.9	0.0102
55	27.2	68.9	0.0099
60	24.2	73.8	0.0092
65	21.5	78.2	0.0079
70	19.3	81.7	0.0062
75	17.5	84.6	0.0060

RUN NUMBER 60

LIGNITE CHAR
5% Ni

WEIGHT OF CHAR=73.6 mg
WEIGHT OF CARBON=58.2 mg
TEMPERATURE=780°C
PARTICLE SIZE=0.500-0.595 mm
FLOW RATE OF CO_2=150 ml/min

TIME (min)	WEIGHT (mg)	CONVERSION (%)	REACTION RATE (min^{-1})
0	73.6	0.0	0.0170
5	68.9	8.1	0.0170
10	63.7	17.0	0.0170
15	59.0	25.1	0.0167
20	54.0	33.7	0.0175
25	48.8	42.6	0.0170
30	44.1	50.7	0.0160
35	39.5	58.6	0.0144
40	35.7	65.1	0.0134
45	31.7	72.0	0.0132
50	28.0	78.4	0.0117
55	24.9	83.7	0.0086
60	23.0	86.9	0.0064
65	21.2	90.0	0.0058
70	19.6	92.8	0.0056
75	18.4	94.8	0.0040

RUN NUMBER 61

LIGNITE CHAR
5% Ni

WEIGHT OF CHAR=72.3 mg
WEIGHT OF CARBON=57.2 mg
TEMPERATURE=780°C
PARTICLE SIZE=0.500-0.595 mm
FLOW RATE OF CO_2=150 ml/min

TIME (min)	WEIGHT (mg)	CONVERSION (%)	REACTION RATE (min^{-1})
0	72.3	0.0	0.0185
5	67.0	9.3	0.0185
10	61.7	18.5	0.0184
15	56.5	27.6	0.0178
20	51.5	36.4	0.0172
25	46.8	44.6	0.0170
30	42.0	53.0	0.0166
35	37.6	60.7	0.0152
40	33.3	68.2	0.0138
45	29.7	74.5	0.0117
50	26.6	79.9	0.0095
55	24.2	84.1	0.0079
60	22.1	87.8	0.0065
65	20.5	90.6	0.0051
70	19.2	92.8	0.0043
75	18.0	94.9	0.0042

RUN NUMBER 62

SUB-BITUMINOUS CHAR
10% K_2CO_3

WEIGHT OF CHAR=65.2 mg
WEIGHT OF CARBON=54.2 mg
TEMPERATURE= 872°C
PARTICLE SIZE=0.500-0.595 mm
FLOW RATE OF CO_2=150 ml/min

TIME (min)	WEIGHT (mg)	CONVERSION (%)	REACTION RATE (min^{-1})
0	65.2	0.0	0.0738
5	45.2	36.9	0.0685
10	28.1	68.5	0.0517
15	17.2	88.6	0.0280
20	12.9	96.5	0.0103
25	11.6	98.9	0.0028
30	11.4	99.3	0.0011
35	11.0	100.0	-

RUN NUMBER 63

SUB-BITUMINOUS CHAR
10% K_2CO_3

WEIGHT OF CHAR=66.8 mg
WEIGHT OF CARBON=56.4 mg
TEMPERATURE=872°C
PARTICLE SIZE=0.500-0.595 mm
FLOW RATE OF CO_2=150 ml/min

TIME (min)	WEIGHT (mg)	CONVERSION (%)	REACTION RATE (min^{-1})
0	66.8	0.0	0.0688
5	48.0	33.3	0.0645
10	30.4	64.5	0.0527
15	18.3	86.0	0.0314
20	12.7	95.9	0.0126
25	11.2	98.6	0.0035
30	10.7	99.5	0.0012
35	10.5	99.8	0.0005
40	10.4	100.0	-

RUN NUMBER 64

LIGNITE CHAR
10% K_2CO_3

WEIGHT OF CHAR=69.2 mg
WEIGHT OF CARBON=53.0 mg
TEMPERATURE=728°C
PARTICLE SIZE=0.500-0.595 mm
FLOW RATE OF CO_2=150 ml/min

TIME (min)	WEIGHT (mg)	CONVERSION (%)	REACTION RATE (min^{-1})
0	69.2	0.0	0.0208
5	63.7	10.4	0.0198
10	58.7	19.4	0.0179
15	54.2	28.3	0.0160
20	50.2	35.8	0.0140
25	46.8	42.3	0.0117
30	44.0	47.6	0.0100
35	41.5	52.3	0.0092
40	39.1	56.8	0.0085
45	37.0	60.7	0.0074
50	35.2	64.2	0.0060
55	33.8	66.8	0.0051
60	32.5	69.3	0.0047
65	31.3	71.5	0.0042
70	30.3	73.4	0.0040
75	29.4	75.1	0.0038

RUN NUMBER 65

LIGNITE CHAR
10% K_2CO_3

WEIGHT OF CHAR=70.2 mg
WEIGHT OF CARBON=53.7 mg
TEMPERATURE=728°C
PARTICLE SIZE=0.500-0.595 mm
FLOW RATE OF CO_2=150 ml/min

TIME (min)	WEIGHT (mg)	CONVERSION (%)	REACTION RATE (min^{-1})
0	70.2	0.0	0.0184
5	65.3	9.1	0.0184
10	60.3	18.4	0.0173
15	56.0	26.4	0.0151
20	52.2	33.5	0.0130
25	49.0	39.5	0.0114
30	46.1	44.9	0.0101
35	43.6	49.5	0.0088
40	41.4	53.6	0.0080
45	39.3	57.4	0.0076
50	37.3	61.3	0.0065
55	35.8	64.1	0.0052
60	34.5	66.5	0.0052
65	33.0	69.3	0.0048
70	31.9	71.3	0.0043
75	31.0	73.0	0.0039